

This work is protected by copyright and other intellectual property rights and duplication or sale of all or part is not permitted, except that material may be duplicated by you for research, private study, criticism/review or educational purposes. Electronic or print copies are for your own personal, non-commercial use and shall not be passed to any other individual. No quotation may be published without proper acknowledgement. For any other use, or to quote extensively from the work, permission must be obtained from the copyright holder/s.

Keele University



Pharmacological analysis of dopaminergic synaptic plasticity in rodent lateral entorhinal cortex

George Pettitt

**A thesis submitted for the degree of
Master of Philosophy**

March 2021

Abstract

Despite receiving the second largest dopaminergic projection from the ventral tegmental area (VTA) and having a pivotal role in conveying non-spatial information received from sensory cortices, the physiological functions of the lateral entorhinal cortex (LEC) are still yet to be fully identified. The LEC is comprised of six distinct layers, with the deep layers (layers V-VI) receiving projections from throughout the hippocampal formation and projecting gamma-aminobutyric acid (GABA) rich neurones to the superficial layers (layers I-III). Preliminary experiments showed that superficial layers also receive the aforementioned dopaminergic input from the VTA, a projection which is highlighted by tyrosine hydroxylase staining. This staining also showing that dopamine (DA) is deposited into pools (referred to as islands) which span these superficial layers. Field excitatory postsynaptic potential (fEPSP) experiments under *ex vivo* conditions studied changes in amplitude, that is the size of postsynaptic responses from localised neurones, and whether they increase (facilitate) or decrease (depress) in size when introduced to various stimuli. Previous studies have shown that application of high concentrations of DA causes significant depression in amplitudes. However, low concentrations of DA show facilitations during bath application of 10 nM DA, or during the washout following 100 nM DA application. Pharmacological analysis of D1-like and D2-like DA receptor function, using the receptor antagonists SCH-23390 and sulpiride respectively, which indicated that both receptors play comparable roles on peak synaptic depression as their co-application with 100 μ M DA showed no statistically significant difference from their individual applications. Gradient analysis during DA application, after exertion of the maximal DA effect, suggests that DA desensitisation, a neurological phenomenon during which receptors lose their sensitivity to a neurotransmitter over time, may be D1-receptor mediated within the LEC. This was shown during SCH-23390 application experiments, sequestering D1-like receptor activity (leaving only D2-like receptor activity) showed an absence of desensitisation, however this was not statistically significantly different from other experiments. Although this effect was seen with 100 μ M DA, co-application with 1000 μ M DA showed no statistical significance from the controls which suggests the agonists competitively bind to the same sites of the receptor as DA. Application of (2R)-Amino-5-Phosphonopentanoate (AP5), an N-Methyl-D-Aspartic Acid receptor (NMDAR) antagonist, showed a greater depression during DA and AP5 co-application. This indicated that recorded amplitudes possess a glutamatergic component to them but are not NMDA dependent. This glutamatergic component was further shown through paired-pulse stimulation experiments, in which two amplitudes are generated over short interpulse intervals (ranging from 10-1000 ms). Paired-pulse stimulations during 100 μ M DA application induced a facilitation over all intervals, which indicated DA affects presynaptic glutamate release probabilities. The combination of these components confirms that recorded amplitudes within the LEC arise predominantly from glutamatergic activity, with DA affecting these amplitudes indirectly by interacting with both presynaptic and postsynaptic glutamatergic receptors.

Contents

Abstract	ii
List of Figures	vi
Abbreviations	viii
1 Introduction	1
1.1 The Hippocampal Formation.....	1
1.1.1 Anatomy of the Hippocampal Formation	1
1.1.2 Projections of the Hippocampal Formation and Parahippocampal Cortices.....	2
1.1.3 The Entorhinal Cortex	3
1.1.3.1 The Medial Entorhinal Cortex and The Lateral Entorhinal Cortex	3
1.1.3.2 The Role of the EC in the Formation of Sensory Memory	3
1.1.3.3 Function and Anatomy of the LEC.....	4
1.1.3.4 Neurotransmitters in the LEC.....	8
1.2 Dopamine	8
1.2.1 Introduction to Dopamine	8
1.2.2 Dopamine Receptors.....	11
1.2.2.1 The D1 Receptor Family	11
1.2.2.2 The D2 Receptor Family	13
1.2.2.3 Dopamine Receptor Pharmacology	15
1.2.3 Dopamine Transmission.....	18
1.2.4 Dopaminergic Neurones in the LEC.....	19
1.3 Plasticity	20
1.3.1 An Overview of Synaptic Plasticity	20
1.3.2 Activity-Dependent Plasticity.....	20
1.3.2.1 Long-Term Potentiation	23
1.3.2.1.1 Postsynaptic Mechanisms of Long-Term Potentiation	23
1.3.2.1.2 Presynaptic Mechanisms of Long-Term Potentiation	25
1.3.2.2 Long-Term Depression	26
1.3.2.2.1 Postsynaptic Mechanisms of Long-Term Depression	26
1.3.2.2.2 Presynaptic Mechanisms of Long-Term Depression.....	27
1.3.2.3 Short-Term Plasticity	28
1.3.3 Dopamine-Mediated Plasticity.....	29
1.3.4 Methods for Inducing Plasticity	31
1.4 Research Aims	34

2	Methods	36
2.1	Slice Preparation	36
2.2	Stimulation and Recording.....	36
2.3	Field Experiments.....	37
2.3.1	Dopamine Application.....	37
2.3.2	Paired-Pulse Stimulation	38
2.4	Immunohistochemistry	38
2.5	Data Analysis	38
3	Results - Controls and Initial Dopamine Experiments	40
3.1	Tyrosine Hydroxylase Immunohistochemistry.....	40
3.2	Control Experiments.....	41
3.2.1	ACSF Changeover Control	41
3.2.2	Sodium Metabisulfite Vehicle Control	42
3.3	Dopamine Applications at Low Concentrations.....	43
3.3.1	Single Application.....	43
3.3.2	Repeated 100 nM Dopamine Application.....	45
4	Results - Pharmacological Analysis of Cell Types Present Within the LEC	47
4.1	Pharmacological Analysis of Antagonists with 100 μ M Dopamine.....	47
4.1.1	AP5 and Dopamine.....	47
4.1.2	SCH-23390, Sulpiride and Dopamine	49
4.2	Pharmacological Analysis of Antagonists with 1000 μ M Dopamine.....	53
4.2.1	Barbadin and Dopamine	53
4.2.2	SCH-23390, Sulpiride and Dopamine	55
4.3	Paired-Pulse Stimulation Tests.....	57
4.3.1	Low Concentration Dopamine (100 nM).....	57
4.3.2	High Concentration Dopamine (100 μ M).....	59
5	Discussion	62
5.1	Summary of Experimental Findings	62
5.2	Justification of Methods.....	62
5.3	Analysis of Results.....	64
5.3.1	Controls and Initial Dopamine Experiments	64
5.3.1.1	Tyrosine Hydroxylase Immunohistochemistry.....	64
5.3.1.2	Control Experiments.....	64
5.3.1.3	Single Application of Low Concentration Dopamine	65

5.3.1.4	Repeated Application of Low Concentration Dopamine	66
5.3.2	Pharmacological Analysis of Cell Types Present Within the LEC.....	66
5.3.2.1	Antagonist Analysis with 100 μ M Dopamine	66
5.3.2.1.1	AP5 with 100 μ M Dopamine	66
5.3.2.1.2	Dopamine Antagonists with 100 μ M Dopamine.....	67
5.3.2.2	Antagonist Analysis with 1000 μ M Dopamine	70
5.3.2.2.1	Barbadin with 1000 μ M Dopamine	70
5.3.2.2.2	Dopamine Antagonists with 1000 μ M Dopamine.....	70
5.3.2.3	Paired-Pulse Stimulation Analysis	71
5.4	Clinical Significance	72
5.4.1	Depression.....	72
5.4.1.1	Overview of Depression	72
5.4.1.2	Anhedonia	74
5.4.1.3	Flinders-Sensitive line (FSL) Rats	74
5.4.2	Schizophrenia	75
5.4.3	Clinical Significance of Results in Neurological Disorders.....	75
5.5	Conclusion	76
5.6	Future Work	77
5.6.1	Refining and Expanding Current Datasets.....	77
5.6.2	Supplementary Pharmacological Experiments	78
5.6.3	Implementing Clinical Relevance	79
6	Acknowledgments	81
7	References	82

List of Figures

1	A Sketch of the Rodent Hippocampal Formation	1
2	Sensory Projections to and From the Entorhinal Cortex and Projections Within the Hippocampal Formation	2
3	Interconnectivity Within the Lateral Entorhinal Cortex	5
4	The Projection of Dopaminergic Neurones From the Ventral Tegmental Area Throughout a Rodent Brain	9
5	The Chemical Structure of Dopamine.....	10
6	The Amino Acid Structure and the Subsequent Signalling Cascade D ₁ and D ₅ Receptors.....	12
7	Signal Cascade of D ₂ -Like Receptors Alongside D ₁ -Like Receptors and the Amino Acid Structure of D ₂ , D ₃ and D ₄ Receptors.....	14
8	Dopamine Release From Vesicles in the Presynaptic Bouton into the Synaptic Cleft.....	18
9	A Simplified Overview of Presynaptic and Postsynaptic Mechanisms in Both Long-Term Potentiation and Depression	22
10	Signal Cascade of Dopamine-Mediated Synaptic Plasticity	30
11	Positions of Electrode Placement During Experiments and a Compartmentalised Waveform	37
12	Tyrosine Hydroxylase Staining Indicates the Presence of Dopaminergic Fibres in the Lateral Entorhinal Cortex	40
13	Changing the Source of ACSF Showed No Significant Change in Synaptic Responses	41
14	Isolated Application of Sodium Metabisulfite Showed No Significant Change in Synaptic Responses	42
15	Application of Low Concentration Dopamine Elicits a Concentration Dependent Effect During Tonic Application and a Facilitative Effect After Removal.....	44
16	Sequential Application of 100 nM Dopamine Shows No Statistically Significant Changes During Either Application.....	46
17	Coapplication of the NMDAR Antagonist AP5 and a High Concentration of Dopamine Yields a Greater Depression than Dopamine on Its Own.....	48
18	Application of the D ₁ -Like Receptor Antagonist SCH-23390, the D ₂ -Like Receptor Antagonist Sulpiride and Their Coapplication Significantly Reduces Both the Onset and the Peak of 100 μ M Dopamine-Mediated fEPSP Depression, but Only SCH-23390 Showed Some Effect on Dopamine Desensitisation	51
19	Coapplying Barbadin and 1000 μ M Dopamine Shows No Statistically Reliable Changes in Either Peak Depression or Dopamine Desensitisation	54
20	Neither Application of the D ₁ -Like Receptor Antagonist SCH-23390 or the D ₂ -Like Receptor Antagonist Sulpiride With 1000 μ M Dopamine Elicit Significant Changes in Peak Depression or Dopamine Desensitisation.....	56
21	Application of 100 nM Dopamine Produces No Statistically Reliable Changes in Paired-Pulse Ratios	58
22	Application of 100 μ M Dopamine Produces Statistically Significant Changes in Paired-Pulse Ratios	60

List of Tables

1	Dopamine Receptor Agonists and Antagonists	17
2	Post Hoc Comparisons Between Low Concentration Dopamine Applications Shows No Statistically Significant Difference Between Any Experiment.....	45
3	Coapplying Dopamine and AP5 Elicits a Statistically Significant Depression in Synaptic Transmission When Compared With Both Dopamine Application and the Untampered Control	47
4	Coapplication of Dopamine Antagonists With Dopamine Shows a Statistically Significant Difference From the Control and Dopamine Application, However No Statistically Significant Difference is Shown Between Antagonists	52
5	There is No Statistically Significant Difference Between Gradients in Any Dataset Following Dopamine Exerting its Maximum Effect on Synaptic Transmission	52
6	Statistically Significant Differences Between Second Pulses in Paired-Pulse Experiments Differs Between Low Concentration (100 nM) and High Concentration (100 μ M) Dopamine Application Experiments.....	61

Abbreviations

5-HT	5-Hydroxytryptamine
AC	Adenylyl Cyclase
ACSF	Artificial Cerebrospinal Fluid
Akt	Protein Kinase B
Akt P	Akt Phosphorylated
AMPA	α -Amino-3-Hydroxy-5-Methyl-4-Isoxazolepropionic Acid
AMPA R	AMPA Receptor
AP2	Clathrin Adaptor Protein 2
AP5	(2 <i>R</i>)-Amino-5-Phosphonopentanoate
BDNF	Brain Derived Neurotrophic Factor
βArr2	β -Arrestin 2
CA	Cornu Ammonis
CaMKII	Calcium-Calmodulin-Dependent Protein Kinase Type II
cAMP	Cyclic 3'5' Adenosine Monophosphate
CaN	Ca ²⁺ -Sensitive Phosphate Calcineurin
Ca²⁺	Calcium Ion
CB₁R	Type 1 Cannabinoid Receptor
cGMP	Cyclic Guanosine Monophosphate
CRE	cAMP Response Element
CREB	cAMP Response Element-Binding Protein
DA	Dopamine
DAG or DGL	Diacylglycerol
DARPP-32	Phosphoprotein of 32 kDa
DAT	Dopamine Transporter
DG	Dentate Gyrus
D₁	Dopamine D1 Receptor
D₂	Dopamine D2 Receptor
D_{2L}	Dopamine D2 Receptor Long
D_{2S}	Dopamine D2 Receptor Short
D₃	Dopamine D3 Receptor
D₄	Dopamine D4 Receptor
D₅	Dopamine D5 Receptor
EC	Entorhinal Cortex
eCB	Endocannabinoid
ERK (1/2)	Extracellular Signal-Regulated Kinase
fEPSP	Field Excitatory Post-Synaptic Potential
FSL	Flinders-Sensitive Line
GABA	Gamma Aminobutyric Acid
GP	Globus Pallidus
GSK-3β	Glycogen Synthase Kinase 3 β

HF	Hippocampal Formation
iGluR	Ionotropic Glutamate Receptor
IPI	Interpulse Intervals
KAR	Kainate Receptors
K⁺	Potassium Ion
LC	Locus Coeruleus
Ld	Lamina Dissecans
LEC	Lateral Entorhinal Cortex
LH	Lateral Habenula
LS	Lateral Septum
LTD	Long-Term Depression
LTP	Long-Term Potentiation
L-DOPA	L-dihydroxyphenylalanine
MAPK	Mitogen-Activated Protein Kinase
MEC	Medial Entorhinal Cortex
mGluR	Metabotropic Glutamate Receptor
Mg²⁺	Magnesium Ion
MOA	Mechanism Of Action
MPNs	Multipolar Neurones
NAc	Nucleus Accumbens
Na⁺	Sodium Ion
NMDA	N-Methyl-D-Aspartic Acid
NMDAR	NMDA Receptor
NO	Nitric Oxide
NOS	Nitric Oxide Synthase
OB	Olfactory Bulb
PB	Parabrachial Nuclei
PFC	Prefrontal Cortex
PI	Phosphatidylinositol
PIP2	Phosphatidylinositol-4;5-Bisphosphate
PIP3	Phosphatidylinositol-3;4;5-Triphosphate
PIP3K	Phosphatidylinositol-3-kinase
PI3K	Phosphoinositide 3-kinase
PKA	Protein Kinase A
PKC	Protein Kinase C
PLC	Phospholipase C
PPD	Paired-Pulse Depression
PPF	Paired-Pulse Facilitation
PPS	Paired-Pulse Stimulation
PPtase 1	Protein Phosphatase 1
PP2A	Protein Phosphatase 2A

preNMDAR	Presynaptic NMDAR
RAP 1	Member of the RAS Family of Small GTP-Binding Proteins
RMTg	Rostromedial Tegmental Nucleus
SN	Substantia Nigra
SNARE	Soluble NSF Attachment Protein Receptor
SNpc	Substantia Nigra pars compacta
SNRI	Selective Norepinephrine Reuptake Inhibitor
SSRI	Selective Serotonin Reuptake Inhibitor
STDP	Spike Timing-Dependent Plasticity
STP	Short-Term Potentiation
TH	Tyrosine Hydroxylase
t-LTD	Timing Dependent LTD
t-LTP	Timing Dependent LTP
TNF-α	Tumour Necrosis Factor-Alpha
VGCC	Voltage-Gated Calcium Channel
VMAT2	Vesicular Monoamine Transporter-2
VTA	Ventral Tegmental Area
WHO	World Health Organisation

1 Introduction

1.1 The Hippocampal Formation

1.1.1 Anatomy of the Hippocampal Formation

With its name derived from the Greek for seahorse, due to the similarities in their shape, the hippocampal formation (HF) is one of the most heavily researched areas of the brain, mostly due to its involvements in neurological diseases. Located in the medial temporal lobe, the anatomical structure of the HF was first depicted in the early 20th century by Santiago Cajal (Figure 1).

Cajal's drawings were significantly advanced for the time the work was published, showing both a theorised direction of synaptic impulses (represented by arrows in Figure 1) and also showing potential subregions of the HF (represented by letters in Figure 1). Despite Cajal publishing this diagram in 1909, it was not until over a decade later that it was first proven that nerve cells (a group of cells which include neurones) communicate through neurotransmitters in one given direction (Loewi, 1921). Similar to the depictions of neurotransmitter direction, the depictions of subregions in the HF were only theorised in Cajal's work in 1909, only to be further supported by later findings (O'Keefe and Nadel, 1978). Of the subregions which Cajal alluded to, subregions B, C and D were all identified as distinct subregions (the entorhinal cortex (EC), subiculum and the dentate gyrus (DG) respectively). There is however a great disparity in the literature as to what lies within the "hippocampal formation", with some authors stating that the EC lies outside of the HF, with others stating that it lies within the HF. Although this disparity exists, the EC shall be regarded as part of the HF henceforth. As well as the aforementioned subregions, the hippocampus (often referred to as the hippocampus proper when discussing the

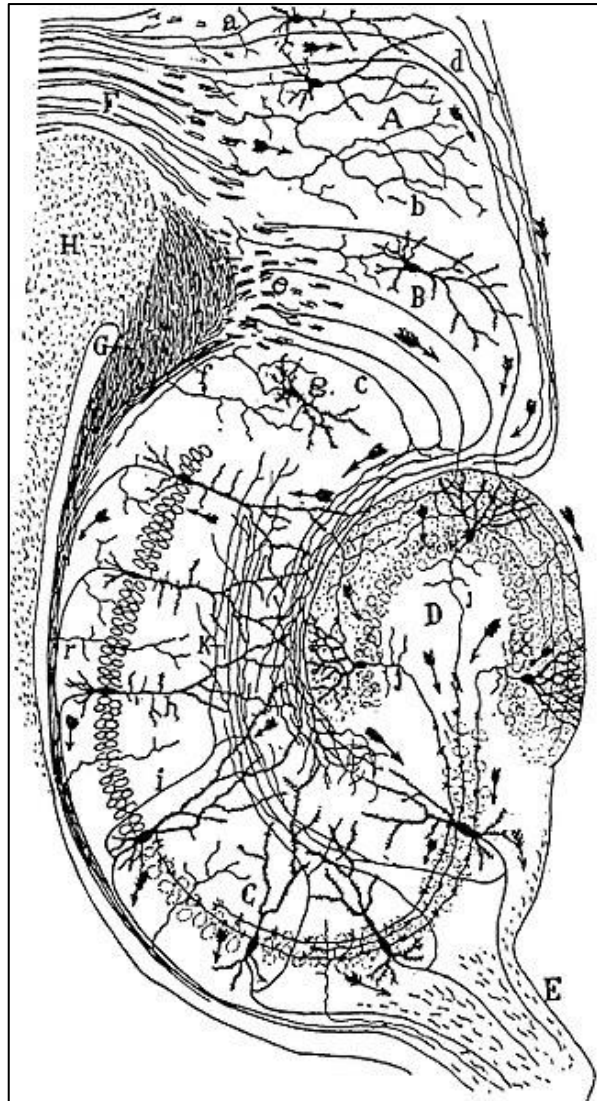


Figure 1 - A Sketch of the Rodent Hippocampal Formation. Santiago Ramón y Cajal's early sketch of the hippocampal formation in 1909. Later studies confirmed Cajal's work, identifying subregions which Cajal had previously alluded to. These subregions include the entorhinal cortex (B), the subiculum (C), the dentate gyrus (D), all of which are identified by their respective capital letter. The hippocampus proper, shown in the bottom left, is depicted by the two rows of ovals, running from CA1 at the top down to CA3. The image also shows Cajal's prediction of direction of information transmission (represented by arrows) (Cajal, 1909).

actual hippocampal structure as opposed to the HF) is comprised of four areas. As the hippocampus proper's layout somewhat resembles the horns of a ram, each of these areas are named Cornu Ammonis (CA) 1-4, after the Egyptian deity Amon (also referred to as Amun, Amen or Ammon) who was depicted as having ram's horns. CA1 lies at the top of the hippocampus, adjacent to the subiculum. CA2 is the smallest of the areas and lies caudal to CA1 (Anand and Dhikav, 2012). CA3 lies approximately at the apex of the curve, bordered rostrally by both CA2 and CA4 (left and right respectively in Figure 1). Finally, CA4 lies in between CA3 and the DG, subsequently CA4 is referred to as the deep, polymorphic layer of the DG (Blackstad, 1956). Each hippocampal area is rich in excitatory pyramidal neurones, which differentiates the hippocampus proper from other regions of the HF (Graves *et al.*, 2013). Despite this depiction being over 100 years old, there have been no significant changes in the anatomical interpretations of subregion layouts since the discovery of the hippocampus's CA1-3 regions (Lorente de Nò, 1934). Despite there being no significant recent changes to the subregions of the HF, our knowledge of the functions and role of each subunit continues to grow.

1.1.2 Projections of the Hippocampal Formation and Parahippocampal Cortices

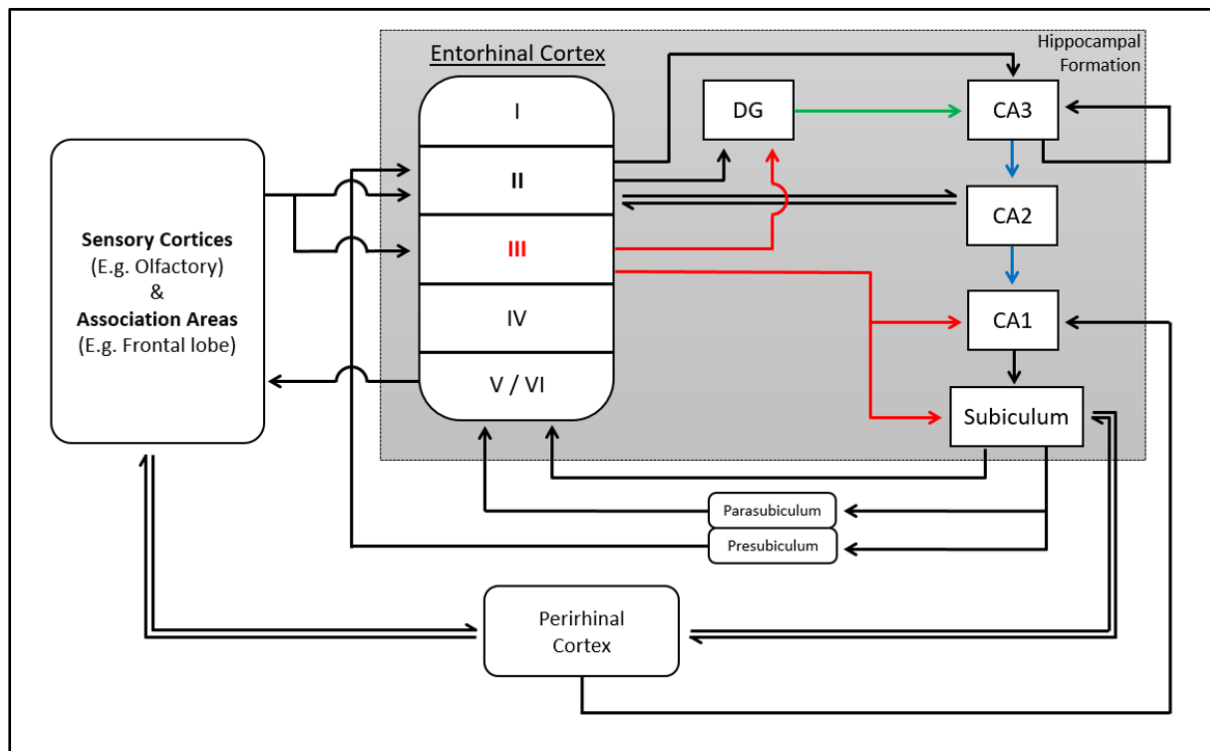


Figure 2 - Sensory Projections to and From the Entorhinal Cortex and Projections Within the Hippocampal Formation. A simplified overview of the connections within the hippocampal formation. This image can be divided into three subsections, sensory cortices and association areas, the parahippocampal formation (namely the perirhinal and pre- and parasubiculum) and the hippocampal formation. All non-spatial sensory information must pass through the entorhinal cortex before entering the hippocampal formation. In this image, black lines represent afferent projections, their arrows represent the direction of the projection and the projections with two half arrow heads show afferent and efferent projections between the two cortices. As well as these projections, green lines represent Mossy Fibre projections from the Dentate Gyrus (DG) to CA3, blue lines represent Schaffer collateral projections from CA3 to CA1 and red lines represent efferent projections from layer III of the entorhinal cortex. The information depicted in this image was derived from a variety of sources, including O'Mara, 2005; Llorens-Martán *et al.*, 2014; Xu *et al.*, 2016; Anand and Dhikav, 2012; Witter, 2007.

Figure 2 shows a simplified overview of the connections within the HF, including mossy fibre projections (connecting the granule cells of the DG to the pyramidal cells of CA3 (Henze *et al.*, 2000)) and Schaffer collateral pathway (a projection between hippocampal regions CA3 and CA1, a region in which long-term potentiation can be easily induced (Vasuta *et al.*, 2015)). CA2 plays a significant intermediate role within the Schaffer collateral pathway (Llorens-Martán *et al.*, 2014) as well as directly sending efferent and receiving afferent projections from layer II of the LEC through the disynaptic cortico-hippocampal loop (Chevalyere and Siegelbaum, 2010; Rowland *et al.*, 2013). As well as these projections, the HF also receives glutamatergic projections from the basolateral amygdala, which is mediated by the EC (Anacker and Hen, 2017; Mandyam, 2013).

1.1.3 The Entorhinal Cortex

1.1.3.1 The Medial Entorhinal Cortex and The Lateral Entorhinal Cortex

The most distal region of the HF, the EC (Brodman area 28) is divided into two distinct subregions, the lateral entorhinal cortex (LEC, Brodman area 28a) and the medial entorhinal cortex (MEC, Brodman area 28b). The latter of the two subregions is somewhat entirely independent from its counterpart, as the MEC has been shown to be implicated in numerous independent processes. These processes include spatial processing and path integration in spatial cognition (Van Cauter *et al.*, 2012); projecting cortical inputs to both the hippocampus (proximal CA1) and the molecular layer of the DG (Knierim *et al.*, 2013), playing a role in episodic memory (Lipton and Eichenbaum, 2008) as well as receiving inputs from the visual cortex via the postrhinal cortex (Agster and Burwell, 2013).

Similarly to the medial division of the EC, the lateral division forms afferent projections to both CA1 and the DG, where layer II of both divisions project to CA3 of the hippocampus through the perforant pathway (van Groen *et al.*, 2003). However, despite these few similarities there are still numerous distinct differences between the two regions. Although both the MEC and the LEC project to CA1, it has been shown that the MEC tends to target the region of CA1 close to CA2 (CA1c) whereas the LEC tends to target the region of CA1 close to the subiculum (CA1a, Masurkar *et al.*, 2017). Furthermore, both project to the DG, however the MEC projects to the middle third of the molecular layer (as was aforementioned), however the LEC projects to the outer third layer (Amaral *et al.*, 2008). Finally, although both the LEC and the MEC receive rich afferent projections from olfactory areas, the unimodal input is approximately 1.5 times greater in the LEC than the MEC (approximately 75% and 50% respectively, Burwell and Amaral, 1998). Functionally, the LEC differs from the MEC, with the MEC conveying spatial information to the hippocampus and the LEC conveying non-spatial information. This is commonly referred to as the “where versus what” model, with the MEC conveying “where” and the LEC conveying “what” (Knierim *et al.*, 2013).

1.1.3.2 The Role of the EC in the Formation of Sensory Memory

As stated in the preceding chapter, the main function of the lateral division of the EC is to relay non-spatial information from sensory cortices to the hippocampus. Of the traditional

senses (not including the somatic senses), the EC receives significant efferent projections from three of the five cortices: Olfactory bulb (OB); auditory cortex and the occipital lobe (for smell, auditory and visual senses respectively). Of these senses, the relationship between the LEC and the olfactory system is the most documented of the three, with the term “entorhinal” deriving from the Greek terms “Ento” and “Rhinal”, meaning inside and nose respectively (Witter *et al.*, 2017). First identified in the late 20th century, the proposed mechanism for the transfer of information is comparable to that shown in Figure 2.

As mentioned in the previous chapter, the OB projects a unimodal input to the EC via the piriform cortex, a projection which has been well reported in rodents and monkeys (Burwell and Amaral, 1998; Amaral *et al.*, 1987 respectively). Although this projection has also been reported in humans, with the piriform cortex receiving the largest bulbar projection (Zhou *et al.*, 2019) and subsequently projecting to both the MEC and the LEC, fewer publications have been published on this projection in humans than in other mammals (Vismer *et al.*, 2015). Upon innervation, the EC then projects to various regions of the hippocampus (Figure 2; Vanderwolf, 1992), with CA1 of the hippocampus projecting back to the EC before the EC then further projects back to the OB in adult mice (Van Groen and Wyss, 1990). It can therefore be concluded that the OB and the hippocampus are directly linked to one another, with the EC playing an intermediate role in their connection.

The formation of auditory memory follows a similar unimodal path to the formation of olfactory memory, innervating the piriform cortex (Engelien *et al.*, 2005) before following the same path through the hippocampus as was aforementioned and shown in Figure 2 (O’Mara, 2005). Furthermore, both the perirhinal cortex and (more importantly) a dorsal lateral strip of layer V neurones of the EC both project back to the auditory cortex (Insausti *et al.*, 1987; Li *et al.*, 2013). Similarly to the formation of auditory memory, the formation of visual memory is governed by the posterior parahippocampal cortex (Baldassano *et al.*, 2013), before following the same path through the hippocampus as the previously mentioned senses (Suzuki and Amaral, 1994). Of these afferent sensory projections to the LEC and the MEC, the projection from the olfactory area is the strongest, followed by the projection from the visual areas with the projection from the auditory areas providing the weakest projection (Burwell and Amaral, 1998; Insausti *et al.*, 1987).

1.1.3.3 Function and Anatomy of the LEC

As well as playing a pivotal role in the aforementioned formation of olfactory, visual and auditory memories, the LEC is also heavily implicated in both the polysynaptic pathway and the direct intra-hippocampal pathway in memory formation (Anand and Dhikav, 2012). In the polysynaptic pathway, afferent information arrives at layers II and III of the EC, before being projected throughout various subregions of the HF and finally terminating at the subiculum. This pathway is implicated in the formation of semantic memory (memory which is acquired through learning outside of personal experience) and can be divided into lateral perforant pathway and medial perforant pathway depending on where the fibres arose from in the EC (Figure 2; Petersen *et al.*, 2013). The direct intra-hippocampal pathway however is implicated

in spatial and episodic memory, memory which is acquired through personal experience. This pathway begins at the temporal association cortex before entering the HF. Once there, layer III of the EC will project to CA1 and then the subiculum, before either returning to the EC or leaving the HF via the alveus and the fimbria (Campbell and Macqueen, 2004). If the signal left the HF, it then terminates in the prefrontal cortex (PFC), inferior temporal cortex or the temporal pole (Anand and Dhikav, 2012). In both of these pathways, the LEC conveys efferent information from sensory cortices, before forming afferent projections to the DG and CA1 respectively (Morgado-Bernal, 2011). Although the LEC is predominantly implicated in non-spatial inputs to the hippocampus, lesions in the LEC reduce the conveyance of spatial information, indicating that the LEC plays some role in conveying both spatial and non-spatial information (Hunsaker *et al.*, 2013). The cell types and projections of both the MEC and LEC are somewhat undistinguishable within most animals, however they are significantly more distinguishable in rats than in any other mammals (Insausti, 1993).

Anatomically speaking, The LEC itself is comprised of six distinguishable layers, with each layer showing a diverse interconnectivity (most notably within layers I-III), with almost every layer forming projections to all other layers (Figure 3).

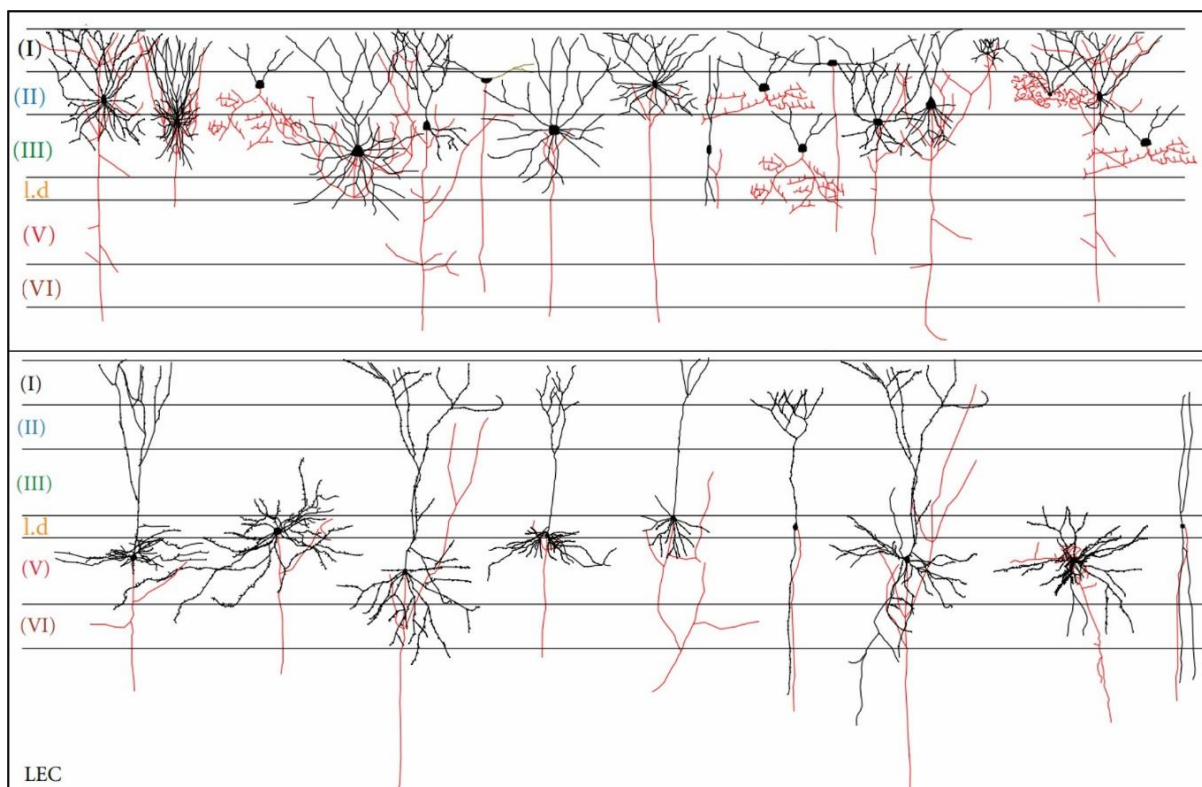


Figure 3 - Interconnectivity Within the Lateral Entorhinal Cortex. Different cell types in different layers of the lateral entorhinal cortex (LEC) and their interconnectivity throughout the subregion. The image depicts two types of neuropil, dendrites (shown as black lines, with the dots representing dendritic spines) and axons (red). The upper portion of the image shows a diverse interconnectivity within layers I-III, with layer I receiving axonal and dendritic projections from all other layers. The lower image shows neurones from the deeper layers V and VI and their projections throughout the LEC. This image was directly adapted from Canto's work (Canto *et al.*, 2008), which is licensed under the Creative Commons Attribution 3.0 Unported License.

The role of layer I of the LEC (the layer which lies most superficial within this region) is mostly for receiving sensory information and infrastructural innervation, where both projections from other layers of the LEC (Figure 3) and afferent projections from sensory cortices terminate (Wouterlood *et al.*, 1985). It has been documented extensively that layer I of the LEC receives afferent projections from both the OB and the olfactory cortex (Habets *et al.*, 1980; Room *et al.*, 1984; Wouterlood *et al.*, 1985), although these projections have been shown to terminate in the deeper lying layers II and III as well (Wouterlood and Nederlof, 1983). Besides from these projections from external cortices, Figure 3 also shows that layer I receives axonal and dendritic projections from all other layers within the LEC. This provides the LEC with a feedback mechanism, as the inhibitory neurones in the deep layers of the LEC receive inputs from other regions of the hippocampus (Figure 2), subsequently depressing afferent projections to layer I (Ohara *et al.*, 2018). As this layer contains few cell bodies and a plethora of myelinated projections, this region is easily distinguishable from deeper layers as layer I is substantially whiter in appearance (Ohara *et al.*, 2009).

Unlike layer I, layer II of the LEC contains a vast array of cell bodies, but similarly to layer I, contains a vast array of projections, a combination which results in a densely packed layer (Figure 3; Canto *et al.*, 2008). Layer II of the LEC also contains a large number of afferent and efferent projections, both from within and outside of the LEC (Figure 2; Witter *et al.*, 2017). Figure 3 shows that layer II of the LEC may not receive inputs from deep layers of the LEC but receives extensive inputs from the superficial layers I and III. Multipolar neurones (MPNs) with laterally extending dendritic trees (one of the three subtypes of MPNs) from both the deep region of layer I and the superficial region of layer III were shown to project into layer II of the ventrolateral LEC (Wouterlood *et al.*, 2000). Externally to the EC, layer II of the LEC receives cortical projections from both the parahippocampal formation and the presubiculum (Figure 2). Layers II and III of the LEC receive cortical projections from the parahippocampal cortex through two pathways, both of which terminate in the hippocampus. However, this projection was shown in rhesus monkeys and is yet to be shown in rodents (Witter *et al.*, 2000). Layer II also receives projections from the presubiculum, an innervation which has been described as dense and extensive (Caballero-Bleda and Witter, 1993). Primarily, layer II of the LEC projects to the DG and CA2/CA3 of the hippocampus through the perforant pathway (Figure 2; Suh *et al.*, 2011; Tamamaki and Nojyo, 1993). Layer II also directly projects to CA2, in conjunction with CA1, through the disynaptic cortico-hippocampal loop (Chevalleyre and Siegelbaum, 2010). A projection from this layer (in conjunction with layer III) back to the parahippocampal cortex has been identified, however this projection has only been identified in humans and is yet to be identified in rodents (Witter *et al.*, 2000).

Similarly to layer II of the LEC, layer III contains a vast array of cell bodies and projections, however this layer receives projections from both deeper layers V and VI as well as the superficial layer II, as is characterised in Figure 3. Layer III also forms projections with other regions of the HF, projecting to the DG, CA1 and the subiculum via the temporoammonic pathway (Figure 2; Ito and Schuman, 2011). Besides from its projections, layer III also receives afferent projections from the parahippocampal cortex, as was

mentioned in the preceding chapter. Another of these inputs to layer III from external to the HF comes from the amygdala, however this has been documented in the MEC and not in the LEC (Pikkarainen *et al.*, 1999). Despite this, layer III has been described as “largely terra incognita” when compared to layers II and V, meaning the region still remains still largely unmapped in comparison (Witter *et al.*, 2017).

Layer IV (also referred to as lamina dissecans, Ld) lies between layers III and V, receiving projections from all other layer’s besides from the superficial layer I (Figure 3). Unlike the other layers in the LEC however, this layer is predominantly devoid of cell bodies, with the name lamina dissecans meaning “a thin layer of separation” (Braak and Braak, 1992). Layer IV of the LEC is substantially less distinguishable than layer IV of the MEC, although there is still evidence showing that the Ld is present in both (Burwell and Agster, 2008).

The deep layers of the LEC are comprised of two layers, V and VI. The more superficial of these deep layers, layer V, can be subdivided into two distinct subregions, Va and Vb, with Va lying superior to Vb. Although layer V receives limited projections from superficial layers of the EC (with only layer III and potentially layer II innervating layer V), layer V projects extensively to both extremities of the EC, innervating layers I and VI, with some axons reaching the pial surface in the case of the former (Figure 3; Canto *et al.*, 2008). These projections come from large MPNs, with are rich in the inhibitory neurotransmitter gamma aminobutyric acid (GABA), indicating that layer V provides an inhibitory role for the superficial layers of the LEC (Miettinen *et al.*, 1997). Functionally, layer Va returns projections back to the cortical and subcortical structures, whereas layer Vb receives cortical projections from the subiculum and the parasubiculum (Figure 2; Ohara *et al.*, 2018). Layer Vb also receives projections from the retrosplenial cortex, the region where the polysynaptic pathway of memory formation terminates (Czajkowski *et al.*, 2013). Functionally, layer Vb receives cortical projections from the subiculum and the parasubiculum, whereas layer Va sends cortical projections back to the cortical and subcortical structures upon innervation (Figure 2; Ohara *et al.*, 2018).

The deepest layer in the LEC, layer VI, is similar to the most superficial layer in that it is identifiable by its high concentration of white matter, indicating the high number of neuropil present within the region. The axons projecting into this region stem from hippocampal/thalamic roots, receiving a rich innervation from CA1 and the subiculum (Figure 2). Cells in this layer project their axons both back to sensory cortices and also throughout the EC, through the deep layers and rarely projecting to layer III (Lingenhöhl and Finch, 1991; Canto *et al.*, 2008). However, the reports which describe the characteristics of layer VI does not distinguish whether these come from the lateral nor the medial division of the EC.

With all this information in mind, it can therefore be concluded that afferent nerve fibres from a sensory cortex can innervate the superficial layers of the LEC, which in turn will innervate the hippocampus through the polysynaptic pathway or the intra-hippocampal pathway (Uva and de Curtis, 2005; Suh *et al.*, 2011; Aggleton *et al.*, 2010). A cascade of innervations throughout the hippocampus culminate in the activation of the subiculum, which in turn activates the deep layers of the LEC (layers V and VI). Excitatory neurones in the

deep layers then feedback processed information throughout the cortex, whereas inhibitory neurones inhibit the activity of superficial layers, suppressing the aforementioned pathways (Miettinen *et al.*, 1997).

1.1.3.4 Neurotransmitters in the LEC

Although preliminary studies in the late 20th century concluded that neurones in the LEC communicate entirely through the neurotransmitter glutamate (Oleskevich *et al.*, 1989; Umbriaco *et al.*, 1995), recent studies have begun to show that other neurotransmitters are in fact present within the LEC. One study showed that the deep layers of the EC (notably layers V and VI) were rich in inhibitory GABAergic neurones, as was mentioned in the previous paragraph (Miettinen *et al.*, 1997). Besides from these predominant neurotransmitters, mRNA expression analysis showed that two serotonin (5-hydroxytryptamine, 5-HT) receptor subtypes, 5-HT_{1C} and 5-HT_{2A} are heavily abundant within the LEC, with 5-HT_{1A}, 5-HT_{1D}, 5-HT_{1E}, 5-HT₃ and 5-HT₆ also being expressed (Wright *et al.*, 1995; Lei, 2012). Although they are all serotonin receptors, each have been shown to induce different responses: 5-HT_{1A} plays a significant role in spatial memory formation (Miheau and Barbara, 1999); 5-HT_{2A} enhances GABAergic neurotransmitter release from deep layer MPNs (Deng and Lei, 2008) and 5-HT₃ inhibits acetylcholine release (Barnes *et al.*, 1989). Although the other receptors have been identified within the LEC, their roles are still yet to be determined (Lei, 2012). The presence and roles of the different 5-HT receptors in the LEC indicates that there are also non-glutamatergic modes of transmission within the region. These receptors stem from afferent serotonergic projections, which originate from the raphe nuclei (Witter *et al.*, 1989). Finally, staining for the rate-limiting enzyme in catecholamine synthesis, tyrosine hydroxylase, showed that superficial layers in the LEC contains rich pools of the neurotransmitter dopamine.

1.2 Dopamine

1.2.1 Introduction to Dopamine

Dopamine (DA) is a neurotransmitter of the catecholamine family, acting as both a cell-cell messenger within the CNS and a hormone within the PNS (Lot, 1993). Within the CNS however, DA is released upon activation of the reward system, primitively as a result of drinking, eating or copulating. The reward system (also referred to as the mesolimbic pathway) originates in the VTA in the midbrain, before projecting to a number of regions in the neocortex. The largest of these projections, the only greater projection than that to the LEC, projects directly to the PFC, the region of the brain associated with intelligence and language to name but two of its functions (Drewe, 1974; Gabrieli *et al.*, 1998; Oades and Halliday, 1987). The VTA also projects extensively to the nucleus accumbens (NAc), the region of the brain associated with reward and subsequently addiction (Wise, 2006). As well as the PFC and the NAc, cells of the VTA project into the limbic system, innervating both the amygdala and the HF, subsequently projecting to the LEC (Tassin *et al.*, 1989). The mesolimbic pathway in a rodent brain is shown in Figure 4 (Swanson, 1982).

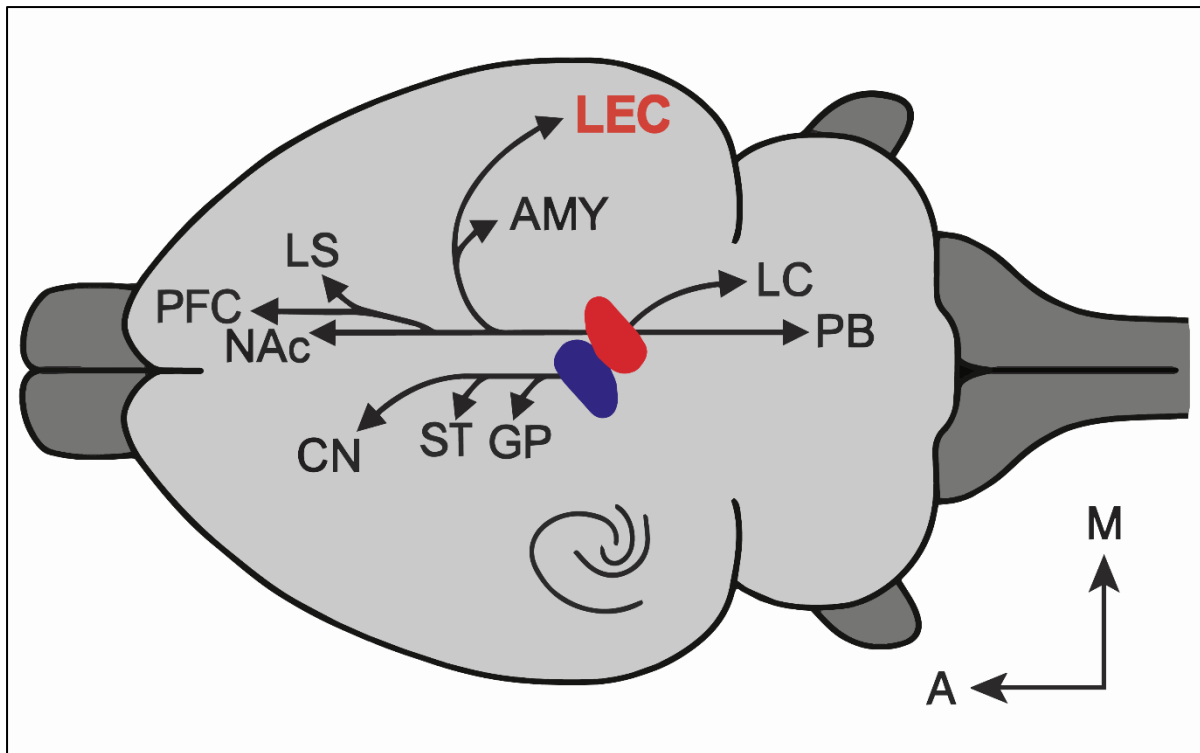


Figure 4 - The Projection of Dopaminergic Neurones From the Ventral Tegmental Area Throughout a Rodent Brain. A transverse section through a rodent brain, identifying the ventral tegmental area (VTA, red) and the dopaminergic projections this region produces. Although it is not identified specifically, the projections made in the mesolimbic pathway are identified, with the VTA projecting to the nucleus accumbens (NAc), the amygdala (AMY) and the lateral entorhinal cortex (LEC, a subregion of the hippocampal formation). Also shown but not directly stated is the mesocorticolimbic pathway, which connects the VTA to the prefrontal cortex (PFC) and the lateral septum (LS). Other projections shown includes a projection from the VTA to both the parabrachial nuclei (PB) and the locus coeruleus (LC). Although all these aforementioned regions have been identified, they are not part of a definitive pathway, however dopaminergic neurones still directly or indirectly innervate these regions (Christoph *et al.*, 1986; Coizet *et al.*, 2010; Deutch *et al.*, 1986). The image also identifies the substantia nigra pars compacta (SNpc, blue) which projects to the globus pallidus (GP), the striatum (ST) and the caudate nucleus (CN) through the nigrostriatal pathway. The scale shown in the bottom right identifies the anatomical orientation on which the section lies, with A denoting anterior (i.e. the NAc lies anterior to the VTA) and M denoting medial (i.e. the LEC lies medial to the VTA). The information depicted in this image was refined from Swanson's 1982 work to match this study (Swanson, 1982).

DA is also the neurotransmitter released in the mesocortical pathway, which, like the mesolimbic pathway, is shown but not specifically identified from its counterpart (Figure 4). The mesocortical pathway follows a similar initial path to the mesolimbic pathway, however this pathway projects to the aforementioned NAc, the lateral septum (LS) and the prefrontal cortex (PFC), all of which are regions in the frontal lobe. Where the mesolimbic pathway is implicated in reward and addiction, the mesocortical pathway's projection to the neocortex associates this pathway with cognitive function (Money and Stanwood, 2013). Besides from these two pathways, DA is the primary neurotransmitter involved in the nigrostriatal and tubular infundibular pathway. The former pathway connects dopaminergic neurones in the excitatory medial subregion of the substantia nigra (SN), the substantia nigra pars compacta (SNpc), with the striatum (ST), projecting directly to the subthalamic nucleus, the globus pallidus (GP) and the caudate nucleus (CN), as shown in Figure 4 (Prensa and Parent, 2001).

This pathway, unlike the two aforementioned pathways, is implicated in motor and behavioural motivation (Gerfen and Wilson, 1996). The final dopaminergic pathway, the tuberoinfundibular (also referred to as the tuberohypophyseal) pathway, is not shown in Figure 4, as this pathway originates in the ventral hypothalamus before projecting to the medial eminence and the pituitary gland (Rang *et al.*, 2019). As well as these pathways, the VTA also directly projects to both the parabrachial nuclei (PB) and the locus coeruleus (LC) of the brainstem through no definitive pathway (Figure 4). The dopaminergic projection from A10 of the VTA to the brainstem yields varying results, as DA suppresses PB activity but stimulates LC activity (Chen *et al.*, 1999; Deutch *et al.*, 1986). Stimulation of the LC also promotes cellular survival of dopaminergic neurones, suggesting at a possible adaptability of this region (Berglöf and Strömberg, 2009). The PB also receives afferent nociceptive projections from the spinal cord, possibly hinting that the PB may act as one of the intermediate steps between the peripheral nervous system (PNS) and dopaminergic projections in the central nervous system (CNS) (Coizet *et al.*, 2010).

Although DA remains excitatory throughout the cortex, indirect dopaminergic innervation of the nigrostriatal pathway, subsequently the lateral habenula (LH) and subsequently the rostromedial tegmental nucleus (RMTg), is shown to suppress VTA activity through the reward prediction error circuit (Watabe-Uchida, Eshel and Uchida, 2017). Figure 4 shows this direct projection between the SNpc and the GP internal segment, with both this and the striatum subsequently innervating the LH (Bourdy and Barrot, 2012). Upon innervation, the LH then projects to the GABA rich RMTg, which subsequently extensively suppresses the activity of both the VTA and the SN by approximately 90% (Christoph *et al.*, 1986). DA also projects to the thalamus (not shown in Figure 4); however this projection is less extensive in the rat than in other mammals (Garcia-Cabezas *et al.*, 2008). In this region, DA appears to have a positive refinement on movement, as reduced dopaminergic inputs to the basal ganglia results in motor complications like that seen in Parkinson's disease (Stoessl *et al.*, 2014).

As DA is a catecholamine (as are the DA derivatives noradrenaline and adrenaline), DA is comprised of a catechol group (also referred to as a benzenediol, 1,2 – dihydroxybenzene) and an ethylamine positioned on carbon 4, a structure which is shown in Figure 5. This structure was first identified in 1910 (as mentioned in Hornykiewicz, 2002), although it was believed that DA was purely a precursor for noradrenaline until 1957, where it was later determined that DA was itself a neurotransmitter (Carlsson, 1993).

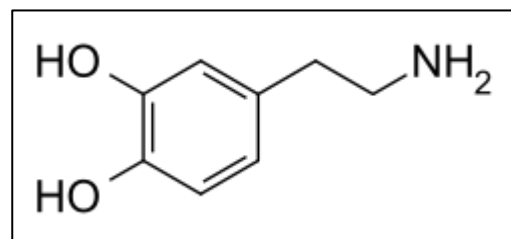


Figure 5 - The Chemical Structure of Dopamine. The structure of the neurotransmitter is comprised of two regions, an ethylamine (located on carbon-4 from the benzene ring, right) and a benzenediol (benzene ring with two hydroxyl groups, left).

1.2.2 Dopamine Receptors

1.2.2.1 The D1 Receptor Family

The D1 family of receptors (containing receptors D_{1A} and D₅ (the latter also referred to as D_{1B})) were first identified by their characteristic of activating adenylyl cyclase (AC) to raise intracellular cyclic 3'5' adenosine monophosphate (cAMP) levels (Andersen *et al.*, 1990). D1-like receptors do this through a cascade reaction upon activation, with D1 receptors solely activating AC through g-protein activation, whereas D5 receptors activate AC, PIP2 (phosphatidylinositol-4;5-bisphosphate) and PLC (phospholipase) all through g-protein activation (Figure 6, Hansen and Manahan-Vaughan, 2012; Sibley *et al.*, 1993). Both of these cascades however culminate in the activation of cAMP response element-binding protein (CREB), a family of transcription factors which bind to cAMP responsive element (CRE) sites on DNA (Silva *et al.*, 1998). Binding of CREB to their respective CRE sites results in the expression of various genes. Some of these genes expressed by CREB include: Arc (Activity-regulated cytoskeleton-associated protein, an ever-present protein in plasticity which alters synaptic strength (Korb and Finkbeiner, 2011)); c-Fos (an oncogene and an immediate early-gene which too is associated with long-term potentiation (Kang *et al.*, 2000)); EGR1 (Early growth response protein 1, which, similarly to c-Fos, is an immediate early-gene which regulates synaptic plasticity (Duclot and Kabbaj, 2017)) and BDNF (Brain derived neurotrophic factor, a protein which too is heavily implicated in cellular plasticity (Leal *et al.*, 2017)) to name a few (Nishi *et al.*, 2011). All of the aforementioned genes are expressed upon the binding of CREB to DNA and are all implicated in long-term neuronal plasticity, indicating that D1-like activation elicits long lasting effects on the neurone.

As well as the cascade reactions that D1-like receptors initiate, Figure 6 also shows the amino acid sequences of both D₁ and D₅ and their relative topographical arrangement on the neuronal membrane (Sibley *et al.*, 1993). The D₁ receptor is comprised of a short amino-acid chain at the N-terminus (approximately 25 residues in length), seven transmembranous domains (culminating in three extracellular and three intracellular loops) before a long amino-acid chain at the C-terminal (Figure 6, upper left). This COOH region in D1-like receptors is significantly larger than in D2-like receptors, with the C-terminal having approximately seven times as many residues in D1-like receptors compared to D2-like receptors (Missale *et al.*, 1998).

The largest of the DA receptors with 475 residues in rats (Sibley *et al.*, 1993), D₅ receptor possesses a very similar structure to D₁, with a short N-terminal, an elongated C-terminal and seven transmembranous regions (also with three extracellular and three intracellular loops, as is shown in Figure 6, upper right). The extracellular N-terminal and the second extracellular loop both contain a CHO group from the amino acid asparagine, an N-Glycosylation site, which is crucial in membrane localisation for D₅ receptors (Karpa *et al.*, 1999). Despite these similarities in overall structure, D₁ and D₅ have extensive differences in their amino acid residues, showing only an approximate 50% homology in their amino acids (Sunahara *et al.*, 1991).

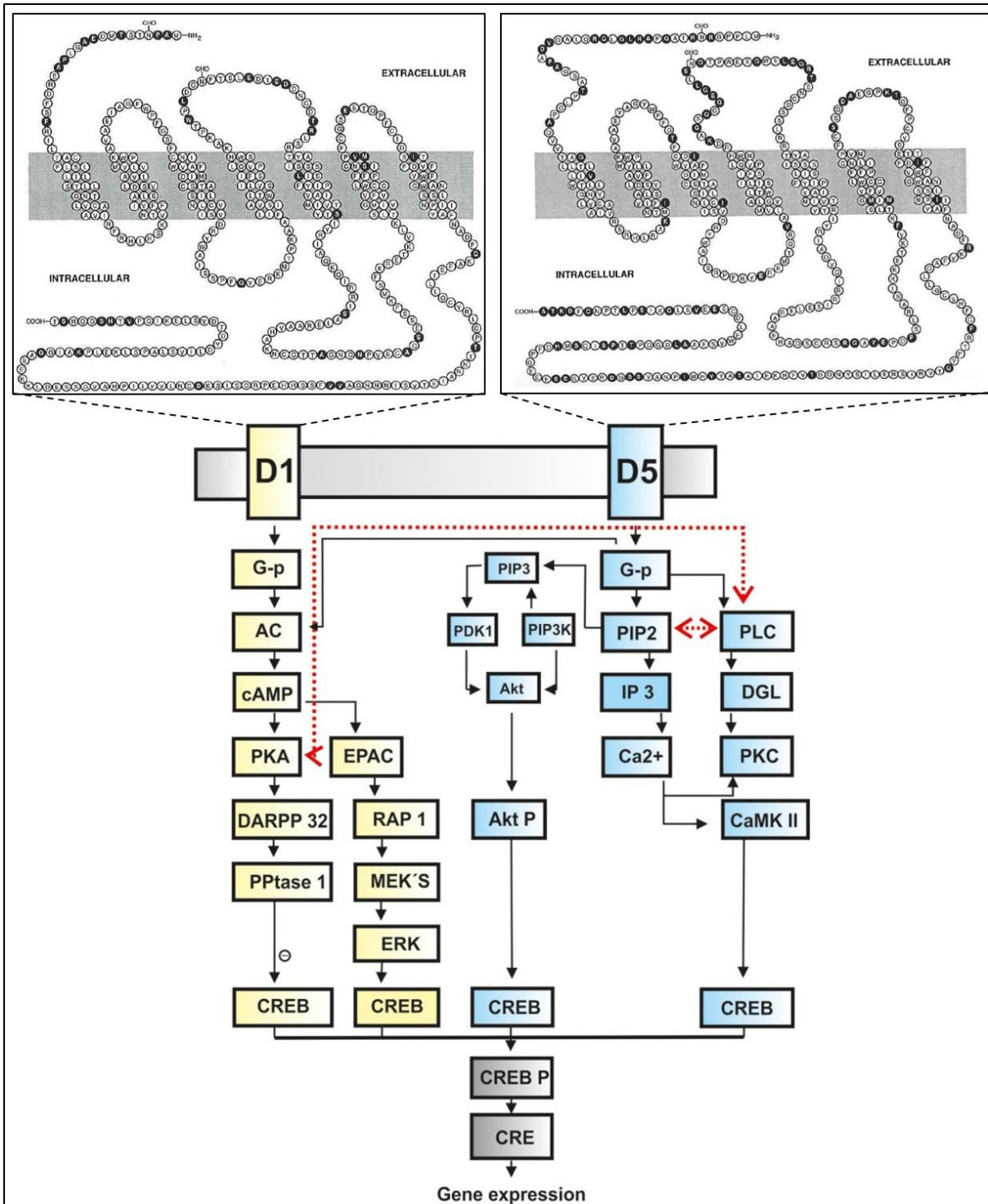


Figure 6 - The Amino Acid Structure and the Subsequent Signalling Cascade D₁ and D₅ Receptors. The topographical organisation and amino acid structure of the D₁-like receptors, D₁ and D₅, are shown in the upper left and upper right respectively. The two extracellular CHO groups on asparagine residues, a region which is susceptible to N-Glycosylation, is also highlighted. The lower region of the image shows the cascade reaction caused by D₁-like receptor activation, with the yellow boxes indicating intermediates in D₁ signalling and blue boxes indicating intermediates in D₅ signalling. A red arrow is used to indicate a communicative link between the two cascades, with and a negative symbol used to indicate a suppressive effect. Abbreviations include (when read from top to bottom, left then right): G-p (G protein); AC (Adenyl cyclase); cAMP (Cyclic 3'5' adenosine monophosphate); PKA (Protein kinase A); EPAC (Exchange protein activated by cAMP); DARPP 32 (Phosphoprotein of 32 kDa); RAP 1 (Member of the RAS family of small GTP-binding proteins); PPTase 1 (Protein phosphatase 1); MEK's (Mitogen-activated kinases); ERK (Extracellular signal-related kinase); PIP₃ (Phosphatidylinositol-3;4;5-trisphosphate); PDK1 (Phosphoinositide-dependent kinase-1); PIP₃K (Phosphatidylinositol-3-kinase); PIP₂

(Phosphatidylinositol-4;5-Bisphosphate); PLC (Phospholipase C); IP3 (Inositol trisphosphate); DGL (Diacylglycerol); PKC (Protein kinase C); Akt P (Phosphorylated Akt); CaMK II (Calcium-calmodulin-dependent protein kinase type II); CREB (cAMP response element-binding protein); CREB P (Phosphorylated CREB); CRE (cAMP response element). The amino acid structures and topography of both D₁ and D₅ were taken directly from International Review of Neurobiology (Sibley *et al.*, 1993, with permission) and the image depicting the cascade reaction was taken directly from Cerebral Cortex (Hansen and Manahan-Vaughan, 2012, with permission). Although the cascade reaction image was depicted in Hansen and Manahan-Vaughan's paper, the information was derived from other sources (Undieh, 2010; Beaulieu and Gainetdinov, 2011).

1.2.2.2 The D2 Receptor Family

Unlike D1-like receptors, the D2 family (comprised of D₂, D₃ and D₄ receptors) inhibit both AC activation and reduce intracellular Akt levels, reducing neuronal hyperexcitability (Figure 7; Bozzi and Borrelli, 2013). Reduced intracellular cAMP and Akt results in a reduced activation of the transcription factor CREB, which subsequently reduces gene expression through CRE. The reduction of intracellular Akt however results in an increase in cellular glycogen synthase kinase 3 β (GSK-3 β), an enzyme that both promotes STAT transcription factors (Beurel and Jope, 2008) and shows implications in cellular apoptosis (Ding *et al.*, 2007) but is downregulated by Akt under physiological conditions. This increase in intracellular GSK-3 β results in an increased expression of β -Catenin from the nucleus, as GSK-3 β directly phosphorylates β -Catenin on three separate residues, which subsequently activates the protein (Beurel *et al.*, 2015). This activation results in a promotion of cellular survival by maintaining the transmembrane protein N-cadherin between neurones and regulating radial glia integrity, a precursor cell for dopaminergic neurones (Tang *et al.*, 2009).

The structures of all three D2-like receptors are remarkably similar, each containing a short N-terminus, seven transmembranous domains and a very short c-terminus (Figure 7, upper). One key characteristic of these D2-like receptors is their elongated intracellular loop between the 5th and 6th transmembranous loop. This is also where the structures differs the most between receptors, with each of the three loops consisting of almost entirely different residues with D₄ containing the shortest loop of the three. This short nature of the loop on D₄ is somewhat shown by the interactions of the receptors, with D₂ and D₃ receptors interacting with the scaffolding proteins calcium-calmodulin-dependent protein kinase type II (CaMKII) and β -arrestin respectively, however D₄ shows no interaction with any other scaffolding protein (Figure 7).

The D₂ receptor exists as two isoforms, D_{2S} D_{2L} (short DA D₂ receptor and long DA D₂ receptor respectively), with the longer isoform containing 29 additional amino acids when compared to the shorter isoform (Dal Toso *et al.*, 1989). Although these isoforms each have different qualities and a majority of functions remain the same (such as lowering AC activity to lower intracellular cAMP), there are still some minor differences between the two (Lindgren *et al.*, 2003). As these isoforms differ in their third intracellular loop (the longest of the three), the N-terminal remains homologous between the two isoforms. This means that the three N-glycosylation sites on the N-terminal remain identical on all variants of D₂, which affect calnexin interaction and cell surface expression of the DA receptor (Free *et al.*, 2007; Min *et al.*, 2015). Figure 7 also shows that β -arrestin and protein phosphatase 2A (PP2A) act

as scaffolding proteins, allowing D₂ to form a G protein like response upon receptor activation (Beaulieu *et al.*, 2005). The role that β -arrestin plays as a scaffolding protein is shown through its inhibition using Barbadin, a new potent drug which blocks prototypical β 2-adrenergic, V2-vasopressin and angiotensin-II type-1 receptor endocytosis (Beautrait *et al.*, 2017).

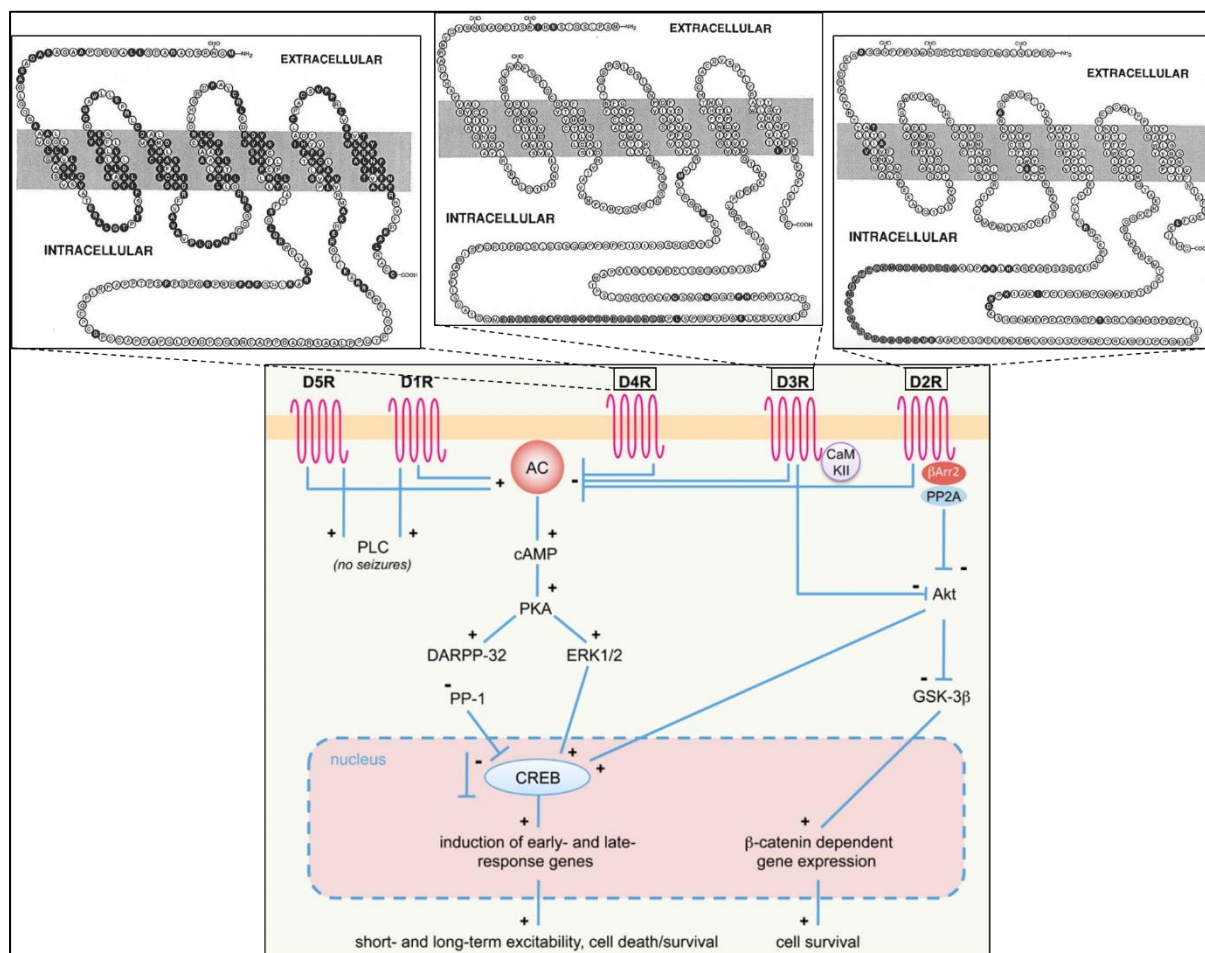


Figure 7 - Signal Cascade of D2-Like Receptors Alongside D1-Like Receptors and the Amino Acid Structure of D₂, D₃ and D₄ Receptors. The topographical organisation and amino acid structure of the D2-like receptors, D₂, D₃ and D₄, are shown in the upper right, upper middle and upper left respectively. The extracellular CHO groups on asparagine residues, a region which is susceptible to N-Glycosylation, is also highlighted. The lower region of the image shows a comparison in the cascade reaction from both D1-like receptors (upper left of the lower image) and D2-like receptors (upper right of the lower image). Positive (+) and negative (-) symbols are used to identify facilitative and suppressive projections respectively. Abbreviations include (when read from top to bottom, left then right): AC (Adenylyl cyclase); PLC (Phospholipase C); cAMP (Cyclic 3'5' adenosine monophosphate); PKA (Protein kinase A); DARPP-32 (Phosphoprotein of 32 kDa); ERK 1/2 (Extracellular signal-related kinase 1/2); PP-1 (Protein phosphatase 1); CaMKII (Calcium-calmodulin-dependent protein kinase type II); β Arr2 (β -arrestin 2); PP2A (Protein phosphatase 2A); GSK-3 β (Glycogen synthase kinase 3 β); CREB (cAMP response element-binding protein). The amino acid structures and topography of D₂, D₃ and D₄ were taken directly from International Review of Neurobiology (Sibley *et al.*, 1993, with permission). Likewise, the image depicting the cascade reaction was taken directly from Frontiers in Cellular Neuroscience (Bozzi and Borrelli, 2013), which is licensed under the Creative Commons Attribution 3.0 Unported License.

The amino acid and topographical structure of D₃ is very similar to that of D₂, in fact the two have approximately a 97% homology to one another (Sibley *et al.*, 1993). One difference however is in the N-glycosylation sites on the N-termini, as D₂ has three binding sites whereas D₃ only has two (with a third appearing in the first extracellular loop and a fourth in the second

extracellular loop for D₃ receptors), however the role of these glycosylation sites on these extracellular loops are yet to be fully identified (Min *et al.*, 2015). Unlike the aforementioned D₂-like receptors, D₄ contains a significantly shorter tertiary intracellular loop, yielding a receptor 30 amino-acids shorter than D_{2S} with only a 41 and 39% homology to D₂ and D₃ receptors respectively (Sibley *et al.*, 1993). Despite the low homology and significant structural difference, D₄ receptors still possess similar properties to the other D₂-like receptors, also reducing hyperexcitability by mediating AC activity and lowering cAMP levels.

1.2.2.3 Dopamine Receptor Pharmacology

Even thirty years before the discovery of the D₂ receptor in the 1980's, there were drugs that targeted DA receptors to treat psychosis (Ban, 2007). Since the discovery of DA receptors however, there have been a vast array of drugs identified (both clinical and non-clinical) that target various sites on these receptors. These drugs primarily have two modes of action, agonists (which help to reinforce receptor activity) and antagonists (which help to attenuate receptor activity). Their efficacy is often reported as an inhibitor constant, K_i, which is defined as the required concentration for half the effect (inhibitory or excitatory) to be observed (Waley, 1982). This K_i value is ultimately determined using a Dixon plot, where lower K_i values indicate a stronger binding affinity (the strength of the bond between the drug and the receptor) within the drug receptor interaction (Cornish-Bowden, 1974).

One of the many D₁-like antagonists, SCH-23390 (also known as (R)-(+)-7-chloro-8-hydroxy-3-methyl-1-phenyl-2,3,4,5-tetrahydro-1H-3-benzazepine) was the first discovered selective D₁-like antagonist (Bourne, 2001). This highly potent benzazepine shows a very high binding affinity with D₁-like receptors and a very low binding affinity to D₂-like receptors (as is shown in Table 1 (Bourne, 2001)). Although the mechanisms behind the binding between SCH-23390 and DA receptors is still yet to be fully identified, this drug will ultimately block dopamine-stimulated AC activity, sequestering the function of D₁-like receptors (Breese and Mueller, 1985). As well as DA receptors, SCH-23390 reduces striatal acetylcholine and choline levels upon infusion, also showing a high affinity for 5-HT_{2A} receptors (K_i = ~11.0nm (Bourne, 2001)). 5-HT_{2A} is heavily abundant within the LEC, enhancing deep layer GABAergic transmission (Deng and Lei, 2008), SCH-23390 being shown to be a 5-HT₂ agonist (Woodward *et al.*, 1992). This therefore suggests that not only does SCH-23390 application attenuate D₁-like receptor activity, it also amplifies 5-HT_{2A} activity, which in turn increases deep layer GABAergic activity, which may result in a greater reduction of activity within the superficial LEC layers I-III. Although this poses an intriguing hypothesis, the role that SCH-23390 application plays in LEC transmission still remains under-reported, with further experimentation needed to better understand this role (Caruana *et al.*, 2006).

Unlike SCH-23390, SKF-38393 acts as a partial D₁-like receptor agonist, functionally facilitating DA signalling in DA receptors but only showing a weak activity (Clark *et al.*, 2011). Also known as (±)-1-phenyl-2,3,4,5-tetrahydro-(1H)-3-benzazepine-7,8-diol, this drug binds extensively with D₁-like receptors, having a higher, though not pharmacologically significant, binding affinity to D₁ than to D₅ (as is also shown in Table 1 (Bourne, 2001)). Also unlike SCH-

23390, the mechanism of action (MOA) is known for this agonist. This group mimics the structure of DA, stimulating AC activity similar to that observed by DA, which gives rise to the agonist property of the drug (Riggs *et al.*, 1987). SKF-38393 may also affect downstream components of the cascade reaction initiated by D1-like receptors, as this agonist in DA knockout rats still exhibits c-Fos expression (Keefe and Gerfen, 1995). This agonist also binds to 5-HT_{2A} receptors; however this binding yielded a K_i value of >10,000 nm, making it pharmacologically insignificant (Neumeyer *et al.*, 2003).

One of the agonists of D2-like receptors is the ergoline derivative quinpirole, however this drug only affects D₂ and D₃ receptors and has no significant affinity for D₄ receptors (Titus *et al.*, 1983; Sullivan *et al.*, 1998). Similarly to the D1-like agonist, quinpirole is shown to directly increase expression of c-Fos, however this effect is only seen in the presence of both quinpirole and SCH-38393 (the aforementioned D1-like receptor agonist). This shows that c-Fos expression is correlated to both D1-like and D2-like receptor activation, however this response is mediated by the D1-like response (Keefe and Gerfen, 1995). As a D2-like agonist, this drug is used in animal models to test obsessive compulsive disorder and schizophrenia, as these disorders arise from an over excitation of D2 receptors (Rodrigo *et al.*, 2011).

An established D2-like receptor antagonist (Fedotova, 2012), both in research and clinically, sulpiride exists in two enantiomeric isoforms, R(+)-sulpiride (where the 1-ethylpyrrolidine group lies below the plane of the remaining groups in the compound) and S(-)-sulpiride (where the 1-ethylpyrrolidine group protrudes above the plane of the remaining groups in the compound). Although they are chemically and functionally identical, binding to D2-like receptors to stimulate AC activity (Wagstaff, Fitton and Benfield, 1994), their orientation affects their binding affinity to D2-like receptors. S(-)-sulpiride shows a significantly higher affinity for D₂ and D₃ than R(+)-sulpiride, with S(-) sulpiride showing a K_i value of 15 nm and 13 nm for D₂ and D₃ receptors respectively, whereas R(+)-sulpiride shows K_i values of 900 nm and 400 nm for D₂ and D₃ receptors respectively. Although both these enantiomers show significant binding to D₂ and D₃ receptors, neither show any pharmacologically significant binding to D₄ receptors, yielding K_i values of 1000 nm and 970 nm for S(-)-sulpiride and R(+)-sulpiride respectively (Bourne, 2001). Upon binding to D₂ and D₃ receptors, sulpiride elicits an antidepressant like response in the mesolimbic area (Tsukamoto *et al.*, 1994), showing no effect on GABA, serotonin, norepinephrine or acetylcholine receptors (Wishart *et al.*, 2006). This blockage of D₂ and D₃ receptors has led to sulpiride being used as an atypical antipsychotic, clinically being prescribed to treat symptoms associated with schizophrenia (Lai *et al.*, 2012). Similar to SCH-23390, the effect of sulpiride on LEC transmission has been tested previously, however more experimentation with this may be required to further understand the role of D2-like receptors during DA application, as outlined in Aim 2 (Caruana *et al.*, 2006).

Asides from the interactions mentioned, all the drugs that have been discussed here interact with 5-HT_{2A} and α 2. Although SCH-23390 showed a high affinity for the serotonin receptor, all others showed a pharmacologically insignificant affinity (K_i = >10,000 nm). Similarly, all showed affinities towards adrenoreceptors α 2, but none of these were pharmacologically significant (K_i = >10,000 nm (Neumeyer *et al.*, 2003)).

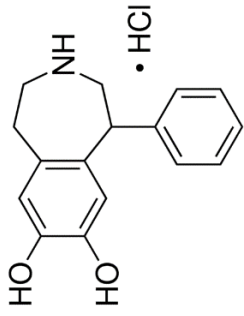
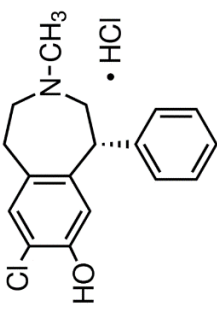
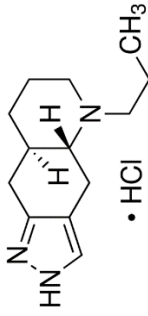
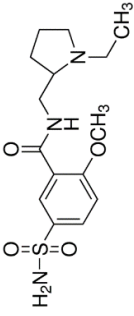
Drug	Description	Structure	MOA	Receptor K _i Values (nM)	References
SKF-38393	A weak partial benzazepine D1-like receptor agonist which promotes glutamate release upon infusion.		The β -phenyldopamine group binds to presynaptic receptors to confer agonist properties, activating adenylyl cyclase.	D ₁ - 1.0 D ₂ - ~150 D ₃ - ~5,000 D ₄ - ~1,000 D ₅ - ~0.5 5-HT _{2A} - >10,000	Description (Bouron and Reuter, 1999; Clark <i>et al.</i> , 2011), MOA (Riggs <i>et al.</i> , 1987), Structures and K _i values (Neumeyer <i>et al.</i> , 2003).
SCH-23390	A highly potent benzazepine D1-like receptor antagonist that reduces striatal acetylcholine and choline upon infusion.		Although the exact mechanism remains unknown, this drug blocks dopamine-stimulated adenylyl cyclase activity.	D ₁ - ~0.2 D ₂ - ~1,100 D ₃ - ~800 D ₄ - ~3,000 D ₅ - 0.3 5-HT _{2A} - ~11.0	Description, Structure and DA receptor K _i values (Bourne, 2001); 5-HT _{2A} K _i value (Neumeyer <i>et al.</i> , 2003); MOA (Breese and Mueller, 1985).
Quinpirole	An ergoline derivative agonist which is selective to D ₂ and D ₃ receptor.		No direct mechanism has been proposed, but the drug has a biphasic effect on locomotion and movement and increases c-fos levels.	D1-like - ~13.0 D ₂ - 4.8 D ₃ - 5.1	Description and structure (Titus <i>et al.</i> , 1983); D1-like K _i value (Seeman, 2007); D2-like K _i values (Seeman and Schaus, 1991); MOA (Eilam and Szechtman,
R(+) Sulpiride	A benzazepine derived D2-like receptor antagonist, also used clinically as an atypical antipsychotic.		MOA's include lack of DA induces adenylyl cyclase stimulation and induction of weak catalepsy in animals.	D ₁ - ~19,000 D ₂ - ~900 D ₃ - ~400 D ₄ - 970 D ₅ - 29,000	DA receptor K _i values (Bourne, 2001); Structure (Sigma Aldrich, Montana, USA); MOA (Wagstaff, Fitton and Benfield, 1994).

Table 1 - Dopamine Receptor Agonists and Antagonists. A comparison between different drugs which target dopamine receptors, including their mechanism of action (MOA), their structure and their inhibitor dissociation constant (K_i). References for the respective information are shown in the furthest right column. Further detail into each can be found in text.

1.2.3 Dopamine Transmission

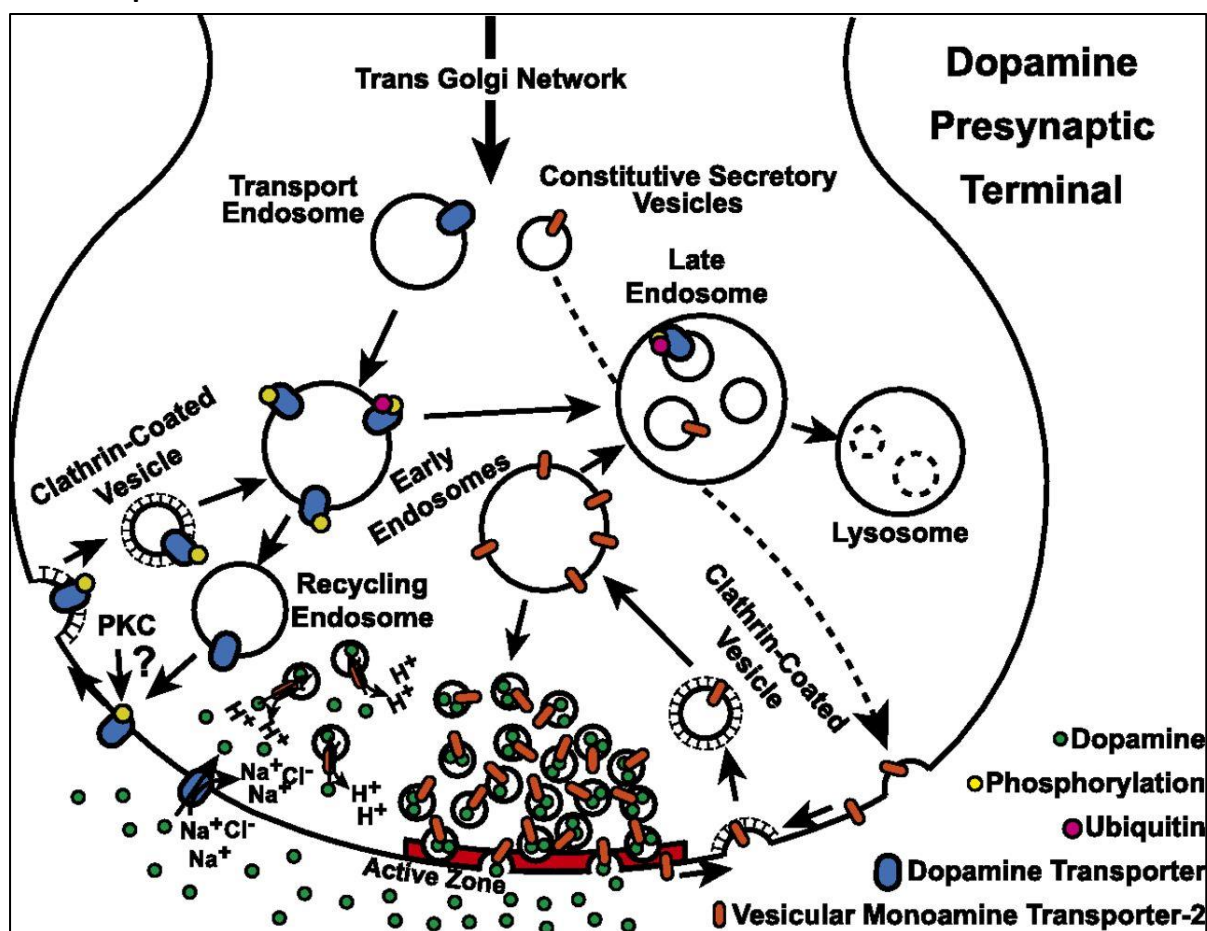


Figure 8 - Dopamine Release From Vesicles in the Presynaptic Bouton into the Synaptic Cleft. The various stages in DA release, from vesicle formation (top) to vesicle budding and neurotransmitter release (bottom). This diagram was taken directly from Pharmacological reviews (German *et al.*, 2015, with permission).

Although DA receptors make novel targets for therapeutic drugs (as was mentioned in the preceding chapter), so too can the dopaminergic production pathway be targeted for drug design. Prior to cellular activation (Figure 8), buds from the trans-Golgi network are released and transported to the synaptic bouton where DA is formed from tyrosine. DA is produced when tyrosine hydroxylase (the rate limiting step in DA synthesis (Levitt *et al.*, 1965)) converts tyrosine into L-dihydroxyphenylalanine (L-DOPA), with aromatic acid decarboxylase (AADC) then converting L-DOPA into DA. At this resting stage of transmission, whilst DA transporters (DAT) remain inactive and internalised within vesicles, DA remains within the cytoplasm of the neurone. From this stage, DAT can migrate in one of two directions. Firstly the channel can be expressed on the surface of the bouton, where it will reuptake DA molecules into the neurone through active transport, a process which is coupled with the transport of one chloride ion and two sodium ions (2Na^+ , Figure 8, bottom left; Vaughan and Foster, 2013). Besides from this pathway, DAT may also be degraded if the endosome which the transporter is enclosed in progresses down the degradation pathway, which would result in the endosome forming a lysosome (Figure 8, right; Daniels and Amara, 1999). DA itself however is formed in the cytoplasm of the neurone (through the aforementioned conversion pathway)

prior to synaptic vesicle packaging in the synaptic bouton (Figure 8, bottom). This packaging is performed by the transport protein Vesicular Monoamine Transporter-2 (VMAT2), which transports DA into the vesicle and protons (H^+ ions) out of the vesicle through the antiporter VMAT2. The protonated nature of the vesicle is maintained by a H^+ -ATPase, which actively transports protons against their concentration gradient back into the vesicle (German *et al.*, 2015). Once DA is packaged into vesicles and an action potential invades the terminal, an influx of calcium ions (Ca^{2+}) into the synaptic terminal results in activation of synaptotagmins (Südhof, 2012). Synaptotagmins couple with phospholipids and SNARE (soluble NSF attachment protein receptor) proteins, which subsequently trigger exocytosis of the DA neurotransmitters into the synaptic cleft (also shown in Figure 8). Simultaneously to DA being released into the cleft, VMAT2 is also released into the cleft, however the synaptic terminal briskly re-uptakes VMAT2 into clathrin-coated vesicles, which are subsequently recycled into endosomes. Once in the synaptic cleft, DA will bind either to a DA receptor (D_1 - D_5), or the presynaptic terminal will reuptake DA through DAT (German *et al.*, 2015).

1.2.4 Dopaminergic Neurones in the LEC

The largest cortical projection from the VTA is to the PFC, with the second largest projection being to the superficial layers of the EC (Oades and Halliday, 1987). These inputs somewhat resemble clumps which span these superficial layers of the LEC, which have previously been referred to as cell islands (Caruana and Chapman, 2008). DA has been previously described as having a bi-directional effect within the LEC (Caruana and Chapman, 2008), providing both a facilitative and depressive effect on the region dependent upon the concentration of tonic DA application (Caruana *et al.*, 2006). These previous DA experiments test the effect that micromolar concentrations (often between 10 and 100 μ M) of DA have on amplitudes, however the exact physiological concentrations of DA have yet to be reported and could be lower than those previously tested. Should DA exist at lower concentrations in the LEC than those tested previously, experiments using nanomolar concentrations of DA (1-1000 nM) may better indicate how the LEC functions under physiological conditions, as is outlined in Aim 1 (Chapter 1.4). Inhibitory pyramidal neurones in layer V, which also project into the superficial layers of the LEC, can themselves be inhibited by DA, creating a partial facilitative effect from DA application as DA reduces this GABAergic suppression (Rosenkranz and Johnston, 2006).

As DA suppresses activity in superficial layers of the LEC, an increase in the concentration of DA in the LEC prevents the LEC from conveying information to the hippocampus through the perforant pathway (Otmakhova and Lisman, 2006). Despite this information however, the *in vivo* effect which DA plays on the superficial layers of the LEC is yet to be fully understood, as the *ex vivo* effect (the effect exhibited when tissue samples are experimented upon outside the living body) is also yet to be fully understood.

1.3 Plasticity

1.3.1 An Overview of Synaptic Plasticity

Plasticity (or a neurones ability to undergo changes over a period of time) occurs when synapses change their shape and function in response to stimuli or damage (von Bernhardt *et al.*, 2017). The concept of plasticity was first coined in the early 20th century, with the Italian psychiatrist Ernesto Lugaro noting “the brain itself will change throughout life to deal with changes in life” (Berlucchi, 2002). The first real breakthrough in synaptic plasticity was made a few decades later, with Hebb’s postulate. Hebb’s postulate stated, “cells that fire together, wire together” (Hebb, 1949), a form of plasticity now called Hebbian plasticity (also referred to as heterosynaptic plasticity; synaptic-specific plasticity). Hebbian plasticity occurs in neurones, notably dopaminergic neurones (Ishikawa *et al.*, 2013), where strengthening of one synapse results in all synapses on the postsynaptic neurone strengthening, not just the individual synapse (Lynch *et al.*, 1977). This synaptic-specific plasticity differs from input-specific plasticity (also referred to as homosynaptic plasticity) as input-specific plasticity occurs solely at the individual synapse that is strengthening, not across all synapses (Castellucci *et al.*, 1970). Although heterosynaptic plasticity has been observed in dopaminergic neurones, homosynaptic plasticity is mostly observed in glutamatergic neurones, the most abundant excitatory neurotransmitter in the cortex and a major mediator of plasticity (Zhou and Danbolt, 2014). One form of homosynaptic plasticity is synaptic scaling, a phenomenon which acts as a negative feedback mechanism in response to elevated chronic activity, whereby total activity is matched by homosynaptic range (Turrigiano *et al.*, 1998; Abbott and Nelson, 2000). Metaplasticity is another variant of plasticity, first denoted in 1996 by Abraham and Bear, metaplasticity governs the form of plasticity whereby a neurone that has previously undergone plasticity goes through further synaptic plasticity (Abraham and Bear, 1996). Also referred to as LTP block, metaplasticity is a critically important phenomenon, as metaplasticity in neurones is a substantial promotor of long-term memory storage (Hulme *et al.*, 2013). All of these are variants of activity-dependent plasticity, a neurological phenomenon which is widely regarded to lay the foundations of learning and memory (Carulli *et al.*, 2011).

1.3.2 Activity-Dependent Plasticity

Although activity-dependent plasticity has been reported throughout the cortex, it predominantly affects glutamatergic neurones due to the involvement of ionotropic glutamate receptors (iGluRs (Rebola *et al.*, 2010)). These receptors are ion channel-associated, purely excitatory and is significantly faster than their metabotropic counterpart (Traynelis *et al.*, 2010). The group of iGluRs includes: Kainate receptors (KARs); N-methyl-D-aspartic acid receptors (NMDARs) and α -amino-3-hydroxy-5-methyl-4-isoxazolepropionic acid receptors (AMPA), all of which are tetramers formed of different glutamatergic subunits (Swanson and Sakai, 2010). Of these three receptors, NMDARs and AMPARs are ligand-gated ion channels active on the synaptic membrane, however KARs are both active within the soma and on the synaptic membrane.

During glutamate transmission, glutamate is released across the synapse upon release from the presynaptic terminal, a similar mechanism to that shown in Figure 8. Within the synaptic cleft, glutamate will initially bind to postsynaptic AMPARs, which in turn opens up the antiport channel protein, allowing an influx of Na^+ ions into the postsynaptic membrane with potassium ions (K^+) transporting out (Chater and Goda, 2014). This results in a positive increase in membrane potential, which in turn repels a magnesium ion (Mg^{2+}) from blocking the NMDARs ion channel, a process referred to as electrostatic repulsion (Nowak *et al.*, 1984). Once the Mg^{2+} ion has dissociated from the ion channel and a glutamate has bound to the ligand binding site, the channel is open and Ca^{2+} (as well as Na^+) flows into the postsynaptic bouton through the NMDAR (Ghasemi *et al.*, 2014). In this cascade of events, NMDARs act as a coincidence indicator, as it requires both presynaptic activity and postsynaptic activity to be present before the receptor becomes active (Seeburg *et al.*, 1995; Sjöström *et al.*, 2003). Once there has been an influx of Ca^{2+} ions into the postsynaptic terminal, the subsequent functions of the neurone change depending on the concentrations of Ca^{2+} entering the cell, with greater Ca^{2+} concentrations yielding synaptic facilitative effects and lower Ca^{2+} yielding depressive effects (as are outlined in Figure 9, left and right respectively; Malenka and Nicoll, 1993). Although AMPARs and NMDARs both play a comparatively significant role in the generation of plasticity, most variants of plasticity are NMDAR mediated (Citri and Malenka, 2008), whereas AMPAR plasticity occurs indirectly, with their phosphorylation state and postsynaptic expression providing their main contribution to synaptic plasticity (Mammen *et al.*, 1997; Noel *et al.*, 1999). This mechanism is known as spike time-dependent plasticity (STDP) and can both increase synaptic activity (expanded in chapter 1.3.2.1) and decrease synaptic activity (expanded in chapter 1.3.2.2).

Although activity-dependent plasticity is primarily conducted through iGluRs, there is evidence that the metabotropic glutamate receptors (mGluRs) also play a role in plasticity (Bortolotto *et al.*, 1999). This group of receptors is significantly slower than its ionotropic counterpart but shows both excitatory (through mGluR1 and mGluR5) and inhibitory (through mGluR2, mGluR3 and all remaining mGluRs) properties (Niswender and Conn, 2010; Blackshaw *et al.*, 2011). In plasticity, mGluRs have been shown to interact with clathrin-dependent endocytosis of AMPARs (Snyder *et al.*, 2001; Wang and Linden, 2000), mGluR5 (a subtype found abundantly within the hippocampus (Ferraguti and Shigemoto, 2006)) activates phospholipase c (PLC) through g-protein activation (Rebola *et al.*, 2010; Popkirov and Manahan-Vaughan, 2010) and plays a more important role in long-term depression, as discussed in chapter 1.3.2.2.

results in those targeted proteins dephosphorylating (P). VGCC and preNMDAR activities are also reduced in LTD, resulting in a significantly reduced influx of calcium, culminating in less glutamate being released across the synapse. This diminished release results in fewer AMPARs activating, thus a smaller sodium influx into the postsynaptic membrane is observed. This means less magnesium ions are repelled from NMDARs, with less calcium ions entering the postsynaptic neurone as a result. This reduction results in PP1 activation as well as glutamate binding to mGluRs, which through two separate mechanisms, results in AMPAR endocytosis (Snyder *et al.*, 2001; Wang and Linden, 2000). In LTD also, eCB shows limited activity and thus, CB₁R shows limited activity as well. In the image, arrows represent a comparison against normal activity, with larger arrows denoting a greater movement and smaller arrows showing a smaller movement. Abbreviations include (when read from top to bottom, left then right): AC (Adenylyl cyclase); PKA (Protein kinase A); DAG (Diacylglycerol); PKC (Protein kinase C); CAMKII (Calcium-calmodulin-dependent protein kinase type II); cAMP (Cyclic 3'5' adenosine monophosphate); CaN (Ca²⁺-Sensitive Phosphate Calcineurin); ERK1/2 (Extracellular signal-related kinase 1/2); PP2B (Protein phosphatase 2B); PP1 (Protein phosphatase 1).

A role for endocannabinoids (eCB) in the induction of activity-dependent plasticity has also been identified. These lipid-based eCB receptors are mostly found on the postsynaptic membrane and, upon activation by either an mGluR1 activated diacylglycerol (DAG) or by an influx of Ca²⁺, *de novo* forms the fatty acids anandamide and 2-arachidonylglycerol which either act as a retrograde messenger on either the homosynapse or the heterosynapse to affect synaptic function (Ohno-Shosaku *et al.*, 2002; Devane *et al.*, 1992; Pierre *et al.*, 2020). The presynaptic type 1 cannabinoid receptor (CB₁R) plays a vital role in eCB activity, although this receptor alone is not sufficient to generate eCB mediated plasticity both within the hippocampus and across the rest of the cortex (Kang-Park *et al.*, 2007; Heifets *et al.*, 2008). Stimulation of eCB, and subsequently CB₁R, can be mediated through the postsynaptic receptors mGluRs, L-type calcium channels and the aforementioned D₂ receptors (Sung *et al.*, 2001; Pisani *et al.*, 2005; Tang *et al.*, 2001). Upon activation of CB₁R, the g-protein Gα_{i/o} dissociates from CB₁R, inhibiting presynaptic AC and subsequently stimulating PKA activity (Heifets and Castillo, 2009). This activation of CB₁R is also reliant on presynaptic NMDAR (preNMDAR) activation, as the influx of Ca²⁺ ions (also through VGCCs as well as the preNMDARs) upregulates Ca²⁺-sensitive phosphate calcineurin (CaN). These changes in both CaN and PKA levels then yield bidirectional effects, with increases in PKA phosphorylating target proteins (producing a long-term increase in activity) and increased CaN levels dephosphorylating target proteins (producing a long-term decrease in activity (Cui *et al.*, 2016)).

1.3.2.1 Long-Term Potentiation

1.3.2.1.1 Postsynaptic Mechanisms of Long-Term Potentiation

Of these forms of activity-dependent plasticity, long-term potentiation (LTP) was the first to be identified in live animals (Bliss and Lømo, 1973) and was first shown in hippocampal slices, which remained potentiated for a long time when stimulated at a low frequency of 0.05Hz (Holland and Wagner, 1998). LTP can be divided into two components, LTP induced through postsynaptic mechanisms and LTP induced through presynaptic mechanisms. Each of these mechanisms presents their own dependence to a stage in their induction throughout the cortex, with postsynaptic mechanisms showing a dependence on NMDAR activity throughout

most of the cortex and presynaptic mechanisms showing a dependence on cAMP activity in mossy fibres (Malenka and Bear, 2004). This importance on NMDAR activity is highlighted in the postsynaptic mechanisms of STDP induced LTP (t-LTP). Instigation of t-LTP requires a secondary pulse to generate a presynaptic spike, which is then followed by a postsynaptic spike ~0-20 ms after, with only LTP observed at over 40 Hz (Bi and Poo, 1998; Markram *et al.*, 1997; Sjöström *et al.*, 2001). At this interval, the subthreshold is potentiated, allowing sufficient time for membranous Ca^{2+} ion concentrations to restabilise, but not sufficient time for the Mg^{2+} block to re-establish (Kampa *et al.*, 2004). This allows for a greater influx of Ca^{2+} ions into the postsynaptic membrane, a process which affects the postsynaptic neurone in two phases. In the first phase, the early phase, the increased concentration of Ca^{2+} ions bind to KARs, which subsequently phosphorylates and activates AMPARs (Diering *et al.*, 2016). This then leads to increased AMPAR expression onto the perisynaptic membrane, mediated by Rab11a (Park *et al.*, 2004), before the receptor migrates to the postsynaptic membrane through diffusion (as shown in Figure 9; Citri and Malenka, 2008). As well as modulating AMPAR expression, this greater influx of Ca^{2+} ions also activates both PKC and CaMKII, both of which also phosphorylate AMPARs (Yang *et al.*, 2004). PKA has been shown to support this CaMKII activity through protein phosphatase inhibition (via inhibition of the phosphoprotein inhibitor 1), with CaMKII subsequently autophosphorylating itself once activated (Blitzer *et al.*, 1998; Barria *et al.*, 1997). The combination of these events results in greater AMPAR expression, allowing a greater influx of Na^+ and subsequently Ca^{2+} ions, which drives LTP induction.

After the early phase has subsided (approximately one hour after first induction (Baltaci *et al.*, 2018)), the second phase, the late phase, begins to take effect. The aforementioned influx of Ca^{2+} ions into the postsynaptic membrane stimulates cAMP production through Ca^{2+} -sensitive AC enzymes (Chetkovich *et al.*, 1991). Increased cAMP concentrations then drive PKA production, in turn activating the extracellular regulated kinase (ERK)/ mitogen-activated protein kinase (MAPK) pathway, which activates CREB (Koga *et al.*, 2019). Activated CREB then binds to CRE sites which, as was discussed in chapter 1.2.2.1, resulting in an increased expression of genes, including: c-Fos (Kang *et al.*, 2000); Zif268/Egr-1 (Thomas and Huganir, 2004); CaMKII (Mayford *et al.*, 1996) and growth factors such as BDNF (Wang *et al.*, 2018). This increase in gene expression leads to protein production, generating more AMPAR and NMDARs, CREBs upstream proteins and growth factors, also forming new synapses between neurones and altering synaptic weights (Yuste and Bonhoeffer, 2001). The long phase therefore acts to reduce threshold potentials, meaning a weaker presynaptic impulse can still yield postsynaptic activity, acting over at least twenty-four hours (Baltaci *et al.*, 2018). This subsequently alludes back to Hebbian plasticity, as two neurones that have “fired together” have now begun to “wire together” (Hebb, 1949).

As well as playing a subsidiary role to NMDARs in t-LTP induction, AMPARs lacking the GluA2 subunit (referred to as calcium-permeable AMPARs) also play an independent role in LTP generation to NMDARs (Park *et al.*, 2018). The proto-oncogene family of Src kinases have

also been shown to increase LTP induction chances by stimulating the activity of NMDARs (Kalia *et al.*, 2004; Wang and Salter, 1994).

1.3.2.1.2 Presynaptic Mechanisms of Long-Term Potentiation

Although evidence for mechanisms involved in LTP was identified a few decades after the first identification of LTP (Staubli *et al.*, 1990; Salin *et al.*, 1996), with a range of mechanisms being identified since (Yang and Calakos, 2013), all presynaptic mechanisms entail increases in presynaptic Ca^{2+} concentrations. This Ca^{2+} concentration is mediated through N-, P/Q and R-type voltage-gated calcium channels (VGCC), with influx through R-type VGCCs significantly lowering the threshold for LTP induction, despite it playing a minimal role in overall Ca^{2+} influx (Qian and Noebels, 2001; Dietrich *et al.*, 2003). Ca^{2+} ion influx is also mediated through glutamate-bound KAR channels, which also lowers the required threshold for LTP induction (Shin *et al.*, 2010). This increase in intracellular Ca^{2+} levels leads to an increase in AC levels which, through cAMP mediated activity, increases PKA levels, allowing phosphorylation of presynaptic substrates, inducing presynaptic LTP (Castillo, 2012; Nicoll and Schmitz, 2005). Another identified mechanism involves retrograde signalling by nitric oxide (NO), a small molecule that is generated by the postsynaptic enzyme nitric oxide synthase (NOS) and can easily diffuse across a cell membrane (Alderton *et al.*, 2001). This enzyme is bound to NMDAR at membrane resting potential, but upon NMDAR activation is activated by Calmodulin and Ca^{2+} , subsequently producing NO molecules which diffuse and act on the heterosynaptic presynapse as a retrograde messenger (Stanton *et al.*, 2003). This possesses a facilitative property through numerous MOAs, namely guanylyl cyclase activation (Zhuo *et al.*, 1994), cyclic guanosine monophosphate (cGMP) activation and cGMP-dependent protein kinase activation (Meffert *et al.*, 1996). LTP is also induced when NO acts on synapses between GABAergic and dopaminergic neurones in the VTA, despite facilitating the release of GABA (Nugent *et al.*, 2007; Bains and Ferguson, 1997). As well as these mechanisms, LTP is also gated through mGluR7b activation and internalisation in mossy fibre synapses, a presynaptic glutamate receptor which plays a key role in cellular de-depression, a form of facilitation in which mechanisms that encode depression are reversed (Pelkey *et al.*, 2005). As well as the aforementioned mechanism of LTP where CB_1R upregulates presynaptic PKA, eCB-LTP has been induced in hippocampal neurones through inhibition of inhibitory GABAergic neurones (Carlson *et al.*, 2002). Homosynaptic eCB-LTP in the hippocampus can also be induced through CB_1R mediated FAK/ROCK pathway, which increases the expression of the presynaptic scaffolding protein, actin. This expression, activated by ROCK upon an increased expression of RhoAGTPase, subsequently increases presynaptic glutamate release (as shown in Figure 9; Wang *et al.*, 2017). Heterosynaptic eCB-LTP is initiated through numerous mechanisms however, namely through a depression of inhibitory transmission (Carlson *et al.*, 2002); through astrocytic support (Navarrete and Araque, 2010) and through dopaminergic signalling (Cachope *et al.*, 2007).

As well as these mechanisms, the roles that preNMDARs play in LTP induction is still poorly understood, as preNMDARs play a much greater role in long-term depression (as

discussed in chapter 1.3.2.2). In both activity-dependent forms of plasticity, these preNMDARs show an autoreceptor function, in which neurotransmitters acts on the same presynaptic terminal which the neurotransmitter was released from as well as the postsynaptic terminal (Duguid and Smart, 2009; Sjöström *et al.*, 2003). This autoreceptor function, first identified in layer II of the EC, allows a further facilitation in excitatory glutamate release, in which metaplastic LTP was induced through preNMDAR enhanced glutamate release (Berretta and Jones, 1996). This mechanism is also shown in CA1-CA3 neurones of the hippocampus, with the two subregions of the HF being the subregions throughout the cortex shown to elicit this form of LTP (McGuinness *et al.*, 2010). PreNMDARs are also required for LTP synthesis in projections from both the striatum and the amygdala, in which preNMDAR only affects cortical afferent synapses (Humeau *et al.*, 2003; Park *et al.*, 2014).

1.3.2.2 Long-Term Depression

1.3.2.2.1 Postsynaptic Mechanisms of Long-Term Depression

Similarly to LTP, long-term depression (LTD) can also be divided into its presynaptic and postsynaptic components, with many mechanisms of LTD showing the reverse of mechanisms shown in LTP. Postsynaptic LTD, like postsynaptic LTP, is dependent on postsynaptic NMDAR activity, with STDP mediated LTD (t-LTD) being induced when a postsynaptic spike is followed by a presynaptic spike (at ~0 and 20-100 ms intervals, 0.1-20 Hz (Bi and Poo, 1998; Markram *et al.*, 1997; Sjöström *et al.*, 2001)). Early phase LTD arises when a diminished Ca^{2+} influx is observed, resulting in Ca^{2+} switching binding switch from KAR (observed in LTP) to protein phosphatase 2B (PP2B (Neveu and Zucker, 1996)). This results in dephosphorylation of AMPARs and subsequent dynamin- and clathrin-dependent endocytosis from the reduced KAR activity (Collingridge *et al.*, 2004; Derkach *et al.*, 2007) and activation of a calcium-dependent protein phosphatase cascade from PP2B activation (Millward *et al.*, 1999). Activation of PP2B, a calcium/calmodulin-dependent phosphate calcineurin heterotrimer, activates protein phosphatase 1 (PP1) which activates the phosphoprotein inhibitor 1, in turn deactivating PP1 (Lisman, 1989). Combination of these pathways results in a suppression of gene expression, thus less proteins (such as the aforementioned receptors and synaptic weighting) are produced, which is indicated in Figure 9. As well as these biomolecules, LTD is heavily correlated with a dephosphorylation of both PKA and PKC, where their dephosphorylation both reduces their activities and also reduces AMPAR activity (Jideama *et al.*, 2006; Kameyama *et al.*, 1998; Yang *et al.*, 2004).

As well as ionotropic-mediated LTD, metabotropic-mediated LTD through mGluRs provides a different induction mechanism to that of NMDAR induced-LTD. Activation of group 1 (excitatory) mGluRs by glutamate neurotransmitters affects both iGluR trafficking and gene expression through a plethora of mechanisms (Gladding *et al.*, 2009; Sanderson *et al.*, 2016). The first mechanism in which mGluR can induce LTD is through AMPAR expression on the postsynaptic membrane. Group 1 mGluRs, upon activation, dephosphorylates and activates striatal-enriched tyrosine phosphatase (STEP), which dephosphorylates AMPARs, initiating

their endocytosis (Zhang *et al.*, 2008). Where this directly affects trafficking, both the p38/MAPK and the ERK 1/2 pathways indirectly affect the trafficking through a cascade reactions, modulating G-actin which results in the endocytosis of AMPARs (Rush *et al.*, 2002; Gallagher *et al.*, 2004). This form of LTD appears to be mediated by downstream mGluR-dependent protein synthesis, as Fragile X mental retardation protein (a protein essential in cognitive development) KO mice show enhanced levels of LTD, potentially providing a therapeutic target in other neurodevelopmental conditions (Hou *et al.*, 2006; Bear *et al.*, 2004). Although mGluRs also trigger eCB activation, thus both branches of postsynaptic LTD can elicit an eCB-mediated response (Ohno-Shosaku *et al.*, 2002), mGluRs have been shown to only contribute to short-term plasticity in hippocampal neurones (Rouach and Nicoll, 2003). The activity of postsynaptic mGluRs is not a prerequisite for LTD induction, instead preNMDAR activation is required in its induction.

1.3.2.2.2 Presynaptic Mechanisms of Long-Term Depression

Where presynaptic LTP stems from an increase in presynaptic Ca^{2+} , presynaptic LTD generally originates in a reduction in Ca^{2+} concentration, which subsequently diminishes levels of respective downstream biomolecules. Where the iGluR, KAR, is activated in LTP, it is the inhibitory metabotropic glutamate receptors mGluR2/3 that are activated in accordance with LTD (Tzounopoulos *et al.*, 1998). Activation of these mGluRs leads to a g-protein linked reaction (through $G\alpha_i$) which culminates in AC suppression and thus cAMP/PKA inhibition (Pin and Duvoisin, 1995). Secondly, where NO plays a facilitative heterosynaptic plastic effect, its effect observed on a homosynapse is depressive (Gage *et al.*, 1997). Upon NOS stimulation and NO production, NO actively passes through the membrane due to its small size and negligible charge. Upon NO entering the homosynaptic presynaptic membrane, it acts on guanylyl cyclase, cGMP and PKG to alter NMDAR dependent LTD (Gage *et al.*, 1997; Li *et al.*, 2003) as well as directly acting on presynaptic K^+ channels (Yang *et al.*, 2007). Although mGluR7b was shown to induce LTP, its counterpart (mGluR7) has been shown to induce LTD. Activation of the mGluR expressed on the presynaptic membrane activated PKC, which downregulates P/Q- VGCC activity (Pelkey *et al.*, 2005). Finally, eCB, and subsequently the presynaptic CB_1R , play a pivotal role in LTD, a role which is subsequently referred to as eCB-LTD (Gerdeman *et al.*, 2002). In CB_1R -mediated LTD, similar to CB_1R -mediated LTP, activation of CB_1R through a retrograde messenger (anandamide or 2-arachidonylglycerol to name a couple) initiates a cascade of events, with CaN levels eventually increasing, dephosphorylating presynaptic targets (as indicated in Figure 9; Heifets and Castillo, 2009). DA receptors also contribute to this eCB-LTD generation, with the presynaptic activity and expression of the DA receptor D_2 dictating whether LTP or LTD is observed (Xu *et al.*, 2018).

Although preNMDARs play a minor role in LTP induction, as discussed in chapter 1.3.2.1.2, they play a significant role in various forms of synaptic LTD induction (Citri and Malenka, 2008; Rodríguez-Moreno, Banerjee and Paulsen, 2010; Heifets and Castillo, 2009; Rodríguez-Moreno *et al.*, 2013; Wang *et al.*, 2012). In their most abundantly studied role, preNMDARs are necessary for STDP induced LTD (t-LTD), acting as a coincidence indicator in

its induction (Bender *et al.*, 2006; Sjöström *et al.*, 2003). STDP induced LTD is observed when a postsynaptic spike is followed by a presynaptic spike, as mentioned previously, yielding a reduced influx of Ca^{2+} ions into the presynaptic membrane (Karmarkar and Buonomano, 2002). PreNMDARs play not only a fundamental role but a necessary role in t-LTD induction, as postsynaptic NMDAR inhibition through MK-801 (an NMDAR antagonist) showed no changes in LTD capabilities, however preNMDAR inhibition through MK-801 blocked LTD almost entirely (Rodríguez-Moreno and Paulsen, 2008). Under the expression of LTD, reduced preNMDAR binding results in a reduction of presynaptic Ca^{2+} influx, which in turn diminishes presynaptic neurotransmitter release, further reducing preNMDAR activity. Instigation of t-LTD also requires postsynaptic mGluR activation, activating eCB and stimulating the production of retrograde messengers (Heifets and Castillo, 2009). These eCB messengers activate the presynaptic CB_1R , activating the g-protein linked cascade and reducing intracellular PKA levels, diminishing presynaptic phosphorylation levels (Cui *et al.*, 2016). This has meant that, similar to preNMDAR, eCB acts as a second coincidence indicator, as its activity in t-LTD is dependent upon the activity of both the presynaptic and postsynaptic receptors (Bender *et al.*, 2006). Despite the important role that both eCB and retrograde signalling molecules play in presynaptic LTD, presynaptic spike pattern-dependent (p-LTD) experiments in rodent barrel (somatosensory) cortex concluded that neither of the aforementioned pathways were required to generate LTD (Rodríguez-Moreno *et al.*, 2013; Banerjee *et al.*, 2009). This preNMDAR mediated LTD can however be almost entirely abolished through inhibition of the NR2B subunit on the NMDAR, a subunit which is shown to be downregulated throughout the EC during mature stages (Massey *et al.*, 2004; Yang *et al.*, 2006; Berretta and Jones, 1996). Application of the subunit antagonist, Ro 25-6981, showed a significant reduction in LTD (with no effect on LTP), most notably in layers II, III and V of the EC (Berretta and Jones, 1996).

1.3.2.3 Short-Term Plasticity

Asides from long-term plasticity, another form of plasticity exists, short-term potentiation (STP), which acts somewhat independently of the aforementioned forms of plasticity. STP occurs within the presynaptic membrane, acting between a few seconds to a few minutes (Citri and Malenka, 2008). This form of plasticity however differs from the early phases of both LTP and LTD, as STP is driven by presynaptic Ca^{2+} ions and few molecular mechanisms surrounding its induction have been observed (Zucker and Regehr, 2002). Similar to LTP and LTD however, the observed influx of Ca^{2+} ions does show a bidirectional effect, with larger concentrations of Ca^{2+} yielding potentiation and smaller concentrations of Ca^{2+} yielding a depression (Fioravante and Regehr, 2011). In STP, frequent firing of the presynaptic neurone results in a transient rise in presynaptic Ca^{2+} concentrations, which gives rise to the mechanisms of STP, augmentation and potentiation (also referred to as post-tetanic potentiation). Both augmentation and potentiation enhance presynaptic neurotransmitter activity by driving vesicle exocytosis through the built-up Ca^{2+} ions (Erulkar and Rahamimoff, 1978; Korogod *et al.*, 2005). The two mechanisms however have slightly different

downstream biomarkers, with augmentation being shorter lasting, stimulating munc13 (a SNARE protein regulator which is modulated by Ca^{2+} (Gioia *et al.*, 2016)) and potentiation being longer lasting, stimulating PKA (Cheng *et al.*, 2018). Although this frequent firing of presynaptic neurones provides mostly a facilitative response, there are synapses at which frequent firing shows a depressive effect (Zucker and Regehr, 2002).

There also appears to be roles for both preNMDARs, eCBs and glial interaction in STP generation. The former, preNMDARs, have been found to mediate glutamate transmission upon activation, an effect which is seen predominantly across frequency dependent short-term facilitation in the EC (Chamberlain *et al.*, 2008). eCBs also mediate STP, this time through the retrograde messenger activities of anandamide and 2-arachidonylglycerol, by which their interaction with CB_1R affects VGCC channel induction, mediating presynaptic Ca^{2+} influx (Chevalleyre *et al.*, 2006). The role that eCBs play in short term plasticity exist as two forms, depolarisation-induced suppression of inhibition and depolarisation-induced suppression of excitation (Llano *et al.*, 1991; Vincent *et al.*, 1992). Besides from preNMDARs and eCBs, glial interaction has been shown to play a supporting role in STP induction, with astrocytes enhancing transmission through their own Ca^{2+} signalling pathways (Sibille *et al.*, 2015).

1.3.3 Dopamine-Mediated Plasticity

Although it was previously thought that only glutamatergic neurones could exhibit plasticity, more recent studies have begun to show that dopaminergic neurones can also undergo plasticity. DA-mediated synaptic plasticity however still remains poorly understood within the LEC; however this phenomenon is significantly better understood in the PFC, the only subregion to receive a larger dopaminergic innervation from the VTA than the EC (Oades and Halliday, 1987). In the PFC, both D1-like receptors and D2-like receptors contribute to both early-phase and late-phase plasticity, as is shown in Figure 10 (Goto *et al.*, 2010). Early-phase plasticity is mediated through AMPAR and NMDARs membrane expression, a process which is stimulated by D1-like transmission but not D2-like transmission (Figure 10, lower; Sun *et al.*, 2005). Activation of D1-like receptors activates AC and then cAMP, activity of which are implemented in both LTP and LTD due to their binding affinities to Ca^{2+} (Chetkovich *et al.*, 1991). PKA is then activated by cAMP, another biomolecule that is heavily implemented in both LTP and LTD for its interactions with CaMKII and also its role in phosphorylating AMPARs (Blitzer *et al.*, 1998; Price *et al.*, 1999). Subsequent activation of DARPP-32 and then PP-1 leads to greater levels of phosphorylated NMDARs as well as stimulating CREB activity, further driving late-phase plasticity (Nishi *et al.*, 2016). This increased CREB activity is also driven through D2-like cascade, in which PLC and PKC, two other biomolecules implemented in plasticity due to their interactions with AMPAR are activated (Yang *et al.*, 2004; Horne and Dell'Acqua, 2007). As these both affect gene expression, they are congruent with late-phase plasticity, a process which is stimulated by both D1-like and D2-like receptor activation (Yamamoto *et al.*, 1988). Both D1-like and D2-like receptors also directly interact with NMDARs, through NMDAR's GluN2A and GluN2B subunits respectively, with both DA receptors inhibiting NMDARs activity (Lee *et al.*, 2002; Liu *et al.*, 2006). Cocaine addiction has

been shown to strengthen this interaction, as well as reducing NMDAR's activity with CaMKII (Liu *et al.*, 2005).

Figure 10 also shows the role which mGluR group II plays in the formation of synaptic plasticity, by interacting with the intermediate biomolecules PLC and ERK 1/2, which has also been shown in other similar reports in both the PFC and the HF (Otani *et al.*, 1999; Zhu *et al.*, 2017). Another factor in DA-mediated synaptic plasticity within the PFC seems to be the interaction between DA receptors and the serotonin receptor 5-HT_{1A}. This 5-HT receptor, whose postsynaptic abundance appears to be on glutamatergic neurons, provides interdependency in DA-mediated plasticity (Meunier *et al.*, 2017). Although experiments testing the role of DA in the HF have been performed, there is yet to be either a conclusive or proposed cascade mechanism like that shown in PFC (Sajikumar and Frey, 2004). There is a similar mGluR-dependency in plasticity formation within the LEC, but the serotonin receptor identified in the PFC (5-HT_{1A}R) is not present in the LEC directly, but is present within the HF (Zhu *et al.*, 2017; Wright *et al.*, 1995; Polter *et al.*, 2012).

One form of DA-mediated STP which has been studied within the LEC is DA receptor

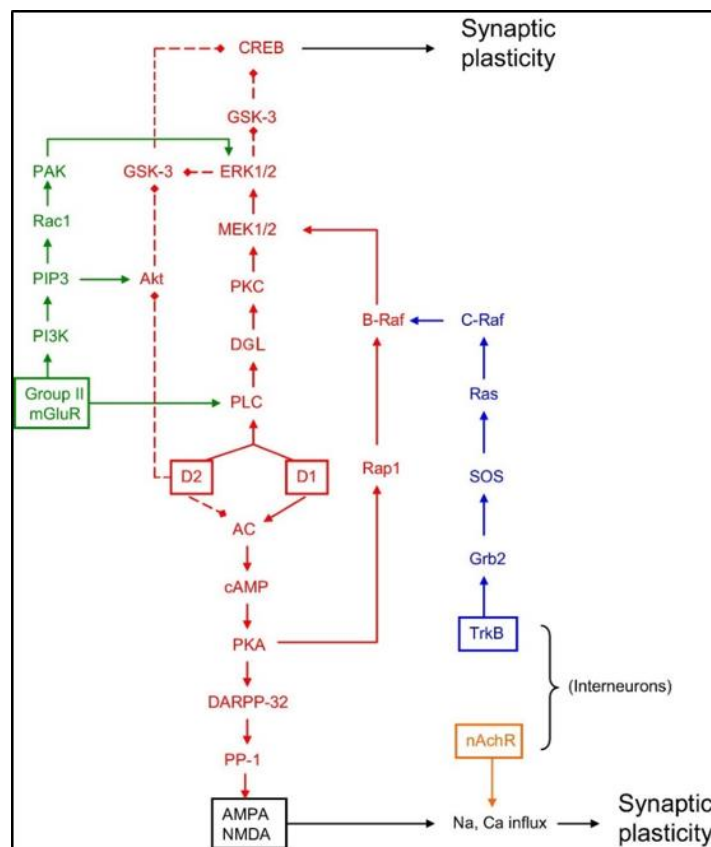


Figure 10 - Signal Cascade of Dopamine-Mediated Synaptic Plasticity. The cascade reaction caused by both D1 and D2 (as well as D1:D2) receptor activation and their role in initiation and propagation of synaptic plasticity in the prefrontal cortex. The predominant signalling pathway, D1/D2 receptor (red), is divided into two separate pathways. The first pathway (ascending) shows the signalling pathway which culminates in decreased cAMP response element-binding protein (CREB) expression. This pathway can be separated into two parts, the excitatory (shown by the solid lines which are D1:D2 mediated) and the inhibitory (shown by dotted lines which is D2-mediated), both of which result in CREB inhibition and subsequent LTP induction (Yamamoto *et al.*, 1988). The other pathway (descending) shows the signalling pathway which culminates in phosphorylation of both N-methyl D-aspartic acid (NMDA) and α -Amino-3-Hydroxy-5-Methyl-4-Isoxazolepropionic Acid (AMPA), increasing postsynaptic calcium and sodium ion influx (Sun *et al.*, 2005). Other signalling factors mediated by dopamine activation are also shown:, including brain-derived neurotropic factor (BDNF, blue); group II metabotropic glutamate receptor (Group II mGluR, green); nicotinic acetylcholine receptor (nAChR). Abbreviations include (when read from top to bottom, left then right): GSK-3 (Glycogen Synthase Kinase 3); PAK (p21-Activated Kinases); ERK 1/2 (Extracellular Signal-Regulated Kinase); Rac1 (Ras-Related C3 Botulinum Toxin Substrate 1); MEK 1/2 (Mitogen-Activated Kinases 1/2); PIP3 (Phosphatidylinositol-3;4;5-Triphosphate); Akt (Protein Kinase B); PKC (Protein Kinase C); PI3K (Phosphoinositide 3-kinase); DGL (Diacylglycerol); PLC (Phospholipase C); Rap 1 (Member of the RAS Family of Small GTP-Binding Proteins); SOS (Son of Sevenless Guanine Nucleotide Exchange Factors); AC (Adenylyl Cyclase); cAMP (Cyclic 3'5' Adenosine Monophosphate); Grb2 (Growth Factor Receptor-Bound Protein 2); PKA (Protein Kinase A); DARPP-32 (Phosphoprotein of 32 kDa); PP-1 (Protein Phosphatase 1). The image depicting the cascade reaction was taken directly from Biological Psychiatry (Goto *et al.*, 2010, with permission).

desensitisation. This neurological phenomenon (also referred to as DA inhibition reversal) arises from a prolonged exposure to the neurotransmitter, where the effect of the neurotransmitter exhibits on the region diminishes over time (Nimitvilai and Brodie, 2010). DA desensitisation was initially only reported in the VTA (Nimitvilai and Brodie, 2010), however it is yet to be directly reported within the LEC. These mechanisms stem from DA receptor concurrent stimulation over prolonged periods (Nimitvilai and Brodie, 2010) and show significant changes in downstream molecules (Goto *et al.*, 2010). Phosphatidylinositol (PI), conventional protein kinase C (cPKC) and PLC have all been implicated in DA desensitisation (Nimitvilai *et al.*, 2014). All of these biomolecules are downstream signalling molecules in the DA signalling cascade, confirming that DA desensitisation is self-mediated.

1.3.4 Methods for Inducing Plasticity

Despite plasticity being a crucial aspect of neurological function, it was not until the early 20th century that artificially induced plasticity could be induced in a laboratory (Markram *et al.*, 2011). Since then, two predominant forms of electrophysiology (physiology that studies the electrical properties of neurones) have been identified intracellular and extracellular recordings. Intracellular recordings provide a detailed insight into a single, specific neurone and its connections, it does not however provide a representation for other nearby neurones. There are three common forms of intracellular recording techniques, voltage clamp, current clamp and patch-clamp recording. The first two techniques are very similar, with voltage clamp maintaining membrane potential and measuring current whereas current clamp maintains current and measures membrane potential (Hodgkin *et al.*, 1952; Brinstock *et al.*, 1975). Patch-clamping however, initially finalised in 1992, can be used to measure either of the aforementioned physical properties of the cell (Neher and Sakmann, 1992). There are numerous types of patch-clamp recording, including whole-cell (where the membrane is broken to allow dispersion of internal fluid) and perforated patch (where the membrane is made permeable to ions so the cytoplasmic contents do not get distilled within the pipette) to name a couple (Cahalan and Neher, 1992).

Should the function of numerous cells in a localised region need to be measured, extracellular recordings can be performed, which consists of single-unit, multi-unit and field recordings. Similar to voltage and current clamps, single-unit and multi-unit recordings are also similar to one another, with single-unit recordings measuring extracellular activity on one neurone and multi-unit recording (using an electrode with a wider diameter) measuring multiple neurones (Hubel and Wiesel, 1962; Recce and O'Keefe, 1989).

The final extracellular recording technique, field recordings, primarily records excitatory postsynaptic potentials, that is the change in postsynaptic membrane potentials driven by excitatory neurone transmission (Bliss and Lømo, 1973). Field excitatory postsynaptic potentials (fEPSPs) were first used in the 1960s and 70s, during which their use in measuring activity in both schaffer collateral-commissural pathway and the perforant path was well researched (Bliss and Lømo, 1973; Collingridge *et al.*, 1983). At this time, fEPSPs were described as reflections in the number of localised cells discharging, subsequently indicating

the excitability of the region (Bliss and Lømo, 1973). Following these experiments, Collingridge determined that these recordings are as a result of excitatory amino-acid activity, later concluded to be the neurotransmitter glutamate (Collingridge *et al.*, 1983). Although initial experiments showed glutamate activity primarily mediates fEPSPs, later studies showed that the inhibitory neurotransmitters GABA (Davies and Collingridge, 1996) and DA (Caruana *et al.*, 2006) can also affect fEPSPs, with the former showing a direct regulation of fEPSPs. The latter however, despite the aforementioned paper showing that DA facilitates and depresses synaptic responses within the LEC, lacks conclusions around whether DA affects fEPSPs directly or indirectly, thus further experimentation is required to determine any conclusion. Individual extracellular postsynaptic potentials may show only a small change in potential; however, neurone rich regions such as the HF have many neurones often converging on a single neurone (Keller *et al.*, 2018). This postsynaptic change in potential is measured by fEPSPs, as relative positively charged ions flood into the neurone upon activation, the extracellular region becomes more relatively negative (Collingridge, 1985; Bean, 2007). Measurement of these changes produces an extracellular waveform, an example of which is shown in Figure 11B. The waveform is comprised of three principal regions, each of which is identified in Figure 11B. The first induced region is the electrical stimulation artefact (1), the non-biological component of the waveform as this shows the recording electrode detecting the activation of the stimulating electrode. The second component (2) shows the presynaptic component of the waveform. Often called the fiber volley, this region shows the changes in membrane potential at the presynaptic terminus upon arrival of the action potential (Hawkins *et al.*, 2017). Analysis of this region can show changes in Ca^{2+} influx, suggesting plastic changes occurring within the presynaptic terminal (Kamiya and Ozawa, 1998). The postsynaptic region (3) of the waveform is the largest and longest region of the three, occurring immediately after the presynaptic component, indicating the presence of a postsynaptic potential. During this postsynaptic potential, activation of few presynaptic cells (as shown by the fiber volley, 2) often leads to the activation of significantly more postsynaptic cells, owing to the dense nature of the HF (Keller *et al.*, 2018). This propagation of an action potential across cells results in a large shift in extracellular ionic concentrations, as Na^+ ions enter cells, causing the largest negative change in the fEPSP waveform (Stolerman, 2010). This postsynaptic component of the waveform can be broken down into various components to measure how the EPSP changes: the initial slope, the peak amplitude, the initial area and the whole area (Liu *et al.*, 2008). Not only can all these components indicate the induction and subsequent form of synaptic plasticity, but they can also show the effects that other neurones or drug application has on the region. This makes fEPSP a reliable experimental technique in the analysis of HF (and subsequently the LEC) activity, as the regions are not only dense in MPNs, but also primarily communicate through excitatory transmission.

The results seen in waveforms would be directly comparable to the induction of plasticity, with LTP producing a larger peak amplitude and LTD yielding a smaller peak amplitude. This occurs as LTP induction conformationally changes postsynaptic receptors to induce larger potentials, thus fEPSPs increase (Daoudal *et al.*, 2002). LTP can be artificially

induced using fEPSP stimulation, with hippocampal neurones showing a significant facilitation after high-frequency (100 Hz for 1 second) tetanic-stimulation (Morishita *et al.*, 2005). LTP can also be induced through theta-burst stimulation (5 pulses at 100 Hz several times over a few minutes (Larson *et al.*, 1986)) as well as other tetanisation timeframes (25-400 Hz (Blundon and Zakharenko, 2008)). Where LTP is induced through high-frequency pulses over a short time, LTD is induced through low-frequency pulses over a long time. This protocol is well versed, one example of this is in hippocampal neurones, where 3 minutes of 5 Hz stimulation yields a significant depression in both fEPSP amplitude and in slope (Morishita *et al.*, 2005). Other stimulation methods which induce LTD include: 15 minutes of 900 pulses at 1 Hz (which induces NMDAR mediated LTD (Dudek and Bear, 1992; Mulkey and Malenka, 1992)) and minutes-long trains of 1-3 Hz (Bear and Malenka, 1994). Stimulation mediated eCB-LTD also shows that both low-frequency (through 2-arachidonylglycerol mediation) and high frequency (mediated by anandamide through CB₁R) can both induce LTD in synapses (Lerner and Kreitzer, 2012). As well as long-term plasticity, STP can be induced through trains (many pulses in quick succession) with augmentation lasting for seconds after the train and post-tetanic potentiation (potentiation observed after tetanisation) lasting minutes after the train (Erulkar and Rahamimoff, 1978).

Synaptic plasticity can also be induced through paired-pulse stimulations (PPS), where two pulses are delivered in quick succession over short interpulse intervals (IPIs). PPS will subsequently induce one of two forms of short-term plasticity, paired-pulse facilitation (PPF, in which an increase in postsynaptic potentials is observed) or paired-pulse depression (PPD, in which a decrease is observed). The mechanisms underlying PPF are predominantly through residual Ca²⁺ build-up in the presynaptic terminal, however it is also heavily dependent on the pool of readily releasable vesicles (Fioravante and Regehr, 2011). Over very short IPIs, PPF observed is at its greatest, as residual Ca²⁺ is at its highest from the previous action potential. This spike in presynaptic Ca²⁺ concentration will subsequently drive greater exocytosis from presynaptic readily releasable vesicles, increasing the presynaptic release probability. This relationship between IPI and the strength of PPF shown appears to be inversely proportional, that is increasing IPI reduces the strength of PPF elicited, as larger IPIs show a much weaker PPF strength (Zucker and Regehr, 2002). One crucial factor in this diminishment of power over time is due to the co-operative effect between Ca²⁺ and vesicles, in which approximately four Ca²⁺ ions are required to drive exocytosis of one vesicle (Dodge and Rahamimoff, 1967). Shorter IPIs will have a substantially greater concentration of presynaptic calcium and thus can drive significantly larger volumes of vesicle release than the lower concentrations observed at longer IPIs. Unlike PPF however, PPD appears to arise through mechanisms entirely independent of both residual presynaptic Ca²⁺ build up and RRP, instead being driven by VGCC inactivation and vesicle endocytosis and replenishment (Fioravante and Regehr, 2011). This not only shows a reduction in intracellular Ca²⁺ pools, but also readily releasable vesicle pools, both of which contribute to a reduction in presynaptic release probabilities. Although PPF has been shown to be greatest at lower IPIs, very short intervals (~10 ms) are often still perceived as a depression when compared to the first pulse, as a multitude of

components (such as aforementioned post-tetanic potentiation and PPD mechanisms) will all contribute to total synaptic activity (Zucker and Regehr, 2002). Although previous whole-cell patch clamping of fan cells in the LEC showed DA increases PPF (Liu, 2020) and previous field experimentation further showed this (Caruana and Chapman, 2008), a greater analysis using both nanomolar and micromolar concentrations of DA will give a better indication into the role DA plays in modulating presynaptic release probabilities within the LEC (as is outlined in Aim 3, Chapter 1.4).

As well as IPIs, the duration of application and how many pairs are both significant in which variant of plasticity is observed. Both 200 and 900 PPS at 1 Hz were shown to induce LTD over 15 minutes, with the latter specifically inducing mGluR mediated LTD (Jo *et al.*, 2010; Mulkey and Malenka, 1992).

1.4 Research Aims

With all this information in mind, analysing not only the role that DA plays on synaptic transmission, but also the roles that the aforementioned antagonists play, will be crucial in further understanding the physiological functions of the LEC and how these functions may change under pathophysiological conditions. This is subsequently the broad aim of this thesis, which can be subdivided into three separate, more specific aims in order to assess them:

- Aim 1: To identify the role that tonic application of low concentrations of DA plays on synaptic transmission within the LEC. The role that high concentrations of DA (between 10-1000 μM) play on transmission is well reported (Caruana *et al.*, 2006; Harvey *et al.*, 2021), however the role that nanomolar concentrations play has yet been previously tested. This will be done by measuring field excitatory postsynaptic potential (fEPSP) amplitudes during tonic applications of low concentration DA (1-1000 nM) and comparing them against high concentration experiments.
- Aim 2: To explore the roles that both D1, D2 receptors and NMDA receptors play on synaptic transmission within the LEC. This will be completed through a pharmacological approach, using receptor antagonists to inhibit specific receptors in order to suggest their roles under physiological conditions. The antagonists to be used are: SCH-23390 (a D1-like receptor antagonist); sulpiride (a D2-receptor antagonist); (2R)-Amino-5-Phosphonopentanoate (AP5, an NMDAR antagonist) and Barbadin (a β -arrestin antagonist). Although both SCH-23390 and sulpiride have been reported previously within the LEC, the antagonistic role of AP5 and Barbadin are yet to be identified in the LEC (the latter of which is yet to be tested in electrophysiology at the time of writing).
- Aim 3: To investigate the role that tonic application of DA may play in altering presynaptic neurotransmitter release probabilities. This will further develop understanding into whether DA interacts with glutamatergic neurones at their presynaptic terminus, as most reports show its effect on the postsynaptic

region (Nakano *et al.*, 2010; Tritsch and Sabatini, 2012). This will be assessed by delivering paired-pulsed stimulations at ranging IPIs (between 10-1000 ms), in the presence of both low (100 nM) and high concentrations (100 μ M) of DA. Although paired-pulses have been delivered to the LEC previously (Caruana *et al.*, 2006), the role which DA plays in this protocol is yet to be identified.

2 Methods

2.1 Slice Preparation

Juvenile Sprague-Dawley rats (aged 14 to 21 days) were euthanised (through means of cervical dislocation) before being decapitated and their brains quickly removed and submerged in cold ($\sim 4^{\circ}\text{C}$), sucrose rich cutting solution saturated with 95% O_2 and 5% CO_2 containing (in mM): 234.00 Sucrose; 26.00 NaHCO_3 ; 10.00 D-Glucose; 2.00 KCl; 1.43 NaH_2PO_4 ; 3.00 $\text{MgCl}_{(\text{aq})}$; 1.00 $\text{CaCl}_{(\text{aq})}$. The cerebellum and the frontal lobes were removed, including a section along the dorsal extent of the cortex. The brain was then flipped upside down on to the exposed region and was separated into the two hemispheres by means of a cut down the longitudinal fissure. Both hemispheres were then subsequently mounted adjacent to a block of sylgard and fixed to the cutting plate. Horizontal slices ($340\ \mu\text{m}$ thick) were prepared using a vibratome (VT1000S, Leica Biosystems, UK) before being transferred to a holding chamber containing $\sim 31^{\circ}\text{C}$ artificial cerebrospinal fluid (ACSF) saturated with 95% O_2 and 5% CO_2 containing (in mM): 124.00 NaCl; 26.00 NaHCO_3 ; 17.00 D-Glucose; 2.50 KCl; 1.43 NaH_2PO_4 ; 2.00 $\text{MgCl}_{(\text{aq})}$; 2.00 $\text{CaCl}_{(\text{aq})}$. All chemicals (including chemicals used in the preparation of cutting solution) were obtained from Sigma Aldrich, Montana, USA. These slices were then left incubated in a heated (controlled using a StableTemp Ceramic Top Hot Plate (Cole-Parmer, Illinois, USA)) and oxygenated holding chamber for 1 hour.

2.2 Stimulation and Recording

Slices were then transferred to and submerged in a slice chamber where $\sim 31^{\circ}\text{C}$ oxygenated ACSF was delivered to the chamber by a peristaltic pump through a negative pressure reservoir at a flow rate of $1.6\ \text{ml}\ \text{min}^{-1}$. Field responses were then produced using stimulating bipolar tungsten electrodes and were then recorded using a pulled glass capillary (pulled using a two-stage pipette puller (Digitimer, UK)) filled with ACSF, attached to a chloride coated silver wire on an amplifier headstage (NPI electronics, Germany). A dissecting microscope and a stereotaxic atlas were then used to best identify the borders of layers I-II of the LEC to allow the accurate placement of the electrodes. The stimulating electrodes were then placed along layers I-II and the recording electrode was then placed caudal to the stimulating electrodes in layers I-III (as depicted in Figure 11A). Once inserted, the stimulating electrode delivered a 1 ms pulse through a DS3 isolated constant current stimulator (Digitimer, UK) with a fixed current between 25-200 μA at 0.05 Hz. Both the timing of each stimulation and each unfiltered evoked response, recorded over 100 ms, was then digitised at 20 kHz and displayed using software (WinLTP, Ltd. WinLTP v2.20, Bristol, UK). The peak amplitude (pkAmp) of these responses, measured as the difference between the resting voltage and the lowest point on the sweep between 2 and 10 ms post stimulation, was then plotted on a pkAmp-time graph. If a response contained population spikes (evoked responses which indicate an electrodes close proximity to neuronal cell bodies), either the polarity of the stimulation was reversed or the electrodes were repositioned to eliminate these spikes. Once a stable 30-minute baseline (defined as a constant pkAmp which showed no deviation) was achieved, then subsequent experiments were carried out.

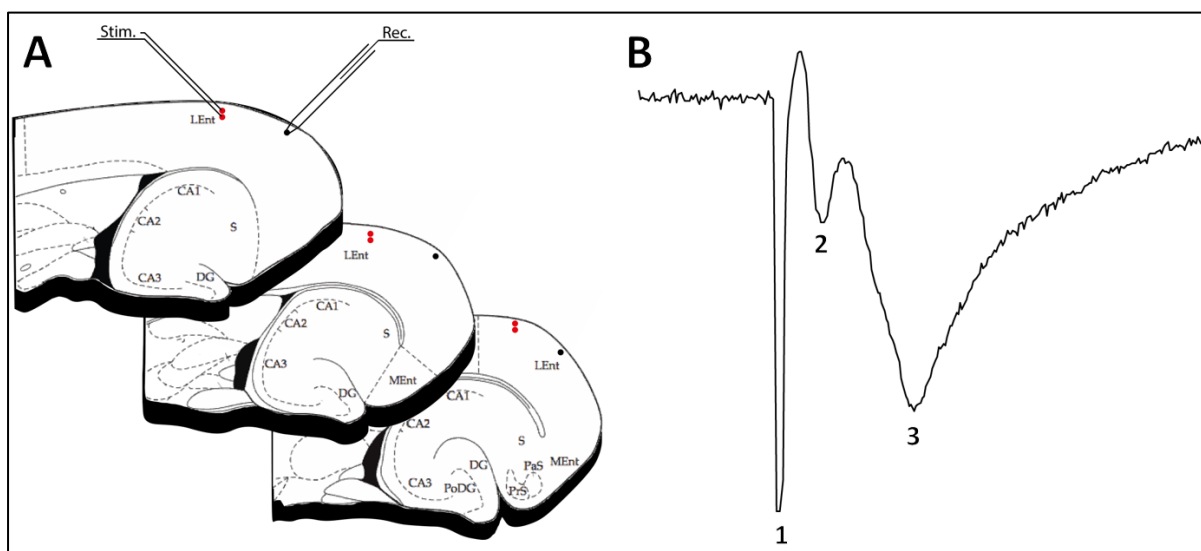


Figure 11 - Positions of Electrode Placement During Experiments and a Compartmentalised Waveform. The stimulating electrodes shown in Figure 11A (left, red) were placed rostral to the recording electrodes (right, black) in each slice. The slices shown were the three most ventral segments of the LEC which shows the largest proportions of the LEC. Figure 11B shows an example waveform, the one depicted being taken from an untampered control experiment. The waveform itself is subdivided into three subsections, the electrical stimulation artefact (1), the fiber volley (2) and the peak fEPSP amplitude (3).

2.3 Field Experiments

2.3.1 Dopamine Application

Pharmacological experiments were started only once evoked field responses were stable for a minimum of 30 minutes. Then, ACSF containing various concentrations (ranging from 1 nM to 1000 μ M) of dopamine hydrochloride (Sigma Aldrich, Montana, USA) was washed onto the slice for 30 minutes. 50 μ M sodium metabisulfite (Sigma Aldrich, Montana, USA) was also added to the ACSF and the room was also darkened, both of which were precautions taken to slow DA oxidation. In the instances where additional pharmacological treatments were also applied as well as DA, the chemical alone was washed onto the slice for an additional 30 minutes prior to their coapplication with DA. The chemicals included: 50 μ M AP5 (Hello Bio, Bristol, UK); 100 μ M Barbadin (Axon Medchem, Groningen, Netherlands); 10 μ M SCH-23390 (Sigma Aldrich, Montana, USA) and 50 μ M sulpiride (Sigma Aldrich, Montana, USA). As SCH-23390 is light-sensitive, the room was darkened upon preparation to prevent drug oxidation. Chemicals were dissolved in either water (sodium metabisulphite, AP5 and sulpiride) or dimethyl sulfoxide (SCH-23390 and Barbadin) and stored at -20°C before being dissolved in ACSF when used.

After this 30-minute application period, each chemical was then coapplied with DA for a further 30 minutes. After the 30-minute application of DA, ACSF alone was re-washed onto the slice for 60 minutes post-DA application as a “washout”. In the instance where 100 nM DA was applied twice, DA was again washed onto the slice following the initial washout, before ACSF was then reapplied for a second 60-minute washout.

2.3.2 Paired-Pulse Stimulation

Similarly to the aforementioned protocol, a 30-minute baseline was first achieved before paired-pulse stimulation (PPS) was induced. During this, 6 paired-pulse trains with logarithmic IPIs (10, 30, 100, 300 and 1000 ms) were delivered across 2 minutes. After this first PPS train, ACSF containing both DA (100 μ M or 100 nM) and sodium metabisulfite (50 μ M) was then washed onto the slice for 10 minutes. Paired-pulse trains with the same IPIs were delivered (again at a frequency of 0.05 Hz) for a further two minutes at the end DA application. The experiment was then terminated after the PPS group in the presence of DA. Each paired-pulse, both before DA application and during DA application, were then expressed as a ratio (the second sweep : the first sweep) and each ratio was plotted on a logarithmic graph.

2.4 Immunohistochemistry

Instead of transferring to the holding chamber, slices which were used for immunohistochemical staining were transferred to a 24-well plate containing 4% paraformaldehyde (PFA, Sigma Aldrich, Montana, USA) in a fume hood and left for 1 hour at room temperature. The slices were then washed three times with 0.1 M phosphate buffered saline (PBS (Thermo Fischer Scientific, Massachusetts, USA)) at 20-minute intervals. The slices were then blocked with PBS containing 10% normal goat serum (NGS, Vector Laboratories, California, USA) and 1% Triton[®] X-100 (Sigma Aldrich, Montana, USA), which was subsequently incubated at room temperature for 2 hours whilst being gently shaken on a standard analogue shaker (VWR, Pennsylvania, USA). After 2 hours, the slices were then incubated in 0.1 M PBS containing 10% NGS, 0.3% Triton[®] X-100 and diluted primary antibody (rabbit anti-TH (Abcam, Cambridge, UK) at 1:1000 dilution) at 4°C for 3 days. The slices were then washed with 0.1 M PBS three times at 10-minute intervals. The slices were then incubated in 0.1 M PBS containing 10% NGS, 0.3% Triton[®] X-100 and diluted secondary antibody (goat anti-rabbit with Alexa 48 (Thermo Fischer Scientific, Massachusetts, USA) at 1:500 dilution) at room temperature on a shaker for 3 hours. Controls were tested adjacent to samples, with the aforementioned secondary antibody being omitted from wells in the last column. The slices were then washed three times with 0.1 M PBS at 20-minute intervals before being transferred to a clean, frozen microscope slide. One drop of Vectashield containing DAPI (Vector Laboratories, California, USA) was then added to the region containing the LEC before a cover slide was placed over the slice. All slices were then individually mounted and imaged using a Hamamatsu ORCA-Flash 2.8 Digital Camera (Hamamatsu Photonics K.K., Shizuoka, Japan), with images being taken as either a single snapshot image or as a Z-stack (multiple superimposed images taken at increments of 1 μ m through the slice).

2.5 Data Analysis

The peak fEPSP amplitude, as defined previously, of every 3 sweeps recorded by WinLTP were averaged, yielding an average synaptic response for each minute of the experiment. The first 30 minutes of the experiment were then averaged, with all successive datapoints being

expressed as a comparative percentage of this average. This mean data and \pm SEM bars were then plotted on a time-fEPSP graph. Once plotted, each group was tested for outliers (using the ROUT method of outlier identification, where the maximum false discovery rate (Q) = 1.0%) and whether each group shows normal Gaussian-distribution (using D'Agostino and Pearson's test). Experiments which saw a statistically significant deviation, with an unpaired t-test between the point of greatest change and its time matched control yielding $P < 0.05$, were then renormalised. This renormalisation was either to a re-established baseline during drug application, or to the final point before DA application if no baseline was re-established. Once the parametric nature of the data was identified and necessary datasets were renormalised, relevant statistical analysis was performed, including unpaired t-tests (when comparing two groups), ANOVAs (when comparing three or more groups) and ANOVAs with various post-hoc comparisons (when comparing three or more groups either against a control or against one another). Linear regression analysis was also used to statistically compare differences in two or more gradients in high concentration DA experiments. In all experiments, a threshold of $P < 0.05$ indicates a statistically reliable difference, with all p-values below this threshold showing a statistically reliable difference. The data handling and subsequent graphical and statistical analysis were all done using Prism (Prism v9.0.0, GraphPad, California, USA). All numbers are reported to 4 significant figures where appropriate.

3 Results - Controls and Initial Dopamine Experiments

3.1 Tyrosine Hydroxylase Immunohistochemistry

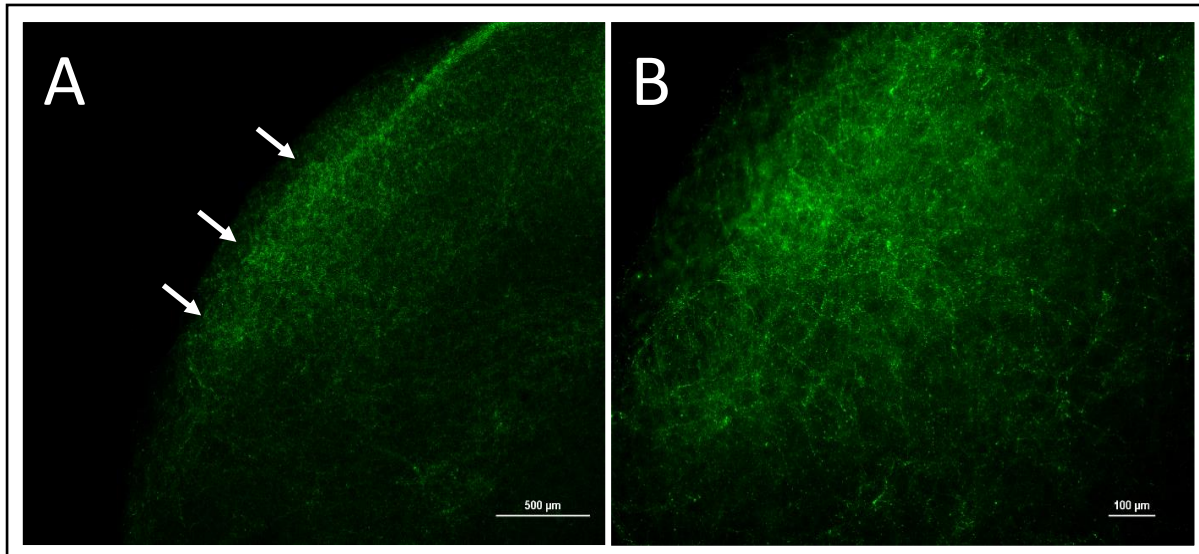


Figure 12 - Tyrosine Hydroxylase Staining Indicates the Presence of Dopaminergic Fibres in the Lateral Entorhinal Cortex. Shown is the tyrosine hydroxylase staining of the lateral entorhinal cortex from two separate rats, both of which P = 14. Figure 12A shows a single image of the upper region of the slice (where the lateral entorhinal cortex is located in the centre of the image) and Figure 12B shows a Z-Stack (where multiple individual images were captured with 1 μm separation along the z-axis, before being superimposed upon one another). Both figures show layers I-II of the LEC are rich in dopaminergic fibres, the region which all electrophysiological experiments were carried out in. Figure 12A also identifies dopaminergic clusters (referred to as islands), which are indicated with white arrows. A measurement scale for both the images is shown in the bottom right of the images, 500 μm and 100 μm for 10A and 10B respectively.

There have been numerous papers which look at both the afferent dopaminergic projections to the LEC and their physiological role, yet experimental evidence of dopaminergic fibres within the region remain somewhat unreported. Immunohistochemical staining for DA fibres in the LEC have been examined previously (D. Caruana, personal communication, October 10, 2018), thus the aim of this experiment was to both support these previous findings and more importantly to confirm that these afferent dopaminergic projections exist within the strains and age of animals used. The results of the tyrosine hydroxylase (TH) immunohistochemistry are shown in Figure 12. Two forms of image capture were used, individual snapshot (Figure 12A) and a z-stack, capturing multiple individual snapshots 1 μm apart (along the z-axis) throughout the slices before being superimposed upon one another (Figure 12B). The presence of TH is indicative of the presence of dopaminergic fibres, meaning the LEC both receives a substantial afferent projection and also shows the island-like deposits (white arrows in Figure 12A), both of which had been reported previously (Caruana and Chapman, 2008).

3.2 Control Experiments

3.2.1 ACSF Changeover Control

A majority of electrophysiological experiments in the LEC assess the changes observed upon the introduction of a new stimulus (for example the introduction of DA), yet no reported experiments have looked to assess if the process of changing solution affects the results in any way. The ACSF changeover control ($n = 5$) experiment was subsequently carried out, which consisted of changing the ACSF source after a 30-minute baseline was achieved, before changing back to the original ACSF source after 30 minutes (Figure 13). Throughout application, fEPSP depressed by an average of $3.419 \pm 1.644\%$ of baseline levels, whereas the control experiment showed a $1.830 \pm 1.567\%$ facilitation of baseline levels. This depression however was not statistically significantly different, [$F_{(2,20)} = 2.13, p > 0.05$]. This was concluded by a 2x3 (group x time) way repeated measures ANOVA over the three distinct subregions. These three subregions (the baseline, application of the new ACSF and the washout) were all averaged across their respective whole duration, with the RM ANOVA being conducted on those averages. Given that the p-value is above the predetermined threshold, changing the ACSF source alone does not induce any significant change in field synaptic transmission.

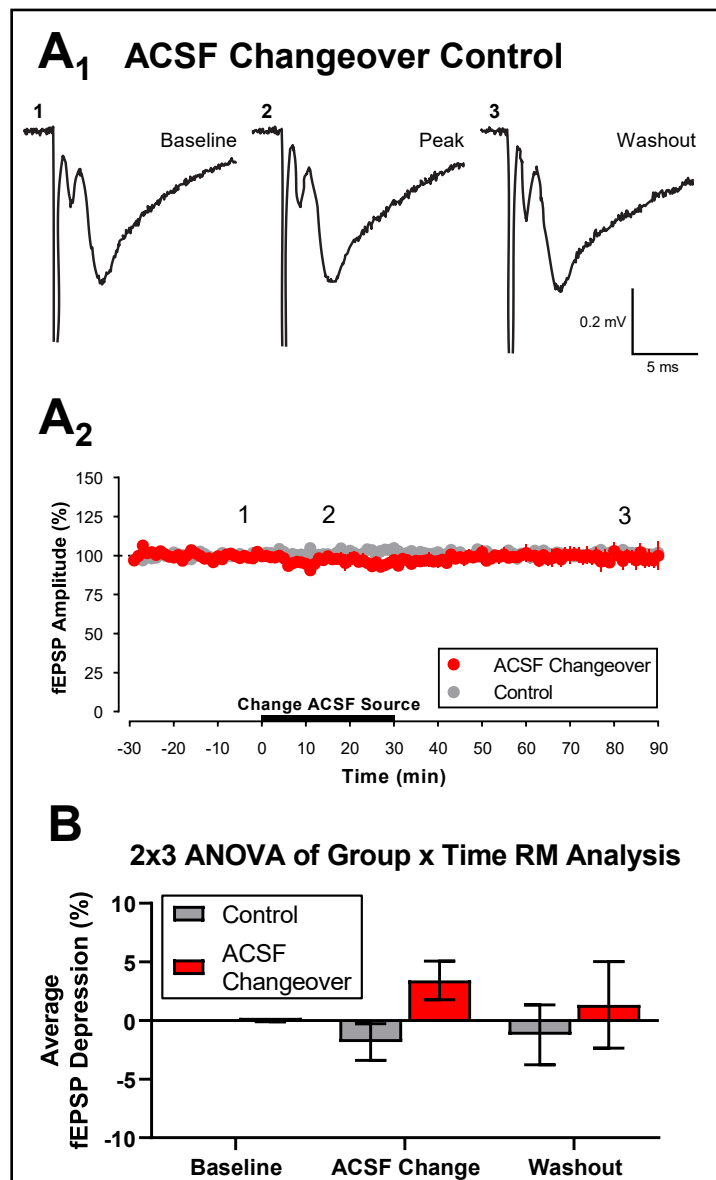


Figure 13 - Changing the Source of ACSF Showed No Significant Change in Synaptic Responses. Amplitudes were averaged over every minute and expressed as a percentage of the baseline levels for this and all successive figures. **(A)** Averaged fEPSPs before, during and after changing the source of ACSF. **(A₁)** Example traces that were taken at three different time points show no change in amplitude throughout the experiment. The numbered traces are taken from specific time points throughout the experiment, corresponding with the numbers shown in A₂. Stimulus artefacts were partially removed at the bottom. **(A₂)** ACSF changeover control experiment superimposed on an untampered control. The ACSF changeover experiment shows a slight diminishment in synaptic response at approximately +7 min which persists throughout the changeover but returns swiftly after the second change in ACSF source. **(B)** A histogram showing the 2x3 RM ANOVA comparing different time points in the experiment (corresponding to the sweeps in A₁ and their time matched controls). Error bars show \pm SEM of the group mean.

3.2.2 Sodium Metabisulfite Vehicle Control

Unlike the ACSF changeover control, this control, isolated application of the antioxidant vehicle (in these experiments sodium metabisulfite) is often reported alongside DA experiments as a control, in all cases showing no statistically significant difference upon application. The sodium metabisulfite vehicle control ($n = 5$) consisted of a 30-minute isolated application of $50\mu\text{M}$ $\text{Na}_2\text{S}_2\text{O}_5$ in ACSF (Figure 14). Application of sodium metabisulfite showed a small depression throughout its application, depressing by an average of $2.223 \pm 3.065\%$ of baseline levels, whereas the control showed a $1.830\% \pm 1.567\%$ facilitation of baseline levels during this time. This depression however was not statistically significantly different, [$F_{(2,18)} = 1.05, p > 0.05$], as was confirmed by a 2x3 (group x time) way repeated measures ANOVA. As with the previous RM ANOVA, the experiment was divided into its three subsections (baseline, vehicle application and washout), each being averaged before a RM ANOVA was conducted on these averages. As the obtained p-value is significantly greater than the predetermined threshold value of 0.05, application of the antioxidant vehicle elicits no significant changes in synaptic transmission, supporting previously reported experiments.

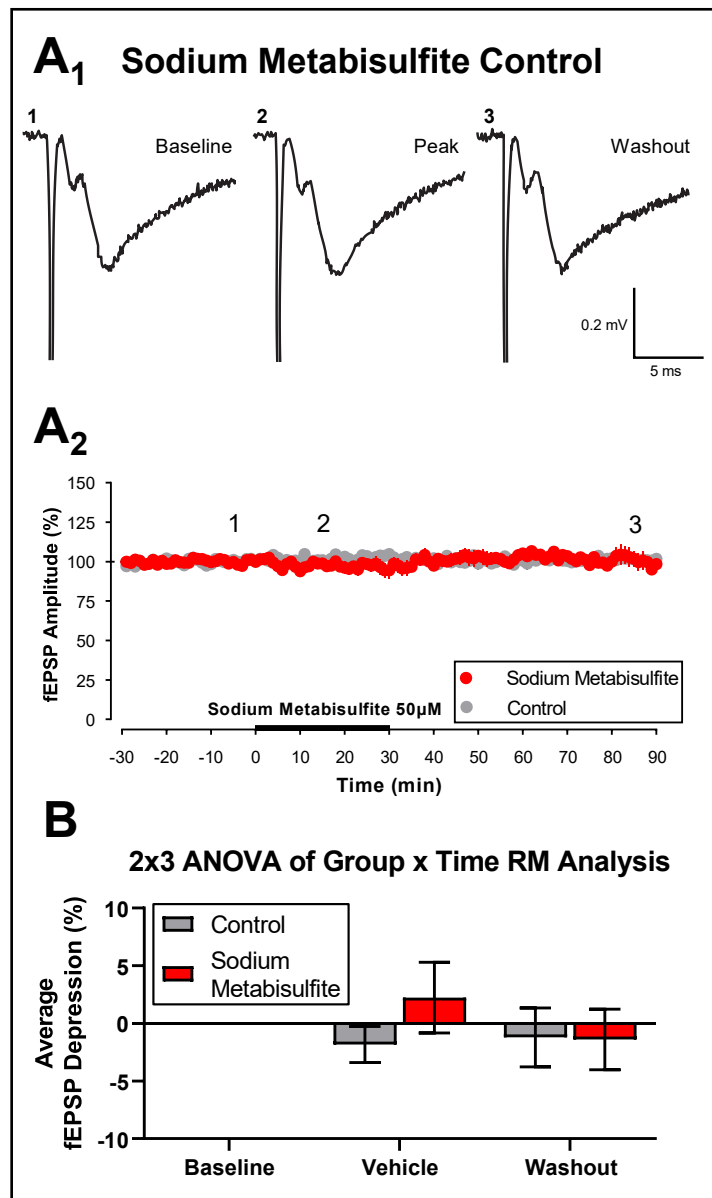


Figure 14 - Isolated Application of Sodium Metabisulfite Showed No Significant Change in Synaptic Responses. (A) Averaged fEPSPs before, during and after changing the addition of sodium metabisulfite (**A₁**) Example traces that were taken at three different time points show no change in amplitude throughout the experiment. The numbered traces are taken from specific time points throughout the experiment, corresponding with the numbers shown in **A₂**. Stimulus artefacts were partially removed at the bottom. (**A₂**) Sodium metabisulfite control experiment superimposed on an untampered control. The sodium metabisulfite experiment shows a slight depression upon application (black bar) but returns to baseline levels swiftly during washout (**B**) A histogram showing the 2x3 RM ANOVA comparing different time points in the experiment (corresponding to the sweeps in **A₁** and their time matched controls). Error bars show \pm SEM of the group mean.

3.3 Dopamine Applications at Low Concentrations

3.3.1 Single Application

Previous field experiments assessing tonic application of DA within the LEC have all looked at tonic application of DA at micromolar concentrations (Caruana *et al.*, 2006; Harvey *et al.*, 2021). However, it may be possible that DA within LEC exists physiologically at much lower concentrations, thus it may be possible that analysis of nanomolar concentrations of DA may provide a more of an understanding of the physiological role of DA. Subsequently, multiple nanomolar concentrations of DA (1 nM, 10 nM, 100 nM and 300 nM, all of which $n = 8$) were individually washed onto the slice, each for a 30-minute duration once a baseline was achieved (as is identified by the black bars in each graph in Figure 15). The experiments were superimposed (Figure 15E), then divided into two distinct subregions, DA application (Figure 15F₁) and the final 15 minutes of the washout (Figure 15G₁).

Peak analysis during DA application, would show whether or not DA application had any immediate or direct effect on synaptic transmission. At their peak changes in fEPSP, application of 1 nM and 10 nM showed a depression of baseline levels, depressing to $94.33\% \pm 3.564\%$ and $91.20\% \pm 3.700\%$ respectively. Application of 100 nM and 300 nM however produced a facilitative response at their peak change in fEPSP, facilitating to $109.2\% \pm 4.297\%$ and $105.8\% \pm 5.361\%$ of baseline levels respectively. Of these applications however, only 10 nM showed a statistically reliable significance compared to its time matched control, $p = 0.0200$ at $t = +28$ minutes. All other applications were not statistically significantly different from their time matched controls (1 nM ($p = 0.2284$); 100 nM ($p = 0.3450$); 300 nM ($p = 0.8518$)), each of which was shown using individual t-tests. Despite this insignificance, each test was statistically reliably different to one another, [$F_{(4,33)} = 3.76, p < 0.05$] and [$F_{(3,28)} = 4.30, p < 0.05$; see Table 2A] respectively, as concluded with a one-way ANOVA between all residuals.

Analysis of the peaks in the second region, the final 15 minutes of the experiment, may indicate if application of nanomolar DA elicited any indirect, long-lasting changes in LEC synaptic transmission. Unlike the bidirectional affect seen during DA application, all concentrations of DA produced a facilitative response during their washout. The largest of these facilitations, 1 nM, facilitated to $121.2\% \pm 8.116\%$ of baseline levels. The next largest facilitation was 100 nM DA application, which facilitated to $114.8\% \pm 4.224\%$ of baseline levels. This was followed by 300 nM, facilitating to $110.7\% \pm 4.034\%$ of baseline levels, with 1 nM facilitating the least, facilitating to $108.2\% \pm 6.457\%$ of baseline levels. These facilitations however were not statistically reliably significant either in the presence or absence of the control, [$F_{(4,33)} = 1.51, p > 0.05$] and [$F_{(3,28)} = 0.91, p > 0.05$; see Table 2B] respectively, with neither of the experiments passing the threshold in either one-way ANOVA. The peak change in fEPSP during 100 nM DA application was however statistically reliably significant from its time matched control ($p = 0.0426, t = 76$ minutes) whereas no other concentration showed this significance through individual t-tests between peaks and their time matched controls (1 nM yielded $p = 0.0813$; 10 nM yielded $p = 0.3450$ and 300 nM yielded $p = 0.0813$).

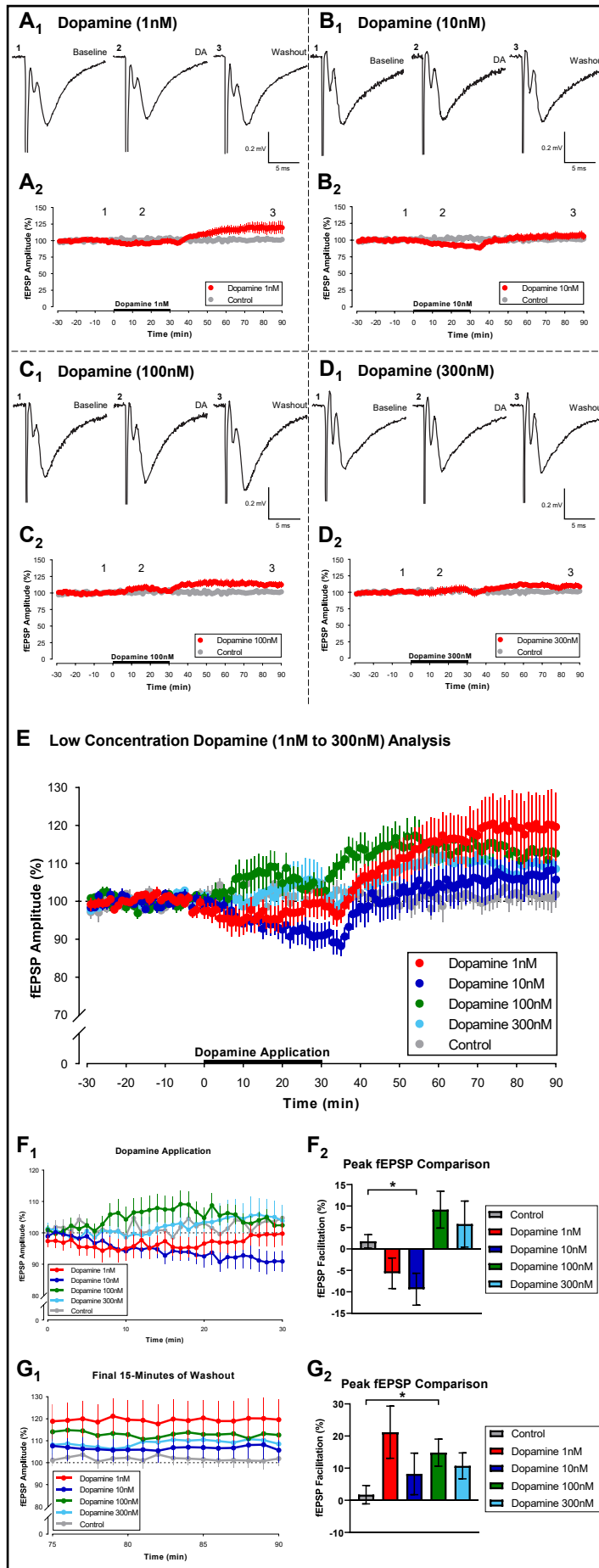


Figure 15 - Application of Low Concentration Dopamine Elicits a Concentration Dependent Effect During Tonic Application and a Facilitative Effect After Removal. (A-D) Averaged fEPSPs before, during and after the addition of low concentration dopamine (abbreviated to DA when reporting traces in A₁-D₁). **(A₁-D₁)** Changes in sweep sizes taken at aforementioned time points (also corresponding with the numbers shown in A₂-D₂ respectively) match the changes shown by their accompanying graphs. Electrical stimulation artefacts were partially removed at the bottom in order to enhance the key aspects of the waveform. **(A₂-D₂)** Low concentration DA experiments superimposed on a control experiment. **(A₂)** DA application shows an initial depression upon application, recovering to baseline levels prior to DA removal. Once removed the amplitude then begins to facilitate and remains facilitated until the end. **(B₂)** DA application causes a gradual decrease in fEPSP amplitude throughout application, before quickly recovering to baseline levels upon removal. **(C₂ and D₂)** Both show a mild facilitative effect upon DA application, which both recover to baseline levels prior to DA removal. Both also show a facilitation upon DA removal, with C₂ showing larger facilitations in both instances than D₂. **(E)** All low concentration DA experiments superimposed upon one another. **(F₁)** Superimposed low concentration DA experiments shortened to show only the region during which DA is applied (t = 0-30 minutes). **(F₂)** A histogram comparing peak fEPSP facilitations of all low concentration DA experiments with one another (as is also shown in Table 2A) and the control. Experiments which fall below the zero line (1 nM and 10 nM) show a depressive response, whereas all other experiments show a facilitative response. **(G₁)** Superimposed low concentration experiments are this time shortened to show only the final 15 minutes of the washout (t = 75-90 minutes). **(G₂)** A histogram comparing peak fEPSP facilitations of all low concentration DA experiments with one another (as is also shown in Table 2B) and the control. Error bars show \pm SEM of the group mean. Asterisks (*) indicate statistically reliable differences between two groups.

Table 2 - Post Hoc Comparisons Between Low Concentration Dopamine Applications Shows No Statistically Significant Difference Between Any Experiment. Post hoc analysis (Dunn's multiple comparisons test) between low concentration experiments of DA, showing their mean rank difference, their significance and their adjusted p-value. **(A)** Post hoc comparisons test during low concentration DA application (t = 0-30 minutes, Figure 15F). **(B)** Post hoc comparisons test for the final 15 minutes of the experiment (t = 75-90 minutes, Figure 15G). In both these multiple comparison tests, no experiments showed any statistically reliable difference.

A - DA Application Comparison			
Dunn's multiple comparisons test	Mean rank diff.	Significant?	Adjusted P Value
Dopamine 1 nM vs. Dopamine 10 nM	3.250	No	>0.9999
Dopamine 1 nM vs. Dopamine 100 nM	-12.00	No	0.3080
Dopamine 1 nM vs. Dopamine 300 nM	-10.00	No	0.7191
Dopamine 10 nM vs. Dopamine 100 nM	-15.25	No	0.0606
Dopamine 10 nM vs. Dopamine 300 nM	-13.25	No	0.1710
Dopamine 100 nM vs. Dopamine 300 nM	2.000	No	>0.9999

B - Washout Comparison			
Dunn's multiple comparisons test	Mean rank Diff.	Significant?	Adjusted P Value
Dopamine 1 nM vs. Dopamine 10 nM	12.97	No	0.8849
Dopamine 1 nM vs. Dopamine 100 nM	6.355	No	0.9970
Dopamine 1 nM vs. Dopamine 300 nM	10.47	No	0.9181
Dopamine 10 nM vs. Dopamine 100 nM	-6.613	No	0.9869
Dopamine 10 nM vs. Dopamine 300 nM	-2.500	No	>0.9999
Dopamine 100 nM vs. Dopamine 300 nM	4.113	No	0.9971

3.3.2 Repeated 100 nM Dopamine Application

As 100 nM DA application was the only nanomolar concentration tested that showed a statistically significant facilitation during its washout, a successive application of 100 nM DA was tested to identify if the observed facilitation during washout possessed additive properties. Previous experiments assessing double applications of DA showed that, at micromolar concentrations, the second application of DA showed a substantially reduced effect on fEPSP (Harvey *et al.*, 2021). This however was only tested on micromolar concentrations of DA, so the effect that nanomolar concentrations of DA may exhibit was yet to be observed. Subsequently, 100 nM DA was applied twice (n = 8), initially between 0 and 30 minutes and secondly between 90 and 120 minutes (Figure 16). Upon initial application, fEPSP showed an average facilitation of $5.251\% \pm 2.752\%$ of baseline levels, showing a greater facilitation during its second application, facilitating by an average of $7.456\% \pm 8.010\%$ of baseline levels (Figure 16B₁). As previous analysis showed that the facilitation during the application of DA was not statistically reliably significant, the peaks during DA application was not assessed again. Instead, the changes in baseline levels over time was measured, which was not shown to be statistically significant, [$F_{(4,48)} = 0.55$, $p > 0.05$]. This was measured using a 2x5 (group x time) way repeated measures ANOVA, with timepoints taken from the peak in: in the baseline (1); during the first DA application (2); during the first washout (3); during the second DA application (4) and during the second washout (5), all of which correspond to the numbers shown in Figure 16A₂. This therefore shows that although both washouts showed facilitation, it is very likely that the observed facilitative effect during washout is not additive.

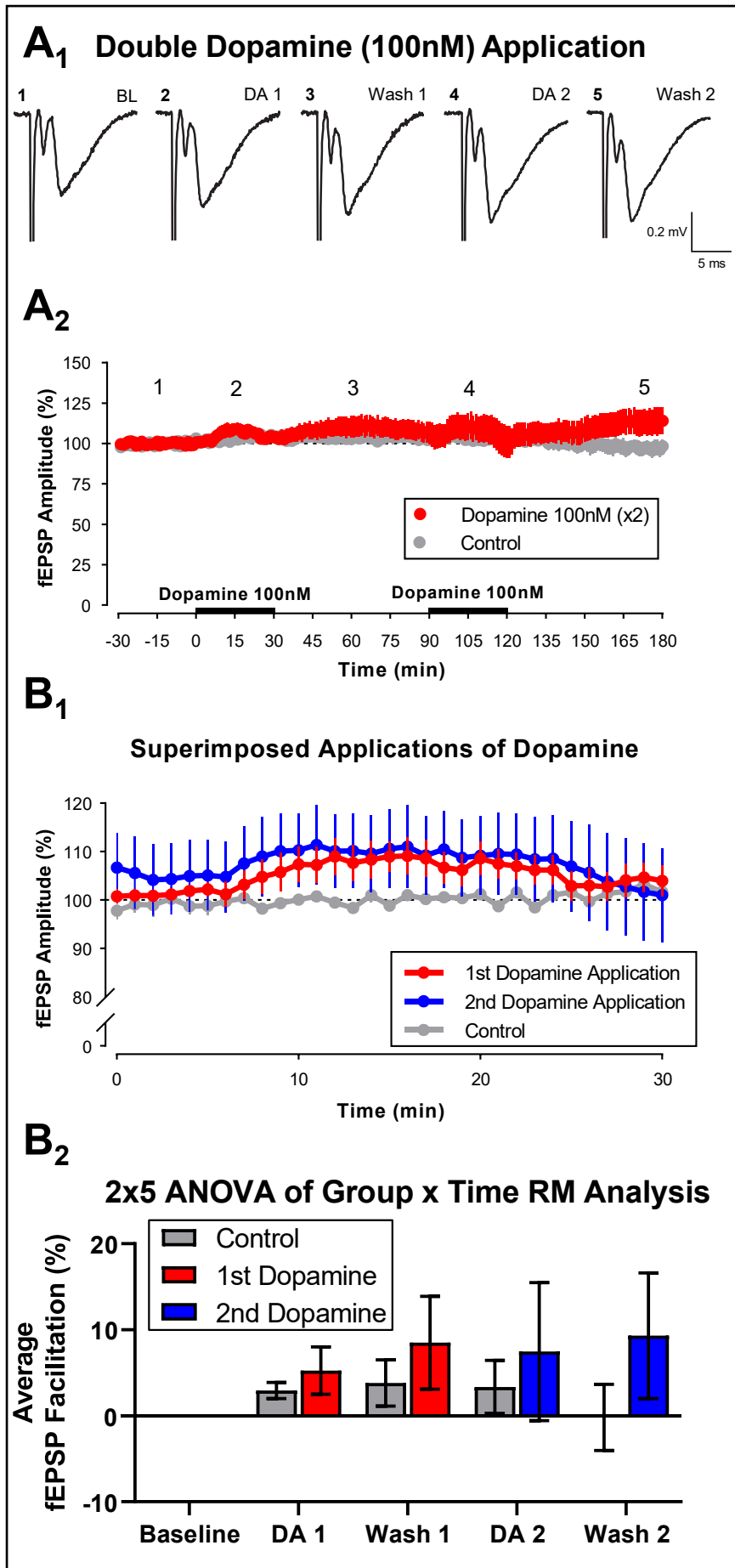


Figure 16 – Sequential Application of 100 nM Dopamine Shows No Statistically Significant Changes During Either Application. (A) Averaged fEPSPs taken before any DA, during the first application of DA, between the two DA applications, during the second DA application and after the last DA application. These time points taken correspond to the numbers shown below in A₂. **(A₁)** Example traces taken from the aforementioned time points throughout the experiment show a gradual increase in the amplitude of the sweeps throughout the experiment. There is minimal increase however between the final two traces, which corresponds to the changes shown below in A₂. Abbreviations shown are BL (Baseline); DA (dopamine application) and wash (washout). Electrical stimulation artefacts were partially removed at the bottom as this highlights the biological components of the waveform clearer. **(A₂)** Double 100 nM DA application experiment superimposed upon an untampered control. The DA experiment shows facilitations during both DA applications (black bars) as well as during both washouts, but all of these facilitations are only temporary, returning back to baseline levels before the end of the respective time points (asides from washout 2). **(B₁)** Both periods of DA application superimposed upon one another against the untampered control. **(B₂)** A histogram showing the 2x5 RM ANOVA comparing different time points (corresponding to both the sweeps in A₁ and the numbers in A₂). Error bars show \pm SEM of the group mean.

4 Results - Pharmacological Analysis of Cell Types Present Within the LEC

4.1 Pharmacological Analysis of Antagonists with 100 μ M Dopamine

As 100 μ M application of DA regularly provides not only a statistically significant response, but also one that is repeatable and thus reliable (Harvey *et al.*, 2021), the following experiments looked at coapplying 100 μ M DA with various receptor inhibitors to observe the roles the targets play in transmission. Comparing changes in fEPSP amplitude between antagonist experiments and isolated 100 μ M DA application experiments may subsequently give an indication into the role each targeted biomolecule plays in synaptic transmission, thus will provide evidence for their physiological role.

4.1.1 AP5 and Dopamine

The first of the targeted receptors, NMDARs, are one of the primary receptor types on excitatory glutamatergic neurones. Although glutamate is heavily implicated throughout the LEC, experiments blocking glutamatergic neurones may provide a better understanding of its physiological role and the role it plays in conjunction with DA.

The NMDAR antagonist AP5 (50 μ M, $n = 8$) was initially applied by itself once a 30-minute baseline was achieved, before being coapplied with 100 μ M DA for a further 30 minutes (Figure 17). As Figure 17A₂ shows a reduction in amplitude upon AP5 application, the experiment was renormalised to $t = +10$ minutes, as highlighted in Figure 17B. In these experiments, application of 100 μ M DA alone showed a depression to 52.80% \pm 2.858% of baseline levels, whereas coapplication of 100 μ M DA and AP5 showed a greater depression, depressing to 38.17% \pm 3.783% of baseline levels. These peak depressions observed were tested against their time matched controls, showing a statistically reliable significance between all four residuals, [$F_{(2,14)} = 128.4$, $p < 0.05$]. Post hoc modifications on the one-way ANOVA compared the ranks of the three groups (the control, 100 μ M DA as well as 100 μ M DA and AP5 applications) showed that all three groups were statistically reliably different from each other ($p < 0.05$), as is reported in Table 3. This further diminishment in fEPSP upon NMDAR antagonist application indicates that not only are measured fEPSPs glutamatergic, but also that DA can directly affect these glutamatergic transmissions, presumably by forming synapses directly onto postsynaptic glutamatergic neurones.

Table 3 - Coapplying Dopamine and AP5 Elicits a Statistically Significant Depression in Synaptic Transmission When Compared With Both Dopamine Application and the Untampered Control. Post hoc analysis (Dunnett's T3 multiple comparisons test) between 100 μ M DA, 100 μ M DA with AP5 and the control. All experiments showed a statistically reliable difference from one another.

Dunnett's T3 multiple comparisons test	Mean Rank Diff.	Significant?	Adjusted P Value
Dopamine + AP5 vs. Control	63.61	Yes	<0.0001
Dopamine + AP5 vs. Dopamine 100 μ M	14.64	Yes	0.0270
Control vs. Dopamine 100 μ M	-48.97	Yes	<0.0001

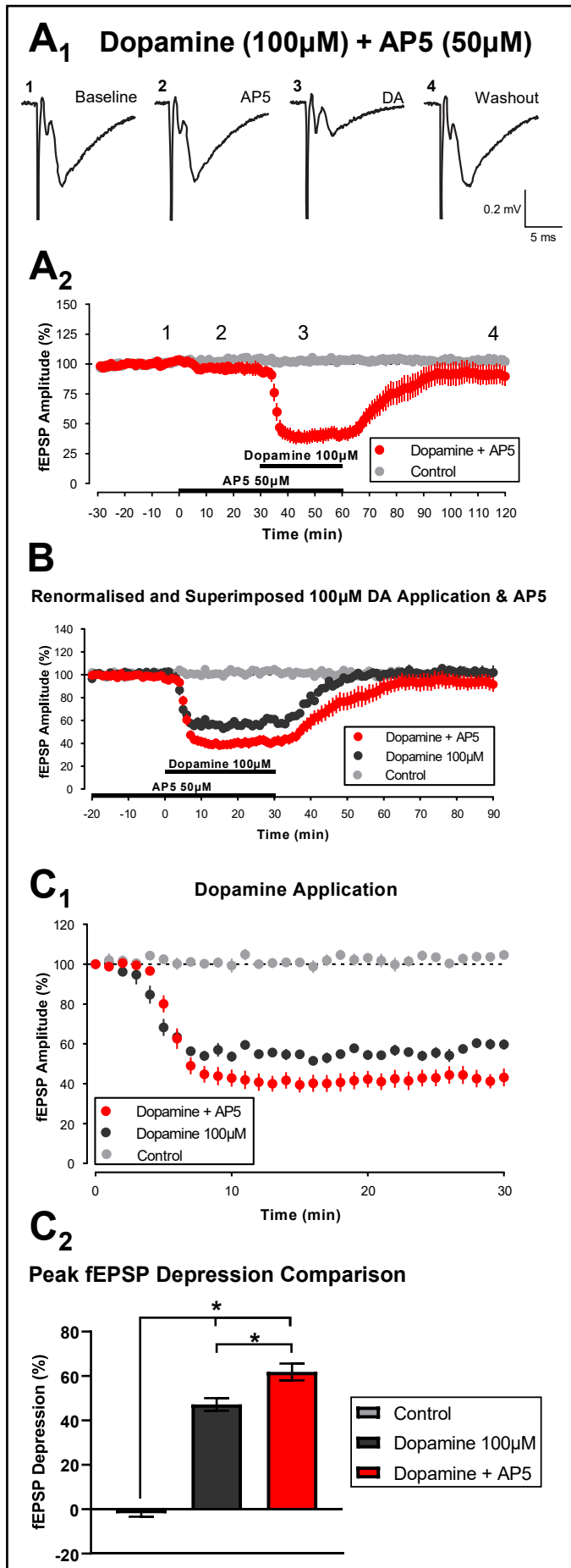


Figure 17 - Coapplication of the NMDAR Antagonist AP5 and a High Concentration of Dopamine Yields a Greater Depression than Dopamine on Its Own. (A) Averaged fEPSPs during the baseline, during AP5 application, during AP5 and DA application and during the washout. **(A₁)** Example traces that were taken at 4 separate time points throughout the experiment (time points which correspond to the numbers shown in A₂) show a minimal depression upon AP5 application (2), a significant depression upon DA application (3) and an approximate return to baseline levels once both chemicals were washed off (4). Electrical stimulation artefacts were partially removed at the bottom in all waveform images. **(A₂)** Superimposed 100 μ M DA with 50 μ M AP5 on an untampered control. This graph also shows a small depression upon AP5 application (lower black bar) and a greater depression upon AP5 DA coapplication (both upper and lower black bars). This depression then gradually returns to baseline levels before plateauing at approximately 90% after 90 minutes. **(B)** As AP5 addition was shown to significantly depress fEPSP amplitudes ($p = 0.0376$, see main text), the data was renormalised to $t = +10$ minutes. This renormalised data was then superimposed on two control experiments, 100 μ M DA and the untampered control. **(C)** The dataset was shortened to show only the region in which DA and AP5 are coapplied ($t = 30$ -60 minutes). **(C₁)** Data was renormalised to $t = 0$, before all aforementioned datasets were superimposed upon one another. **(C₂)** A histogram comparing the peak fEPSP depressions during DA and AP5 coapplication. Error bars show \pm SEM of the group mean. Asterisks (*) indicate statistically reliable differences between two groups.

4.1.2 SCH-23390, Sulpiride and Dopamine

Previous papers have shown that a high concentration of DA plays a predominantly depressive role within the LEC, however coapplication with the D1-like receptor antagonist (SCH-23390) and the D2-like receptor antagonist (sulpiride) with DA significantly reduces the depressive effect that DA plays on synaptic transmission (Caruana *et al.*, 2006). These experiments aimed to not only replicate the results shown previously, but also for a comparison between the two to be made.

The D1-like receptor antagonist SCH-23390 (10 μ M, n = 8) and the D2-like receptor antagonist sulpiride (50 μ M, n = 8), as well as the coapplication of both the antagonists (n = 8) were initially applied for 30 minutes once a 30-minute baseline was achieved. Each isolated drug application, as well as their coapplication, yielded a significant reduction on fEPSP amplitude, so all three datasets were subsequently renormalised (Figure 18D). These experiments, as well as isolated DA application and an untampered control, were superimposed and then broken down into two different subsections, initial onset of DA-mediated fEPSP depression (the initial 10 minutes of DA application, Figure 18E) and the entirety of the 30-minute DA application period (Figure 18F). The 30-minute DA application was then subdivided into two further subsections, the peak fEPSP depression (Figure 18F₂) and the final 18 minutes of DA application (Figure 18F₃).

Analysis of the first of these subregions (initial onset of DA-mediated fEPSP depression) using linear regression analysis would indicate any changes in the rate at which DA reaches its maximum observed effect, the shallower the slope the longer DA takes to elicit its maximum affect. This initial 10 minutes was further constricted to minutes 3-8, before a straight line of best fit for each experiment was generated (Figure 18E). Each experimental line of best fit showed a statistical significance from zero (as is shown by the key in Figure 18E₁), showing that each experimental condition elicited a significant effect on postsynaptic responses. Comparison between each gradient showed that experiments using DA antagonists were statistically reliably different to experiments without antagonists, but they were not significant between themselves. This was shown using a simple linear regression analysis, which compared each experiment by assessing the SEM of the gradient and its degrees of freedom. This therefore shows that application of DA antagonists suppresses the cellular mechanisms underpinning DA-induced fEPSP depression, resulting in DA taking significantly longer for it to exhibit its maximum affect. These results do however suggest that this rate is neither D1-like nor D2-like receptor-mediated, as there was no statistically reliable difference between any of the antagonist application experiments.

The second of these subregions, peak fEPSP depression by DA, was shown to be statistically significant in all instances where 100 μ M DA was applied to the slice. SCH-23390 application depressed responses to 67.55% \pm 3.104% of baseline levels, sulpiride application depressed responses to 67.54% \pm 3.527% of baseline levels and their coapplication depressed responses to 64.56% \pm 3.190% of baseline levels. Although coapplication of SCH-23390 and sulpiride appeared to show a slightly greater depression in fEPSP amplitude, the three groups were not statistically significant from one another, [$F_{(2,21)} = 0.2755$, $p > 0.05$], as was indicated

using a one-way ANOVA. All three of these observed changes in responses did however show a smaller reduction in amplitude compared to isolated 100 μM DA application, which showed a depression to 48.69% \pm 2.171% of baseline levels at its peak effect. Statistical analysis between DA application with and without antagonists confirmed this observation, as the p-value was below the threshold, [$F_{(4,27)} = 33.17$, $p < 0.05$], as shown using a one-way ANOVA with post hoc comparisons (Table 4) and reported graphically in Figure 18F₂. As DA antagonist application showed statistically reliable differences from both the control and 100 μM DA application, the DA-mediated response was not entirely blocked but instead was significantly reduced. However, similarly to the results shown in the previous paragraph, these results suggest that effect is neither D1-like nor D2-like receptor-mediated, as there was no statistically reliable significance between any of the DA antagonist application experiments (as concluded in the post hoc analysis).

Lastly, gradient analysis of each experimental condition after DA had exerted its maximum effect on fEPSP amplitude (in these experiments this was defined as the final 18 minutes) may indicate the different roles each DA receptor may play in DA desensitisation, potentially suggesting one receptor may lose its sensitivity to DA faster than the other. The gradient of each experiment was then tested against zero, which concluded that experiments which contained SCH-23390 were not statistically non-zero, with its isolated application and its coapplication with sulpiride yielding [$F_{(1,150)} = 0.75$, $p > 0.05$] and [$F_{(1,150)} = 0.21$, $p > 0.05$] respectively. These results were shown through a linear regression analysis, similar to that shown two paragraphs ago, which also showed that all three other experiments were statistically reliably non-zero ($p = 0.0053$ and $p = 0.0173$ for isolated DA application and the coapplication of DA and sulpiride respectively). Although experiments in which SCH-23390 was applied was not shown to be statistically significant from zero, the gradients (as well as the standard error of the slope) of each experiment are not statistically significant from one another, [$F_{(4,4)} = 1.104$, $p > 0.05$], as was shown by the one-way ANOVA with post hoc modifications shown in Table 5. These results therefore indicate that SCH-23390 may in fact block DA desensitisation during application as neither experiment that applied the D1-like antagonist showed a statistically significant difference from zero. However, as the one-way ANOVA shows that there is no statistical significance between the slopes of each experimental condition, it may be the case that addition of D1-like and D2-like receptor antagonists shows no change in DA desensitisation, however this test showed a reduced statistical power compared to each individual linear regression analysis.

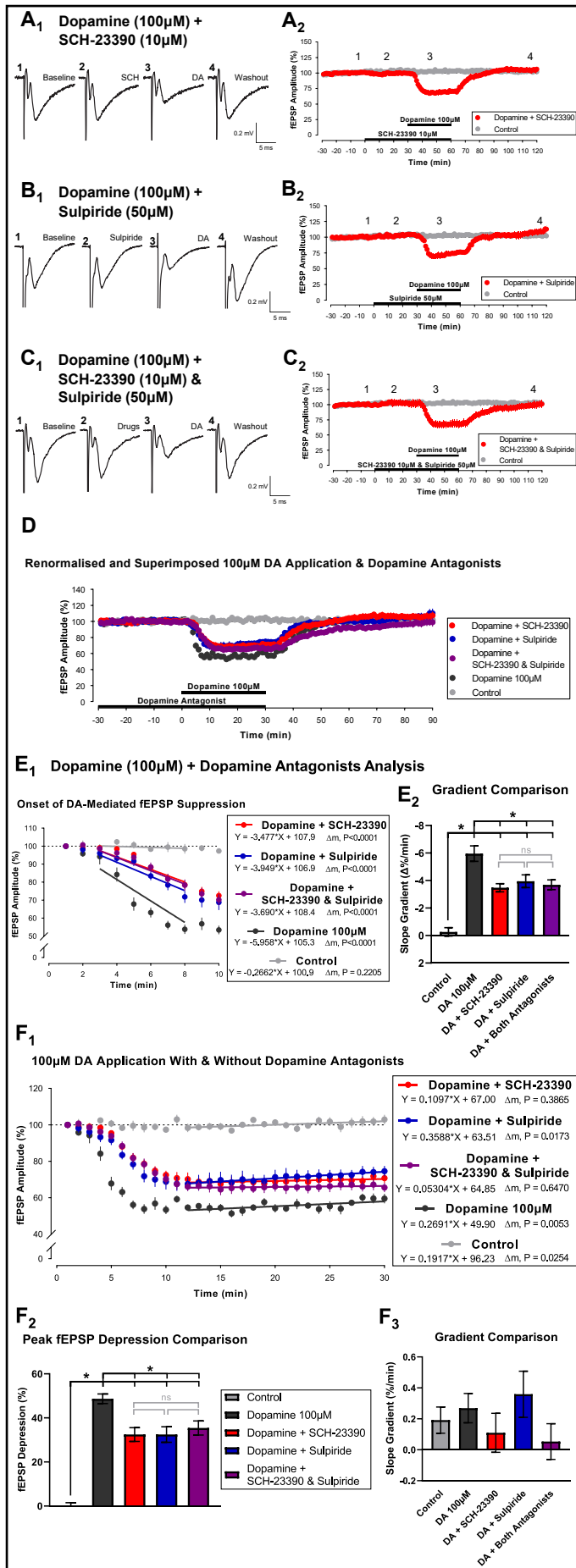


Figure 18 - Application of the D1-Like Receptor Antagonist SCH-23390, the D2-Like Receptor Antagonist Sulpiride and Their Coapplication Significantly Reduces Both the Onset and the Peak of 100 μM Dopamine-Mediated fEPSP Depression, but Only SCH-23390 Showed Some Effect on Dopamine Desensitisation. (A-C) Averaged fEPSPs during the baseline, during DA antagonist application, during DA antagonist and DA coapplication and during the washout. (A₁-C₁) Example traces taken from highlighted time points across the experiment (corresponding to the numbers shown in A₂-C₂) match the changes shown by their accompanying graphs, showing little change when the DA antagonist is added (2), a large change when DA is added (3) and returning to baseline levels (4). Electrical stimulation artefacts were partially removed at the bottom as this is the non-biological component to the waveform. (A₂-C₂) All experiments show respective DA antagonist experiments superimposed upon an untampered control. (D) As all DA antagonist experiments showed statistically significant changes upon application when compared to their time matched controls (see main text), all experiments were renormalised to t = 0, which was subsequently superimposed upon the untampered control. (E) The dataset was shortened to show only the initial 10 minutes of DA application, highlighting the onset of DA-mediated depression. (E₁) Data was renormalised to the first point (t = +1 minute) and a straight line of best fit was plotted through minutes +3-8 for each experiment. The gradient of each line, as well as each lines comparison against zero, is shown in the key. (E₂) A histogram comparing the gradients shown in E₁. (F) The dataset was shortened to show only the region in which DA antagonists and 100 μM DA are coapplied together (t = 0-30 minutes). (F₁) Data was again renormalised, this time again to the time point t = +1 minute, before a straight line of best fit is then plotted through points between +12-30 minutes for each experiment. The gradient of each line, as well as each lines comparison against zero, is shown in the key. (F₂ and F₃) Histograms showing comparisons between peak fEPSP facilitation during DA application and the gradients of the lines of best fit produced in F₁. Error bars show ±SEM of the group mean. Asterisks (*) indicate statistically reliable differences between two groups and "ns" is used to identify groups which are not statistically significant from one another.

Table 4 - Coapplication of Dopamine Antagonists With Dopamine Shows a Statistically Significant Difference From the Control and Dopamine Application, However No Statistically Significant Difference is Shown Between Antagonists. Post hoc analysis (Dunnett's T3 multiple comparisons test) between 100 μ M DA, 100 μ M DA with SCH-23390, 100 μ M DA with sulpiride, 100 μ M DA with both SCH-23390 and sulpiride and the control. The results show a range of comparisons are not statistically reliably significant from one another ($p > 0.05$) and a range of comparisons are statistically reliably different ($p < 0.05$).

Dunnett's T3 multiple comparisons test	Mean Rank Diff.	Significant?	Adjusted P Value
Dopamine + SCH-23390 vs. Dopamine + Sulpiride	-0.01139	No	>0.9999
Dopamine + SCH-23390 vs. Dopamine + SCH-23390 & Sulpiride	-2.986	No	0.9980
Dopamine + SCH-23390 vs. 100 μ M Dopamine	-16.24	Yes	0.0096
Dopamine + SCH-23390 vs. Control	32.37	Yes	<0.0001
Dopamine + Sulpiride vs. Dopamine + SCH-23390 & Sulpiride	-2.975	No	0.9989
Dopamine + Sulpiride vs. 100 μ M Dopamine	-16.23	Yes	0.0210
Dopamine + Sulpiride vs. Control	32.38	Yes	0.0001
Dopamine + SCH-23390 & Sulpiride vs. 100 μ M Dopamine	-13.25	Yes	0.0427
Dopamine + SCH-23390 & Sulpiride vs. Control	35.36	Yes	<0.0001
100 μ M Dopamine vs. Control	48.61	Yes	<0.0001

Table 5 - There is No Statistically Significant Difference Between Gradients in Any Dataset Following Dopamine Exerting its Maximum Effect on Synaptic Transmission. Post hoc analysis (Dunnett's T3 multiple comparisons test) between 100 μ M DA, 100 μ M DA with SCH-23390, 100 μ M DA with sulpiride, 100 μ M DA with both SCH-23390 and sulpiride and the control. The summary for all comparisons shows no statistically significant difference between any groups ($p > 0.05$).

Dunnett's T3 multiple comparisons test	Mean Rank Diff.	Significant?	Adjusted P Value
Dopamine + SCH-23390 vs. Dopamine + Sulpiride	-0.2491	No	0.8343
Dopamine + SCH-23390 vs. Dopamine + SCH-23390 & Sulpiride	0.05666	No	>0.9999
Dopamine + SCH-23390 vs. 100 μ M Dopamine	-0.1594	No	0.9236
Dopamine + SCH-23390 vs. Control	0.08200	No	0.9971
Dopamine + Sulpiride vs. Dopamine + SCH-23390 & Sulpiride	0.3058	No	0.7015
Dopamine + Sulpiride vs. 100 μ M Dopamine	0.08970	No	0.9980
Dopamine + Sulpiride vs. Control	-0.1671	No	0.9335
Dopamine + SCH-23390 & Sulpiride vs. 100 μ M Dopamine	-0.2161	No	0.7685
Dopamine + SCH-23390 & Sulpiride vs. Control	0.1387	No	0.9354
100 μ M Dopamine vs. Control	-0.07740	No	0.9936

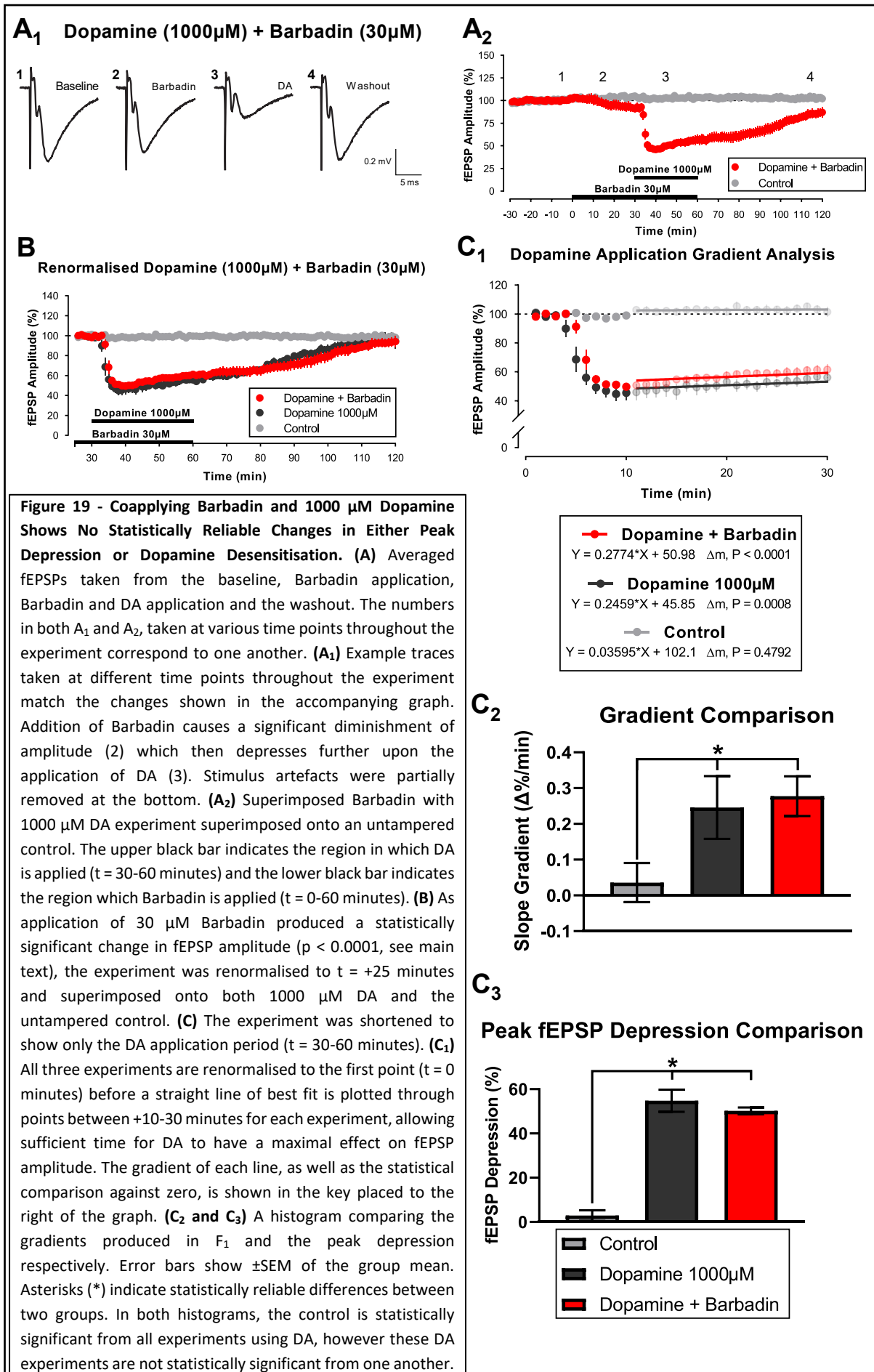
4.2 Pharmacological Analysis of Antagonists with 1000 μ M Dopamine

4.2.1 Barbadin and Dopamine

The final of the three receptor antagonists, Barbadin, targets the scaffolding protein β -arrestin. This protein is one of the two scaffolding proteins which allow D₂ receptors to elicit a G protein like response upon DA receptor activation, as was outlined in Chapter 1.2.2.2. This inhibition of D₂ receptor activation using Barbadin may therefore sequester the effect that D₂ receptors play in synaptic transmission, without affecting D1-like receptors (as β -arrestin is not present in the D1-like receptor cascade reaction). Although 100 μ M DA provides a significant and reliable response, DA-mediated desensitisation is not always observed. Previous experiments using 1000 μ M DA however (Harvey *et al.*, 2021) showed desensitisation during every experiment, so this concentration was chosen so that the potential effect elicited by these antagonists on desensitisation could be observed.

Barbadin (30 μ M, n = 8) was initially applied by itself for 30 minutes once the 30-minute baseline was achieved, before being coapplied with 1000 μ M DA for a further 30 minutes (Figure 19). Application of Barbadin resulted in a depression in fEPSP amplitude, through an unknown mechanism, so the data was renormalised to t = +25 minutes (Figure 19B). This experiment was, as with previous experiments, broken down into two subsections, the first 10 minutes of DA application (to compare peak fEPSP depressions) and the final 20 minutes of DA application (to compare linear regressions). Application of 1000 μ M DA showed a substantial depression in amplitude, depressing to 54.81% \pm 4.975% of baseline levels and an even greater depression to 50.23% \pm 1.537% of baseline levels when coapplied with Barbadin. Although addition of Barbadin appeared to enhance the depressive effect, the two peak changes in fEPSP were not shown to be statistically significant ($p > 0.9999$) by a one-way ANOVA with post hoc comparisons analysis. This therefore also shows that, under these experimental conditions, Barbadin had no statistically significant effect on the maximal depression that DA elicits on postsynaptic glutamatergic transmission.

As well as the peak depression during the first 10 minutes of DA application, the gradient in the final 20 minutes was also assessed. Comparing the gradients of isolated DA application and coapplication of DA and Barbadin showed that both were statistically non-zero ($p = 0.0008$ and $p < 0.0001$ respectively), however there was no statistically reliable difference between the two [$F_{(1,227)} = 0.13$, $p > 0.05$]. These results from a linear regression analysis, as shown in Figure 19C and 19C₂, shows that Barbadin plays no effect on DA desensitisation under these experimental conditions.



4.2.2 SCH-23390, Sulpiride and Dopamine

Chapter 4.2.1 showed that DA desensitisation may be mediated through D1-like receptors as blockage of β -Arrestin, thus D2-like receptors, showed no change in desensitisation. This however contradicts with previous experiments in other parts of the cortex, which show desensitisation is through D2-like receptors (Kim *et al.*, 2003; Nimitvilai *et al.*, 2014 as further elaborated in Chapter 5.3.2.1.2), so further testing using previously tested antagonists was performed to test the reliability and repeatability of the previous outcome. The following experiments were therefore designed to assess the role of both SCH-23390 and sulpiride on DA desensitisation when coapplied with 1000 μ M DA because, as was mentioned in the previous paragraph, 1000 μ M DA reliably induces DA desensitisation during its application.

The D1-like antagonist SCH-23390 (10 μ M, $n = 8$) and the D₂-like antagonist sulpiride (50 μ M, $n = 8$) were again initially applied by themselves for 30 minutes once a 30-minute baseline was achieved, before being coapplied with 1000 μ M DA for a further 30 minutes (Figure 20). Of both these experiments, only sulpiride showed a statistically significant depression during its application, so that experiment was renormalised to $t = +29$ minutes. Application of 1000 μ M DA appeared to elicit a similar response in each experimental group, with SCH-23390 and DA depressing amplitude to 47.32% \pm 3.586% of baseline levels, sulpiride and DA depressing amplitude to 52.19% \pm 3.683% of baseline levels and 1000 μ M alone depressing amplitude to 54.81% \pm 4.975% of baseline levels. Statistical analysis between the groups confirmed this, as a one-way ANOVA showed a statistical significance between the experimental groups from the untampered control, [$F_{(3,21)} = 38.83$, $p < 0.05$], but not between themselves [$F_{(2,16)} = 0.85$, $p > 0.05$]. This non-significance observed on peak fEPSP during DA application, as is shown in Figure 20C₂, matches the results shown when Barbadin was coapplied with 1000 μ M DA, but contradicts with the results shown when the same antagonists were coapplied with the lower 100 μ M DA (Figures 19 and 18 respectively). This suggests that the observed fEPSP depression during 1000 μ M DA application acts entirely independently to antagonist application, a phenomenon which was not observed at any lower concentration.

The experiment was then shortened to show only region where DA was applied (Figure 20D₁), with a subsequent linear regression analysis being performed on the final 20 minutes, ensuring DA had exerted its maximum effect on fEPSP amplitude. This linear regression analysis (Figure 20D₁) produced lines of best fit for each experiment, with each lines gradient and statistical difference from zero both reported in the accompanying key. Although all gradients produced in experiments containing DA were statistically non-zero, comparisons between each gradient (and their respective SEMs) showed no statistical significance between the groups [$F_{(3,4)} = 2.40$, $p > 0.05$]. The one-way ANOVA comparing these gradients, as well as their SEMs, is shown in Figure 20D₂. This statistical insignificance shows that despite DA antagonists showing statistically significant changes under lower concentrations of DA, higher concentrations of DA in the presence of antagonists elicits no significant effect on synaptic transmission.

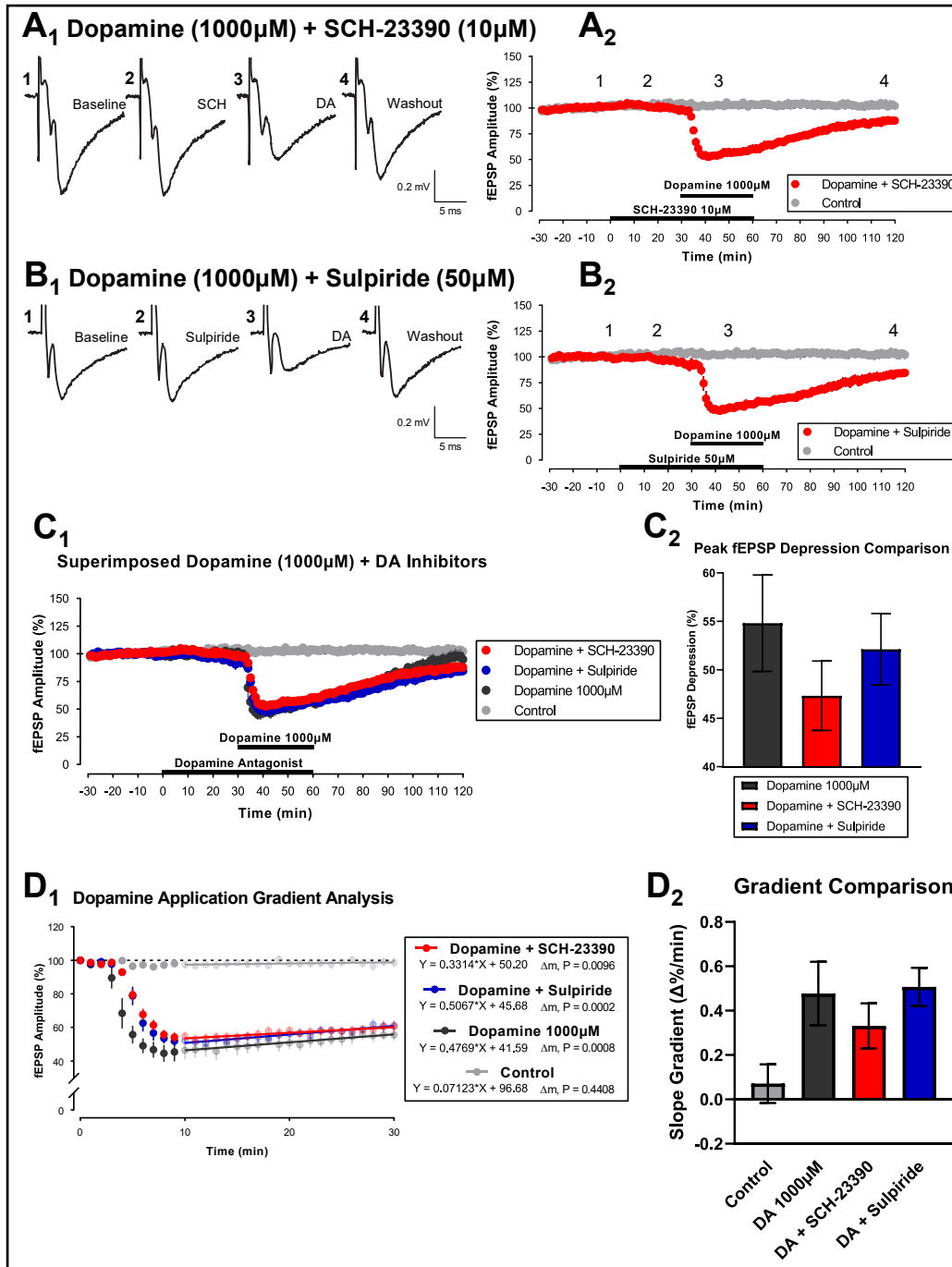


Figure 20 - Neither Application of the D1-Like Receptor Antagonist SCH-23390 or the D2-Like Receptor Antagonist Sulpiride With 1000 µM Dopamine Elicit Significant Changes in Peak Depression or Dopamine Desensitisation. (A and B) Averaged fEPSPs taken from time points corresponding to the numbers indicated in A₂ and B₂. (A₁ and B₁) Example traces taken throughout the experiment, during the baseline (1), drug application (2), drug and DA coapplication (3) and washout (4). Amplitudes represented by these traces matches the changes shown in the adjacent graph. Electrical stimulation artefacts were partially removed at the bottom in order to show the biological components to the waveform clearer. (A₂ and B₂) 100 µM DA with 10 µM SCH-23390 (A₂) and 50 µM sulpiride (B₂) experiments each superimposed on an untampered control. Both experiments show similar responses, showing a gradual depression during drug application (lower black bar) before rapidly depressing upon DA application (upper black bar) (C₁) All DA with DA antagonist experiments were superimposed on one another. (C₂) A histogram comparing peak fEPSP facilitation during DA application. (D₁) The experiment was renormalised to the first point (t = 0) and shortened to show just the DA application region (t = 0-30 minutes). A straight line of best fit is then plotted through points between +10-30 minutes for each experiment, with the lines gradient and its statistical comparison against zero, is shown in the accompanying key. (D₂) A histogram comparing the gradients produced in D₁. Error bars show ±SEM of the group mean.

4.3 Paired-Pulse Stimulation Tests

As mentioned in Chapter 1.3.4, methods for inducing plasticity, PPS across short IPIs moderate presynaptic release probabilities in glutamatergic neurones. Previous studies showed an optimum facilitation between 20-30 ms IPIs (Schulz *et al.*, 1994), however this paper looked at PPS within the hippocampus proper instead of the LEC directly. These experiments therefore aim to assess if the LEC possesses similar paired-pulse characteristics to the hippocampus, also providing a greater understanding of the role which glutamatergic and dopaminergic neurones play within the LEC.

4.3.1 Low Concentration Dopamine (100 nM)

Once the baseline was achieved, paired-pulses at logarithmic IPIs (10, 30, 100, 300 and 1000 ms) were delivered prior to DA application. 100 nM DA ($n = 6$) was then applied for 10 minutes, allowing sufficient time for DA to elicit its maximal effect, before paired-pulses (at the same IPIs as aforementioned) were again delivered to the slices. Pulse two was then expressed as a ratio of pulse one, with each paired-pulse being superimposed onto the same logarithmic graph (Figure 21). Although 100 nM application of DA previously showed a facilitation during application (see Chapter 3.3.1), application of 100 nM after the first PPS showed no statistical change in amplitude. Although this may indicate that 100 nM application of DA is not facilitative, neither dataset were statistically significant and both had changes in their respective parameters.

Comparing differences in IPIs before and after DA application was then analysed in two separate ways, comparing each IPI before and after DA application together, and comparing each IPI against one another. Comparisons between individual IPIs showed no identifiable change after DA application when compared to before application. Individual *t*-tests confirmed this, as 10 ms ($p = 0.9805$), 30 ms ($p = 0.6991$), 100 ms ($p = 0.8182$), 300 ms ($p = 0.8182$) and 1000 ms ($p = 0.1320$) were all above the statistical threshold. This therefore shows that application of 100 nM DA had no significant effect on the release probability within the presynaptic neurone, as none of these paired-pulses intervals showed any change. Although IPIs were not statistically significantly different between themselves, IPIs were statistically reliably different from one another. This was shown both before DA application [$F_{(4,11)} = 43.09$, $p < 0.05$] and during DA application [$F_{(4,11)} = 53.03$, $p < 0.05$]. As individual IPIs before and during DA application were not statistically significantly different from one another, they can be treated as similar. Post-hoc modifications of the previously tested one-way ANOVA between IPIs was then performed in IPIs during DA application. This post-hoc comparison showed that only 10 ms was statistically significantly different from all other IPIs, showing statistical significance from 30 ms ($p = 0.0003$), 100 ms ($p = 0.0004$), 300 ms ($p = 0.0014$) and 1000 ms ($p = 0.0016$). Each of these post hoc comparisons between IPIs during DA application are shown in Table 6. This comparison further reinforces the previous statement, as the same IPI interval curve is shown both before and during application, thus DA showed no statistical changes on IPI ratios at this concentration.

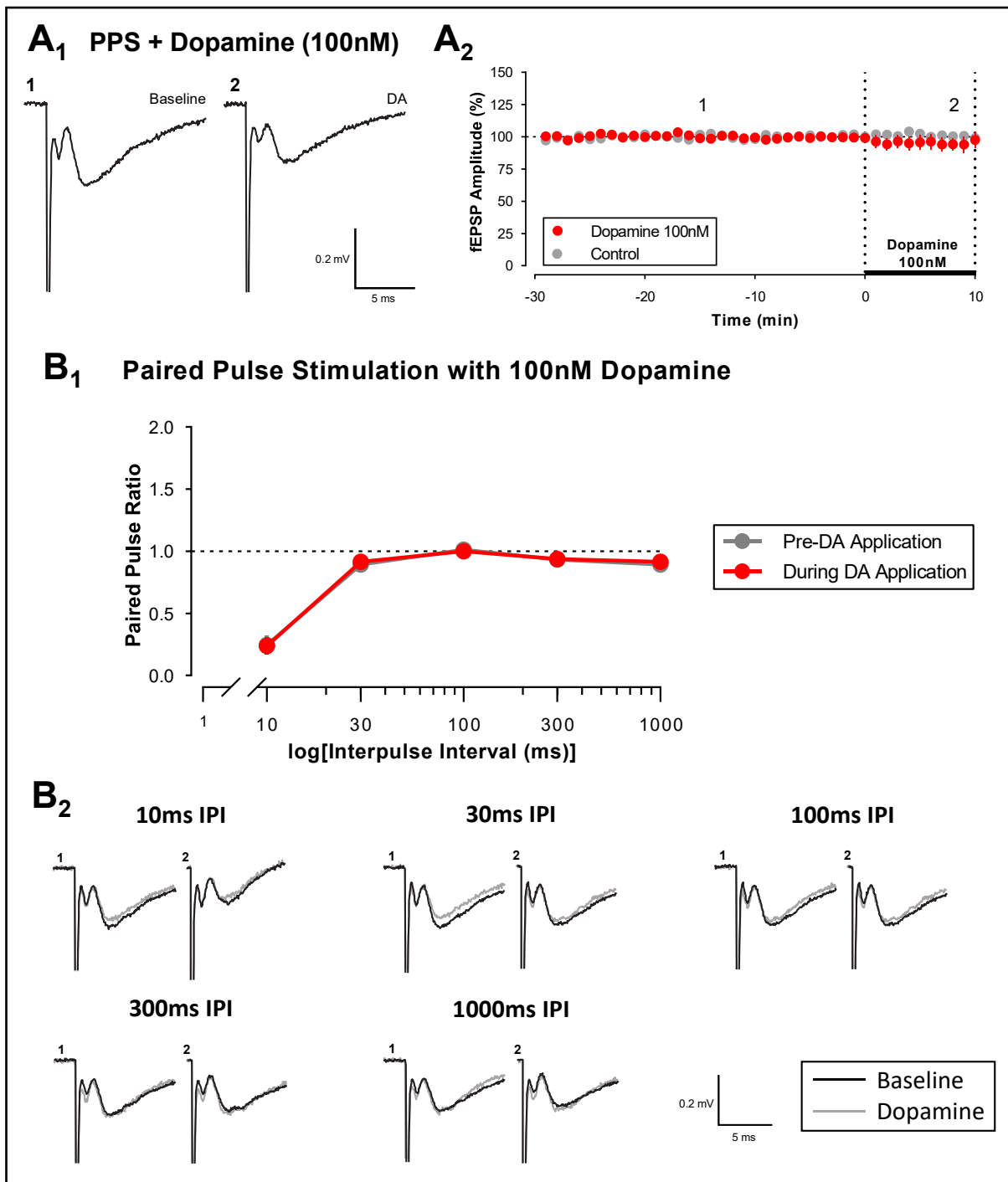


Figure 21 - Application of 100 nM Dopamine Produces No Statistically Reliable Changes in Paired-Pulse Ratios. (A) Averaged fEPSPs were taken from two timepoints across the experiment, baseline (1) and during DA application (2), time points which correspond to the numbers shown in A₂. (A₁) Example traces from the baseline and during DA application match the changes observed throughout the experiment, with DA application showing a minor (yet not significant) change in fEPSP amplitude. Electrical stimulation artefacts were partially removed at the bottom to best highlight the biological components of the waveform. (A₂) 100 nM DA application (black bar) superimposed onto an untampered control, with vertical dotted lines (indicated at t = 0 and +10 minutes) indicating the time point which paired-pulses were delivered. (B) Comparisons between paired-pulses prior to DA application and during DA application. (B₁) Paired-pulse ratios (measured as sweep 1 compared against sweep 2) from both before DA application (grey) and during DA application (black) were superimposed upon one another on a logarithmic scale. (B₂) Paired-pulse sweeps at noted interpulse intervals (IPI) both before DA and during DA superimposed upon one another. Error bars shown in A₂ and B₁ show \pm SEM of the group mean.

4.3.2 High Concentration Dopamine (100 μ M)

Although 100 nM application showed no statistically significant difference in either its single application (Chapter 3.3.1) or in paired-pulse experiments (Chapter 4.3.1), 100 μ M DA was tested again because of its reliability of yielding a consistently statistically significant response (as mentioned and shown throughout Chapter 4.1.2). Similarly to 100 nM DA paired-pulse experiments, paired-pulses (at the same logarithmic IPIs as mentioned previously) were delivered prior to and during DA application before both ratios (again pulse two to pulse one) were superimposed on a logarithmic graph (Figure 22). 100 μ M DA ($n = 6$) was then applied for 10 minutes, again allowing sufficient time for DA to exert its maximal effect on fEPSP amplitude. This maximal effect, at which a depression in amplitude to $40.66\% \pm 2.529\%$ of baseline levels, was shown to be significantly statistically different from the time matched control ($p < 0.0001$), indicating that the concentration of DA was large enough to significantly, and reliably, alter fEPSP amplitudes.

This experimental group was then analysed through the same parameters as 100 nM application PPS was, by assessing IPIs within each experimental group as well as IPIs between one another both before and during DA application. Unlike 100 nM PPS however, all IPIs were statistically significantly different during DA application compared to before application of DA. Confirmed by individual t-tests between each IPI, 10 ms ($p = 0.0022$), 30 ms ($p = 0.0022$), 100 ms ($p = 0.0087$), 300 ms ($p = 0.0325$) and 1000 ms ($p = 0.0087$) all yielded p-values below the required threshold ($p < 0.05$). As each of these IPIs showed statistical significance between themselves, comparisons between each other would be tested in both before and during DA application datasets. Comparison of IPIs before DA application showed a similar response to that observed in 100 nM application, also showing a statistically reliable significance before 100 μ M application [$F_{(4,17)} = 71.76$, $p < 0.05$]. In fact, before DA application IPI ratios in both 100 nM and 100 μ M PPS experiments were very similar to one another ($p = 0.2222$), as shown by a t-test between each IPI within the two experiments. Comparing IPIs during DA application also showed a statistically reliable difference between ranks also showed statistical significance, [$F_{(4,14)} = 9.00$, $p < 0.05$], as also confirmed by a one-way ANOVA. The post hoc comparisons for this ANOVA, as well as the post hoc comparisons from 100 nM DA PPS, is shown in Table 6. This indicates that a high-concentration application of DA plays a significant role in affecting presynaptic release probability, as all IPIs assessed here show not only a statistically significant difference, but paired-pulse facilitation is observed.

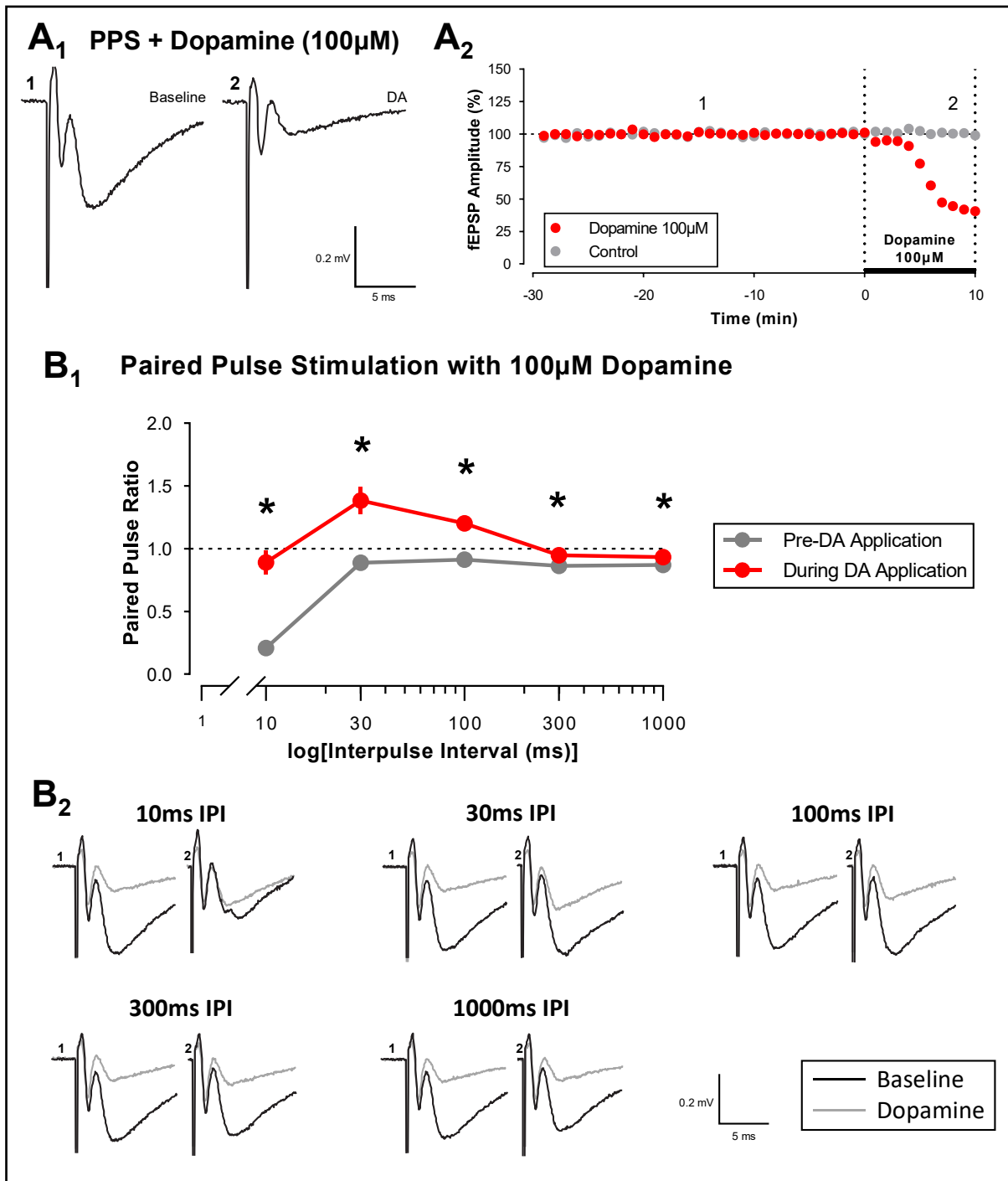


Figure 22 - Application of 100 μ M Dopamine Produces Statistically Significant Changes in Paired-Pulse Ratios. (A) Averaged fEPSPs were taken from two timepoints across the experiment, baseline (1) and during DA application (2), time points which correspond to the numbers shown in A₂. (A₁) Example traces from the baseline and during DA application match the changes observed throughout the experiment, with DA application showing a large (and significant) fEPSP depression. Electrical stimulation artefacts were partially removed at the bottom to best show the biological components to the waveform. (A₂) 100 μ M DA application (black bar) superimposed onto an untampered control, with vertical dotted lines (indicated at t = 0 and +10 minutes) indicating the time point which paired-pulses were delivered. (B) Comparisons between paired-pulses prior to DA application and during DA application. (B₁) Paired-pulse ratios (measured as sweep 1 compared against sweep 2) from both before DA application (grey) and during DA application (black) were superimposed upon one another on a logarithmic scale. Asterisks (*) indicate statistically reliable differences within IPIs. (B₂) Paired-pulse sweeps at noted interpulse intervals (IPI) both before DA and during DA superimposed upon one another. Error bars shown in A₂ and B₁ show \pm SEM of the group mean.

Table 6 – Statistically Significant Differences Between Second Pulses in Paired-Pulse Experiments Differs Between Low Concentration (100 nM) and High Concentration (100 μ M) Dopamine Application Experiments. Post hoc analysis (Dunn's multiple comparisons test) between the second pulse during paired-pulse experiments at different interpulse intervals (IPIs) compared against one another. Comparisons were made between 10, 30, 100, 300 and 1000 ms IPIs during both 100 nM and 100 μ M DA application experiments. These results show statistically significantly different comparisons ($p < 0.05$) and comparisons which were not statistically reliably different ($p > 0.05$).

A - 100 nM Pulse 2 Comparisons			
Dunn's multiple comparisons test	Mean rank diff.	Significant?	Adjusted P Value
10ms vs. 30ms	-13.17	No	0.0958
10ms vs. 100ms	-21.50	Yes	0.0002
10ms vs. 300ms	-14.00	No	0.0588
10ms vs. 1000ms	-11.33	No	0.2576
30ms vs. 100ms	-8.333	No	>0.9999
30ms vs. 300ms	-0.8333	No	>0.9999
30ms vs. 1000ms	1.833	No	>0.9999
100ms vs. 300ms	7.500	No	>0.9999
100ms vs. 1000ms	10.17	No	0.4547
300ms vs. 1000ms	2.667	No	>0.9999
B - 100 μM Pulse 2 Comparisons			
Dunn's multiple comparisons test	Mean rank diff.	Significant?	Adjusted P Value
10ms vs. 30ms	-16.67	Yes	0.0104
10ms vs. 100ms	-13.50	No	0.0791
10ms vs. 300ms	-2.667	No	>0.9999
10ms vs. 1000ms	-1.333	No	>0.9999
30ms vs. 100ms	3.167	No	>0.9999
30ms vs. 300ms	14.00	No	0.0588
30ms vs. 1000ms	15.33	Yes	0.0255
100ms vs. 300ms	10.83	No	0.3305
100ms vs. 1000ms	12.17	No	0.1668
300ms vs. 1000ms	1.333	No	>0.9999

5 Discussion

As was mentioned in the introduction, the LEC plays a crucial role in the conversion and storage of non-spatial memory but the exact mechanisms underlying synaptic plasticity mediated by DA, most notably receptor desensitisation to the neurotransmitter, still remains somewhat unknown. The experiments performed here, in comparison and conjunction with prior experiments completed in this field, aim to further understand these mechanisms.

5.1 Summary of Experimental Findings

These experimental findings show that previous and subsequent dopaminergic experiments are physiologically relevant as the superficial layers I and II of the LEC possess rich pools of dopaminergic deposits. Controls assessing changing solutions and vehicle addition (changing ACSF or addition of sodium metabisulphite) both showed no statistically significant changes in responses. Application of nanomolar concentrations of DA showed a statistically reliable depression during application during 10 nM addition, as well as a statistically reliable facilitation during 100 nM DA washout. High concentrations of DA not only showed statistical difference from the untampered control but coapplication with receptor antagonists also allowed subsequent identification of the roles many biomolecules play in the physiological functions of the LEC. These antagonist applications showed that NMDA plays a facilitative role on transmission in the presence of DA, increasing the size and amplitude of fEPSP responses, as antagonist coapplication with DA depresses amplitude greater than DA alone. DA itself however plays an entirely depressive role at high concentrations, with DA antagonist application diminishing this depression. Application of very high concentrations of DA appeared to saturate receptors which prevented antagonists from affecting responses, indicating the antagonists used possessed a competitive MOA (as was shown by both DA antagonists and Barbadin). Finally, not only does DA affect glutamatergic postsynaptic receptors, as seen by the depression during DA application, but paired-pulse experiments indicate that DA also affects glutamatergic neurones on the presynapse as well.

5.2 Justification of Methods

The physiological intercranial temperature of a rat fluctuates between 36.5-38.5°C (Briese, 1998), however slices were placed in a holding chamber and experiments were performed in solutions around 31-32°C. Studies have shown that electrophysiological recordings at physiological temperatures (~37°C) can induce spontaneous seizures, which may be in part due to neuronal hypoxia, as oxygen may fail to penetrate the slice to reach inner cells. Reducing this temperature (to 32°C) showed a reduction in the metabolic demand of neurones, as well as slowing the kinetics of seizure-generating components, such as K⁺ ions (Morris *et al.*, 2016). Experiments were therefore performed at 32°C, as this ensured slices would not become epileptic during the experiment.

Whilst the rat brain was being sliced, sucrose rich cold (4°C) cutting solution (also referred to as low sodium ACSF or sucrose ACSF) was used during slicing with the brain in the

Vibratome. Without this protective solution, an influx of Na^+ into the cell would result in an osmolarity gradient imbalance, forcing water into the cells, inducing neuronal swelling and subsequent cytolysis (Aghajanian and Rasmussen, 1989). The equiosmolar replacement of NaCl with sucrose (subsequently reducing this excessive addition of sodium) prevents this neuronal swelling, subsequently allowing greater amplitudes to be recorded as more neurones survive surgery (Ting *et al.*, 2014). During this procedure, the solution is held at $\sim 4^\circ\text{C}$ (the conventional cutting temperature) because this both prevents cellular damage and hardens the brain for cleaner slices to be made (Ballanyi and Ruangkittisakul, 2008). Although slicing at 4°C is the conventional temperature and was successful in these experiments, recent studies have shown that slicing at physiological temperatures may also be a viable option (Huang and Uusisaari, 2013; Ankri *et al.*, 2014).

Once slices were cut and placed into the ACSF holding chamber, they were left for approximately 1 hour for a “protective recovery” stage. First described in 2003, the protective recovery period gradually reintroduces Na^+ ions to the slice to ensure the osmolarity gradient is maintained, preventing cytolysis (Fiala *et al.*, 2003). Other papers show that 1 hour in a protective recovery state is sufficient enough for glycogen granules reappearing in astrocytic processing (Fiala *et al.*, 2003), but most importantly is sufficient time for *ex vivo* synaptic recovery (Kirov, Sorra and Harris, 1999; Schurr *et al.*, 1984).

As DA is an unstable chemical under certain conditions, numerous precautionary measures were taken in order to extend its activity and slow its oxidation. Firstly, addition of the antioxidant sodium metabisulfite is itself reduced in the presence of H_2O_2 , a by-product formed in the autoxidation of DA in Neuro-2A cells (Pedrosa and Soares-da-Silva, 2002). This reduction protects the cell from the cytotoxic product, slowing any potential degradative effect that DA plays on the neurone. Applying $50\ \mu\text{M}$ of the antioxidant has previously shown to slow DA oxidation whilst showing no statistical changes in fEPSP measurements during its isolated application (Yang and Seamans, 1996; Caruana *et al.*, 2006), thus this concentration was co-applied with DA in these experiments. Secondly, the room was darkened to stymie the rapidly oxidising nature of the catechol group into its quinoid form, with light exposure accounting for approximately 20% this oxidative nature (Sánchez-Rivera *et al.*, 2003).

During statistical analysis of datasets using one-way ANOVAs, a Tukey test was selected when using a multiple comparisons test. Although the power of the significance ($p < 0.05$) is significantly reduced during these comparisons, the datasets were not analysed using tests that alter this power (such as the Bonferroni or the Šídák corrections (Blakesley *et al.*, 2009)) due to the size and nature of these experiments. It may there be perceived to be beneficial to show type two errors (false negatives) than it may be to show type one errors (false positives), as initially accepting the null hypothesis would require further testing to disprove, whereas initially rejecting the null hypothesis may lead experimental attention elsewhere. Furthermore, datasets which were shown to contain outliers, using the ROUT method, were removed to ensure the datasets showed accurate results and were not misled by any one experiment. The ROUT method identifies outliers by generating a nonlinear regression curve, analysing residuals and removing subsequent outliers (Motulsky and Brown,

2006). The parameters were set to the middle of the ROUT scale, $Q = 1.0\%$, to ensure the removal of outliers was strict enough to remove datasets that were outliers, but not so strict as to remove experiments that may have resulted from a physiological effect. These parameters were then applied to each dataset, eight individual experiments being subsequently removed, two of which were control experiments and six of which contained DA receptor antagonists. The two control experiments (one ACSF changeover and one sodium metabisulfite control) were likely caused by inconsistencies in solution preparation, with varying temperatures and excessive bubbling likely accounting for the diminishment. The remaining six experiments each contained DA receptor antagonists, which highlighted the varying effects DA application had on responses. The outliers were removed using method to avoid scientific bias, as only experiments which statistically differ from the others are removed, rather than ones which best yield a favourable result.

5.3 Analysis of Results

5.3.1 Controls and Initial Dopamine Experiments

5.3.1.1 Tyrosine Hydroxylase Immunohistochemistry

As all successive experiments used DA (asides from control experiments), immunohistochemical staining for the enzyme TH would confirm the presence of dopaminergic fibres within the region. These results show there is a clear presence of dopaminergic fibres within the LEC, also showing some a clear resemblance of clusters of richer TH deposits (as previously alluded to in previous TH staining (D. Caruana, person and Chapman, 2008)). All control experiments in this dataset were conducted alongside slices, in which secondary antibody was omitted, none of which showed these dopaminergic fibres. No statistical analysis was performed on these experiments, but a visual comparison between samples and the controls showed that DA is evidently present within layers I-III of the LEC, thus subsequent DA experiments can be deemed valid. These clusters of dopaminergic cells within the LEC may also account for the variation in amplitude between experiments, as electrodes placed within these islands may show a greater depression upon DA application than electrodes placed outside these islands.

5.3.1.2 Control Experiments

These control experiments were designed to test if either changing the source of ACSF or adding the vehicle would significantly alter the response, as both these changes would be used in all successive experiments. Although both experiments showed a small depression, neither showed a statistically significant difference, as was concluded by a RM ANOVA. This indicates that both control variables have no significant effect on any underlying mechanisms in fEPSP induction, with further experimentation likely removing the small diminishment observed. It is likely that the small diminishment observed is due to inconsistencies in solution preparation methods, specifically fluctuations in temperature or excessive bubbling during application, factors which can be attributed to initial inexperience using the electrophysiological apparatus. As vehicle addition showed no statistical significance, it is

therefore congruent with previous experiments testing the same parameter, which also showed that isolated application of sodium metabisulphite showed no statistically significant change in amplitude (Caruana and Chapman, 2008). The ACSF changeover experiment however cannot be compared against any previous experiments, as although the control will have likely been tested in labs, no reports were present within the literature.

5.3.1.3 Single Application of Low Concentration Dopamine

As most previous experiments looked at the role which high concentration DA plays within the LEC, this experimental group was created to identify the role which nanomolar concentrations of DA, a potentially more physiologically viable range, may play in affecting transmission. Although each nanomolar concentration of DA elicited different responses during DA application and during the washout, individual t-tests comparing peak changes in fEPSP against their time matched controls showed that 10 nM application of DA elicited a statistically significant response. During DA application, the lower nanomolar concentrations (1 and 10 nM DA) showed a depression in fEPSP amplitudes, whereas the higher concentrations (100 and 300 nM DA) showed facilitation. Although these higher concentrations failed to show a statistically reliable significance, they did show that the LEC may potentially possess some facilitative properties. Previous experiments which showed this facilitation showed that 1-10 μ M DA facilitated fEPSP amplitude during application (Caruana *et al.*, 2006), however recent experiments testing these same parameters have failed to replicate this facilitative response. This lack of replicability could be as a consequence of many factors, such as strain and age of the rat, the electrophysiological equipment itself and also the experimenter performing the tests. What has been shown, in both these experiments and in the aforementioned report, is that application of lower concentrations of DA generates a facilitation whereas application of higher concentrations elicits a depression. This facilitation may therefore have a physiological component to it, as inhibitory GABAergic MPNs within deep layers of the LEC (layers V-VI) can themselves be inhibited by DA (Rosenkranz and Johnston, 2006), which may induce a temporary facilitative effect. For this to be confirmed however, more testing using these parameters would need to be performed and statistically significant results would need to be obtained.

The amplitude during washout also differs for each experiment, however this shows no correlative pattern, with 1 nM DA eliciting the largest rebound (119.6% \pm 9.148%), followed by 100 nM, 10 nM and 300 nM eliciting the smallest rebound (108.5% \pm 3.600%). Despite there being no clear pattern with these rebounds, the rebound observed by 100 nM was shown to be statistically significantly different from its time matched control. This therefore means that it is very likely that an underlying mechanism causes these facilitations. One mechanism, as mentioned in the previous paragraph, could be long term inhibition of deep layer inhibitory neurones, which (as inhibition of inhibitory neurones prevents their firing) may lead to an increase in activity within the superficial layers. Another mechanism, as further outlined in Figure 10, could be that D1-like/D2-like receptor activation (but not saturation) may induce a cascade which culminates in temporarily increased AMPAR and NMDAR expression on

glutamatergic neurones, increasing excitatory activity through early-phase plasticity induction (Sun *et al.*, 2005). This suggests that although underlying mechanisms may contribute to the observed effect, more testing, such as elongating experiments after the 60-minute washout is complete, may provide more information into the results seen. DA induced facilitation may also play a key role in memory formation, as increased activity may lead to greater sensitivity of the HF when responding to weaker stimuli, meaning a greater amount of non-spatial information may be conserved and processed.

5.3.1.4 Repeated Application of Low Concentration Dopamine

As 100 nM applications of DA produced a statistically significant facilitation during its washout (as elaborated in the previous chapter), repeated addition of 100 nM DA may indicate if this facilitation is through cellular mechanisms or not. The second application of DA showed a similar magnitude of facilitation to the first application, showing a small facilitation upon application, rising to 111.4% \pm 8.219% and 109.1% \pm 3.787% of baseline levels respectively. However, a RM ANOVA showed that neither facilitation during DA application was statistically significantly different which, similar to previous experiments using nanomolar DA, concludes that although facilitation may be physiological, more testing for a significant result would be required before any conclusions can be drawn.

Furthermore, these results also cannot be compared against previous experiments, as no previous reports in the LEC have looked at nanomolar concentrations of DA, as the lowest concentration previously studied was 1 μ M (Caruana *et al.*, 2006; Caruana and Chapman, 2008; Glovaci and Chapman, 2015). Although not in the LEC, one study looked at the tonic application of DA in the stomatogastric ganglion, a region of the stomach which contains the lateral pyloric neurone, a dopaminergic neurone which expresses only D1-like receptors (Rodgers, Krenz and Baro, 2011). This experiment showed that nanomolar concentrations of DA can regulate the densities of voltage-gated ion currents through multiple mechanisms, one such proposed includes maximum potassium ion channel conductance. This experiment looked at dopaminergic neurones in lateral pyloric neurones as opposed to the LEC neurones, but it may give some indication into how nanomolar concentrations of DA may affect neighbouring neurones through D1-like receptors, a concept which is yet to be brought into the HF.

5.3.2 Pharmacological Analysis of Cell Types Present Within the LEC

5.3.2.1 Antagonist Analysis with 100 μ M Dopamine

5.3.2.1.1 AP5 with 100 μ M Dopamine

The allosteric modulator of the NMDAR antagonist, AP5 was used to identify the role which glutamatergic neurones play within basal transmission of the LEC and how tonic application of 100 μ M DA may affect this. The experiment conclusively shows that AP5 application significantly changes amplitudes both before and during its coapplication with DA. The concentration of 50 μ M AP5 was chosen because at this concentration, NMDAR activity is reduced to approximately 0% activity in wild type cells when compared to the control (Chen

et al., 2015). Initially, AP5 application in isolation significantly depressed fEPSP amplitude, with the dataset subsequently being renormalised as a result of this change. This fEPSP has been shown in previous experiments which look at the role NMDARs have within the hippocampus, as CA1 fEPSPs significantly depress (although substantially more in CA1 than in the LEC) upon AP5 application (Kang *et al.*, 2017). This depressive effect is however physiologically relevant, as NMDAR inhibition reduces excitatory glutamate efficiency, reducing both maximal excitability and measured fEPSP. This reduction in excitability is further shown during DA application, as DA and AP5 coapplication is significantly lower than DA alone (as shown in Chapter 4.1.1). As NMDARs are found both on the presynaptic and the postsynaptic membrane, bath application of AP5 would inhibit NMDAR activity on both membranes. This would subsequently reduce both presynaptic and postsynaptic Ca²⁺ influx, diminishing neurotransmitter exocytosis within the presynaptic terminal and sequestering postsynaptic cascade events triggered by Ca²⁺ influx through NMDARs. Despite the aforementioned Ca²⁺ sequestering playing a key role in the formation of LTD (Figure 9), a RM ANOVA (2x2) showed no statistically reliable difference between the baseline and the washout. Although this indicates that no form of long-term plasticity was induced, the experimental parameters were not designed to induce LTP or LTD and AP5 would block any NMDAR mediated LTD as NMDAR-LTD is predominantly activity dependent (Lüscher and Malenka, 2012).

5.3.2.1.2 Dopamine Antagonists with 100 µM Dopamine

Similarly to NMDA inhibition, coapplication of both D1-like and D2-like antagonists with DA showed statistically significant changes in fEPSP amplitudes. Despite a comprehensive pharmacokinetic analysis of AP5 showing a concentration at which it is fully potent, definitively categorising these DA antagonists' pharmacokinetics has posed somewhat of a greater challenge. As such, neither the D1-like antagonist (SCH-23390) nor the D2-like antagonist (sulpiride) are yet to have their pharmacokinetics fully identified, thus no definitive concentration at which 100% of receptors have been saturated has been alluded to previously. One previous experiment however showed application of 100 µM DA with 10 µM SCH-23390 or 50 µM sulpiride both showed a statistically significant result, so these concentrations were replicated here (Caruana *et al.*, 2006). Isolated application of both these drugs significantly depressed fEPSP amplitude, with each experiment subsequently being renormalised as a result of this significance. This result however differs from the aforementioned experiments looking at these antagonists, which showed no change in amplitude, despite SCH-23390 being used at a higher concentration (50 µM in the previous experiment compared to 10 µM here (Caruana *et al.*, 2006)). However, as was mentioned in Chapter 5.3.1.3, as previous aspects of that paper also have not been replicated, this change may too be as a result of changes in other control variables (age and strain of rat or electrophysiological apparatus to name a couple) that these results differed from one another. As the aforementioned paper and this report are (as of time of writing) the only two reports testing these experimental conditions, the results obtained through this experiment cannot be supported. Furthermore, as

coapplication of both SCH-23390 and sulpiride is also yet to be reported elsewhere, the results obtained in that experiment also cannot be cross-referenced against any other yet published article.

The first analysed aspect of the superimposed DA antagonists with DA was the gradient during the initial onset of DA-mediated fEPSP suppression. This analysis concluded that all experiments which used DA were statistically non-zero and DA antagonists showed a statistically reliable difference to isolated DA application. This difference will be due to two different factors, peak fEPSP depression and the time taken for DA to exert its maximum effect on fEPSP. The former factor, peak fEPSP depression is significant in determining this gradient as fEPSP depression in the presence of DA antagonists is significantly less than without DA antagonists (thus Δy is less in the presence of DA antagonists). The latter factor is significant in determining the gradient as the time taken for maximum dopaminergic effect is longer in the presence of DA antagonists (~12 minutes) than in the absence of these antagonists (~8 minutes). This delay and suppression of depression of amplitude is due to the DA antagonists binding to DA receptors, both of which show partial antagonism to their respective receptors at a saturated concentration. Their individual applications show a suppression in dopaminergic neurone efficiency, with subsequent action potentials, thus postsynaptic glutamate activity, being suppressed. Their coapplication also showed little difference from individual applications, suggesting that there is no significant change in receptor blocking as increasing antagonist concentration showed no significant change in depression. Although this DA onset gradient is yet to be tested with these parameters outside this experiment, this statistically reliable significance concludes that application of DA antagonists dampens the onset gradient.

The second analysed aspect of DA antagonist application is the attenuation of the affect 100 μM DA elicits on response. In the presence of either (or both) antagonists, fEPSP depression is restricted by approximately 15% of baseline levels (25% less depression than DA application without the antagonists, which itself showed a 20% depression). In these experiments, both DA antagonists display non-competitive binding properties to their respective receptors. Primarily, if these antagonists were competitive, each experiment would gradually slope towards the 100 μM DA control as the antagonist dissociates from receptors due to the high concentration of DA. Secondly, coapplication of both antagonists not only still shows DA-mediated depression, but this experiment also shows no statistically significant changes from each antagonist individually. This indicates the antagonists are non-competitive as the effects are not superimposable (where if both antagonists were competitive, a significantly smaller depression would be observed as both D1-like and D2-like receptors would be occupied). Furthermore, preliminary reports looking at these antagonists show that although SCH-23390 shows a high affinity for D1-like receptors and sulpiride shows a high affinity for D2-like receptors, both drugs show some interaction with both receptor subtypes (Bourne, 2001). Therefore, it may be inferred from this experiment that both antagonists bind to their respective receptors through a non-competitive mechanism whilst also showing some binding to the other receptor subtype.

The final analysed aspect of DA antagonist and 100 μ M DA complication experiments assessed the final 18 minutes of DA application, the period immediately after peak depression was observed for each experiment. A one-way ANOVA comparing the slope of each experiment showed no statistically significant differences, though linear regression comparisons showed that all experiments which used SCH-23390 showed no statistically significant difference from zero. As all other experiments which did not include this D1-like receptor antagonist were statistically non-zero, it indicates that D1-like receptors may be the types of DA receptors which are responsible for dopaminergic desensitisation within the LEC. Use of sulpiride supports this as blocking only D2-like receptors (thus only D1-like receptors will be present during sulpiride application) shows not only statistical significance from zero, but also shows the steepest gradient of all experiments ($m = 0.3588$). This D1-mediated desensitisation is supported within the literature, with Kim *et al.* reporting the same conclusion (Kim *et al.*, 2003). Although this experiment and the aforementioned paper show the prominence of D1-like receptors in desensitisation, the general consensus surrounding literature states that D2-like receptors are the main DA subtypes which exhibit desensitisation (Nimitvilai *et al.*, 2014 and Nimitvilai and Brodie, 2010). Despite this, blocking D1-like receptors (using SCH-23390) to isolate D2-like receptors appeared to show no desensitisation, as these experiments showed no statistical significance from zero, however this showed no statistical significance. However, despite all these experiments showing DA desensitisation, most studies were conducted in other regions of the brain (mostly the VTA). This could suggest that dopaminergic neurones in the LEC behave differently compared to dopaminergic neurones in other regions of the brain, however concluding this would require further, more extensive experimentation and repeatable results when compared to other cortical regions.

Despite the two receptor antagonists affecting two separate receptors, with limited interaction for the other respective receptor (Bourne, 2001), their effects shown through these experiments contradicts the information shown in the D1/D2 signalling mediated plasticity pathway, Figure 10. This figure indicates that AC activity, activated by D1-like activity and inhibited by D2-like activity, resulted in greater AMPAR and NMDAR expression in glutamatergic neurones. This modulation of postsynaptic iGluRs may suggest that fEPSPs would be different under each antagonist application, with a greater depression likely being observed through SCH-23390 application, as inhibiting D1-like receptor activation in turn reduces AC levels, thus yielding a greater depression than what would be observed through sulpiride application. If this were to be observed, it would be likely that their coapplication with lie between the two results, with the AMPAR and NMDAR concentration modulations cancelling out one another, however the observed results contradicts this.

The conclusion that can be drawn from all these experiments is that at their current concentrations, the DA antagonists were unable to fully inhibit the effect of DA on transmission. This may be due to the antagonists' inability to fully inhibit DA activity, hence explaining why the pharmacokinetics surrounding the antagonists is somewhat scarce, as differentiating between maximal and minimal activity remains challenging. Alternatively, not observing a complete inhibition of DA activity may be because the antagonist concentration

applied was not large enough, something which a comprehensive concentration-activity curve would indicate. This could therefore be an avenue which could have been further explored, as observing the percentage decrease in peak fEPSP compared to 100 μM DA application without antagonists across ranging concentrations could be used to generate concentration-activity curves for both SCH-23390 and sulpiride, subsequently better understanding both.

5.3.2.2 Antagonist Analysis with 1000 μM Dopamine

5.3.2.2.1 Barbadin with 1000 μM Dopamine

As of completing the Barbadin experiments, the β -arrestin antagonist was a very novel drug, only being discovered about a year prior to its use in its experiments (Beautrait *et al.*, 2017). At the time of writing, only a handful of papers have previously used Barbadin (Beautrait *et al.*, 2017; Aberoumandi *et al.*, 2019; Zhang *et al.*, 2019; Khalid and Chang, 2020; Wang *et al.*, 2019), none of which have looked at the role that Barbadin plays in fEPSPs, let alone the role of Barbadin in the LEC. This therefore meant that not only was the previous experiment the first use of Barbadin in the LEC and the HF, but also the first experiment using Barbadin in fEPSP research. The disadvantage of this however is that no previous data exists into viable concentrations that could be applied during the experiment, which was observed during 100 μM Barbadin application. Application at this concentration resulted in fEPSP collapse soon after its coapplication with DA so the dataset was abandoned. Subsequently, 30 μM Barbadin would be used to assess β -arrestin, the D₂ receptor scaffolding protein, function in synaptic transmission. Tonic application of this β -arrestin antagonist before and during coapplication with DA significantly diminished fEPSP amplitude compared to the untampered control but not compared to 1000 μM DA itself. This statistical insignificance of Barbadin is further shown in both peak fEPSP depression and in the gradient during the final 20 minutes of DA application. This initial diminishment in amplitude may be physiologically relevant, as Barbadin blocks internalisation through clathrin adaptor protein 2 (AP2) interaction, preventing neurones from recycling cleaved neurotransmitters and thus pools of neurotransmitters would diminish. This statistical insignificance compared to 1000 μM DA may too be physiologically relevant, as Barbadin has not previously been shown to permeate the neuronal membrane, preventing its binding with β -arrestin.

5.3.2.2.2 Dopamine Antagonists with 1000 μM Dopamine

Unlike when coapplied with 100 μM DA, coapplication of 1000 μM DA with SCH-23390 showed no statistically significant change during its application. Although this was not statistically reliably different at $t = 30$ ($p = 0.0503$), fEPSP amplitude showed a gradual reduction during SCH-23390 application, indicating an effect was observed during drug application, even if this was not significant. Sulpiride however did show statistical significance during its application and was subsequently renormalised. Although previous experiments applying sulpiride showed no statistically significant changes during its application (during its coapplication with 100 μM DA; Caruana *et al.*, 2006), the depression observed during the D2-

like antagonists' application may be physiologically relevant, however determining this would require further testing. This Previous dopaminergic experiments in the LEC showed that 1000 μM DA, the concentration used in conjunction with Barbadin, is highly concentrated enough to fully saturate DA receptors. This saturation is characterised by the observed recovery even throughout the washout phase, whereas 100 μM DA will rapidly return to baseline. Although DA antagonists should theoretically block the observed changes in fEPSP amplitude mediated by DA, saturation with 1000 μM DA occupies DA receptor active sites, preventing antagonist binding. This may go some way to determining the underlying mechanisms of how the antagonists block DA suppression, as these experiments (unlike the 100 μM DA experiments) shows the drug interaction may bind to the receptors through a competitive mechanism.

The results seen when coapplying 1000 μM DA with these receptor antagonists, as well as when coapplied with Barbadin, appear to possess a metaplastic effect. This variant of plasticity, similar to Hebbian plasticity, is heavily dependent upon NMDAR activity, which is in turn theorised to alter Ca^{2+} related activities (Izumi *et al.*, 1992). This dependency is further shown as activities of other postsynaptic receptors, namely AMPAR and mGluRs, act entirely independently of metaplasticity (Zorumski and Izumi, 2012). Subsequently, metaplasticity induced through prolonged DA exposure would culminate in a reduction in DA's efficacy during its application, a phenomenon that was observed in all experiments which applied both 100 μM and 1000 μM DA (this experimental group as well as the last group). Despite this, the exact mechanisms underlying metaplasticity still remains somewhat idiopathic, however these results should aid in further understanding the phenomenon, as neither D1-like, D2-like nor β -arrestin show any effect on the metaplastic affect at the tested parameters within the LEC.

5.3.2.3 Paired-Pulse Stimulation Analysis

PPS experiments were used to determine if DA mediated glutamatergic transmission through acting on the glutamatergic presynapse within the LEC, affecting presynaptic glutamate release probabilities. Previous studies looked at how PPS and high concentration DA affect these release probabilities (Caruana and Chapman, 2008), however this study did not assess PPS and low concentrations DA. Although the application of 100 nM DA showed no statistically reliable difference, as was also observed during its single application, the response elicited was different from previous experiments, showing a slight depression upon application. The two cannot be compared however, as parameters between experiments differ, with PPS potentially inhibiting the facilitative properties of 100 nM DA, suggesting a potential presynaptic release mechanism to the previously observed facilitation. The ratios observed in both parameters in this experiment are also congruent to those shown previously, with IPIs shorter than 30 ms (10 ms (Hamam *et al.*, 2007; Bouras and Chapman, 2003) and 20 ms (Waldbaum and Dudek, 2009; Jiang *et al.*, 2000)), showing a depression during the second pulse. This experimental group also showed no difference before and during DA application, thus concluding that although DA had elicited an insignificant change in amplitude, this facilitation was not driven through a mechanism based on presynaptic glutamate release.

PPS during high concentration DA application however shows a change from paired-pulse depression into a paired-pulse facilitation. Although this facilitation is greater at shorter IPIs (10, 30 and 100), all IPIs showed a statistically significant facilitation compared to before DA application. The longest IPI paired-pulse, 1000 ms, was also shown to be statistically significant, despite the two pulses acting as two entirely independent action potentials (Jonas, 2000). Although a facilitation after 1 second is yet to be reported elsewhere, this may likely be because shorter facilitative IPIs had been delivered to the slice prior to the delivery of 1000 ms IPI pulses which may affect presynaptic pools to alter presynaptic release probabilities. This may also be due to activation of mechanisms associated with early-phase LTP generation (Sun *et al.*, 2005). Of these different IPIs, 30 ms yielded the largest PPR (1.383 ± 0.106), an IPI which had also been shown in previous experiments, often being described as the “optimal PPF IPI”. At this IPI the presynaptic release probability is at its highest, with extracellular Ca^{2+} pools restabilising and intracellular pools not yet fully clearing, a second sweep will initiate an influx of more calcium into the presynaptic terminal, leading to a greater exocytosis of neurotransmitters (Caruana and Chapman, 2008; Jo *et al.*, 2010; Zucker and Regehr, 2002). This therefore shows a presynaptic influence that DA has on glutamatergic neurones, where most evidence would suggest that DA acts on the postsynaptic neurone (Nakano *et al.*, 2010; Tritsch and Sabatini, 2012), supporting the aforementioned experiments which tested PPS in the LEC (Liu, 2020; Caruana and Chapman, 2008). Although this presynaptic release probability is yet to have an exact mechanism proposed, it is likely that this occurs through VGCC and subsequently Ca^{2+} mediation, as altering both these to increase intracellular Ca^{2+} concentrations would facilitate presynaptic neurotransmitter release, altering the terminals probability. Should this occur through presynaptic VGCC activation, it would match one such previous study by Berretta and Jones (Berretta and Jones, 1996). In their study, it was shown that preNMDARs induce LTP in EC layer II, whereas it is predominantly involved in LTD induction across the rest of the brain. Although this experiment showed a similar result to this experiment, their facilitation observed at 50 ms IPI was insignificant, whereas these show statistically significantly reliable differences. In order to identify the presynaptic mechanisms in which DA affects neurotransmitter release, a range of further experiments would need to be performed, such as blocking glutamate transmission (through AP5 inhibition of NMDARs, a concept which was tested in the aforementioned paper), blocking DA receptors (through SCH-23390 or sulpiride application and their coapplication) as well as potentially targeting other downstream molecules and assessing their function in paired-pulse facilitation.

5.4 Clinical Significance

5.4.1 Depression

5.4.1.1 Overview of Depression

Depression has been described as a multifaceted neurological disorder, in which a variety of dysfunctions all contribute to significant cortical activity suppression (Hasler, 2010). This neurological disorder affects more than 300 million people worldwide and is the world’s leading cause of disability as reported by the World Health Organisation (WHO). Depression

has been shown to affect women more than men, but age is an irrelevant factor as people from all ages can be diagnosed with the disorder (WHO, 2021). Depression can be subdivided into two categories, the first of which is unipolar depression, where the sufferer only experiences depressive episodes (Cuellar *et al.*, 2005). The term unipolar depression is somewhat of a broad umbrella which covers five further subcategories, major depression, seasonal affective disorder, adjustment disorder, postpartum depression and dysthymic disorder (Benazzi, 2006). The second of the two subcategories of depression, bipolar depression can also be subdivided into two distinct categories, bipolar I and bipolar II, which indicates a history of mania and hypomania (which describes periods of euphoria and is a milder variant of mania) respectively (Angst and Cassano, 2005).

Similarly to the ranging types of depression, the mechanisms underlying the disorder are also extensive. These mechanisms vary from stemming from an inflammatory disorder, a dysregulation of the neurotransmitter glutamate and as a neurodegenerative disorder (to name a few from Lang and Borgwardt's review (Lang and Borgwardt, 2013)). The first of these mechanisms involves changes in inflammatory homeostasis, with changes in interleukin-6, tumour necrosis factor-alpha (TNF- α), interleukin-2 receptors and c-reactive protein all directly affect the inflammation of the various cortical regions (Liu *et al.*, 2012; Dowlati *et al.*, 2010). Elevation of these proteins (asides from TNF- α which is lowered) results in reduced phosphoinositide 3-kinase (PI3K) levels, which may subsequently trigger depression (Lang and Borgwardt, 2013). Stimulation of the mammalian target of rapamycin (mTOR) pathway through ketamine administration is also widely implicated in various forms of depression (Abelaira *et al.*, 2014). Aside from cellular mechanisms, depression is considered as a neurodegenerative disorder due to its reduction in hippocampal volumes and BDNF levels which are both observed in depressed patients (Campbell and MacQueen, 2006; Pittenger and Duman, 2007). As well as decreases in these factors, neurotrophin-3, erythropoietin and glial cell-derived neurotrophic factor (GDNF) are all lowered in brains of depressed subjects. These changes result in a decrease in CREB, which subsequently reduces BDNF levels, which in turn reduced PI3K levels which (as was previously mentioned) that all contribute to leading to depression (Lang and Borgwardt, 2013). Aside from these mechanisms underpinning depression, depression has also been shown to occur from a reduction in DA levels throughout the cortex, with depressed patients showing a reduction in DA transporter binding when observed with a PET scan (Sarchiapone *et al.*, 2006). As well as this reduced binding, depression has also been shown to stem from reduced levels of DA, which may in fact result in the aforementioned binding reduction (Kilbourn *et al.*, 1992). It may therefore be possible that targeting the dopaminergic system may provide a therapeutic alternative when treating depression.

Clinically, depression is currently treated primarily using medications that block neurotransmitter reuptake, including the reuptake of selective serotonin (SSRIs, such as citalopram, fluoxetine and sertraline) and serotonin and noradrenaline (SNRIs, including duloxetine and venlafaxine (Faquih *et al.*, 2019)). Although SSRIs and SNRIs dominate clinically used antidepressants, there are other medications that target the dopaminergic system.

These medicines, such as quetiapine and bupropion, are not selective to DA receptors, acting on serotonergic and norepinephrine receptors as well (Kondo *et al.*, 2013; Stahl *et al.*, 2004).

5.4.1.2 Anhedonia

Described as the “hallmark of depression”, anhedonia is the most common characteristic observed in people with depression, so much so that this symptom is required for depression to be diagnosed. First described in 1897, anhedonia is defined as the reduced ability to experience pleasure (Ribot, 1897) and although it is well implicated in major depression, it is also a side effect of Parkinson’s disease and drug abuse (Klein, 1984; Isella *et al.*, 2003; Volkow *et al.*, 2002). Despite this reduced experience of pleasure, depressed patients have shown an increased refinement in their senses, with some patients showing higher sweet taste perception than those without depression (Berlin *et al.*, 1998). Although the exact mechanisms underlying anhedonia still remain somewhat idiopathic, correlations between the disorder and both DA (and subsequently serotonin due to the correlation between the two neurotransmitters (Yan, 2000)) and glutamate receptors have still been shown (Der-Avakian and Markou, 2012). Despite this however directly analysing and quantifying anhedonia in depression possesses a challenge, as the variety of mood disorders in depression are somewhat entangled (Gorwood, 2008). There may still be a crucial role for the LEC to play in anhedonia, as this subregion conveys non-spatial information from sensory cortices before projecting the information throughout the hippocampus. As long-term retention of non-spatial information from the hippocampus plays a fundamental role in anhedonia (Der-Avakian and Markou, 2012), it may be possible that the LEC plays a substantial role in its development (Lally *et al.*, 2015).

5.4.1.3 Flinders-Sensitive line (FSL) Rats

Studying depression in humans holds many challenges, however using rat models may subsequently yield a better and alternative. DA receptors are highly conserved between the two species, as rats’ brains possesses a 91% identical D1 receptor and a 96% identical D2 receptor amino acid sequence to humans (Sibley *et al.*, 1993). As well as the receptors, DA transporters are highly conserved amongst mammals, with rats having a 92% homology to humans for these transporters (Giros *et al.*, 1992). The Flinders-sensitive line of rats (FSL) act as a genetic model of depression, being used since their discovery in 1993 by D. Overstreet (Overstreet, 1993). This line of rats are overly sensitive to the acetylcholinesterase agonist diisopropyl fluorophosphate, a chemical which has recently been shown to lead to develop cognitive depression (Phillips and Deshpande, 2016). Comparing experiments using this pathophysiological model of rat to the physiological Sprague-Dawley rats may also indicate changes in LEC structure and function in depression, further increasing knowledge of both the LEC and of depression.

5.4.2 Schizophrenia

Deriving from the Greek roots of split (*schizen*) and mind (*phren*), schizophrenia affects much less people than depression, with approximately 20 million people worldwide suffering from this disorder (James *et al.*, 2018). Where depression stems from reduced cortical DA levels, schizophrenia is believed to be the other side of the same coin, stemming from increased levels of DA (namely D₂) transmission. This alteration in cortical DA levels results in a range of symptoms, all of which fall into three generic clusters. The first group, positive symptoms, defines symptoms which arise due to cortical overexcitation and includes symptoms such as hallucinations and erratic behaviour. This group is potentially the most important group when identifying schizophrenia, as at least one of these symptoms must be present for the disorder to be fully diagnosed (Patel *et al.*, 2014). The second group is the opposite to the first group, both in name and in nature. The negative symptoms associated with schizophrenia arise from cortical suppression and includes symptoms such as reduced expressions and social withdrawal. The final group, cognitive symptoms, are associated with any side effects that do not fall into the aforementioned groups and primarily include diminishment in cognitive abilities (all three groups are discussed in Joseph *et al.*, 2015). Similarly to that observed in depression, the structure of the brain is also changed in patients who suffer from schizophrenia, which includes an enlargement of the major ventricles (Davis *et al.*, 1998) as well as a reduction in dendritic spine densities on a cellular level (Moyer *et al.*, 2015). Although DA (as well as other neurotransmitters) dysfunction and cortical changes have all been well reported in schizophrenia, the exact cellular mechanisms underlying the disorder are still largely unknown.

Clinically, schizophrenia is treated with antipsychotics, medications that subsequently target a range of neurotransmitter systems associated with the disorder. Antipsychotics are classified in two groups, the first discovered typical antipsychotics (medications which show more extrapyramidal symptoms, such as haloperidol and trifluoperazine) and the later discovered atypical antipsychotics (medications which show less extrapyramidal symptoms, such as aripiprazole and quetiapine (Faay *et al.*, 2018)). Sulpiride, the D₂-like antagonist coapplied with 100 μ M and 1000 μ M, is also an atypical antipsychotic, currently being used clinically as a treatment for schizophrenia (Lai *et al.*, 2012).

5.4.3 Clinical Significance of Results in Neurological Disorders

As outlined in Chapter 5.4.1.2, the LEC may play a crucial role in anhedonia, as this region conveys non-spatial information from sensory cortices and projects the information throughout the hippocampus for long-term storage. If a patient suffers from diminished neurological glutamate and DA levels, non-spatial information is less likely to be conveyed as the activity of the LEC fails to suppress to allow memory to be conveyed, a mechanism which was outlined in Chapter 1.1.3.3. These experiments further support this statement, as more potentially physiological lower concentrations of DA elicit a much lower level of fEPSP depression than higher concentrations, which may support this link between low inter-neural DA and depression (which can be observed through anhedonia like symptoms). The most

notable of these concentrations, 100 nM, may provide a therapeutic alternative to currently used medications, as this facilitation of localised activity may reduce anhedonia like symptoms, potentially suppressing symptoms of depression in patients. This facilitation of LEC activity could also result in an increased conveyance of non-spatial memory through the HF, which may provide another avenue of treatment for anhedonia. Besides from anhedonia, the findings in this study could influence pharmacological targets in DA related neurological disorder (such as Parkinson's and schizophrenia), as localised DA application could offer new insights into new potential targets for treatment (Yiannopoulou and Papageorgiou, 2013).

However, these implications cannot be fully confirmed until these experiments are performed against the aforementioned depressed model FSL rats, a comparison between which would show if any proposed therapeutic alternative may show any clinical significance. Furthermore, making conclusions on neurological disorders through *ex vivo* experiments that target one region, within a segment of the brain, brain would be illogical, as neurological disorders are complex and arise from a variety of defects from a plethora of cortices.

5.5 Conclusion

In conclusion, the role that the LEC plays under physiological conditions still remains largely unknown. However, this report will go some way to directly (through the experiments completed here) and indirectly (through further experiments completed as a result and expansion of the ones completed here) improving our knowledge on the mechanisms underlying LEC function. Tyrosine hydroxylation identification in the LEC has confirmed that previous and subsequent DA-mediated experiments are physiologically relevant, and that DA is released in islands throughout the superficial layers of the region. These experiments also show that DA may be expressed in the LEC at lower concentrations under physiological conditions, with 10 nM DA showing a statistically reliable depression during application and 100 nM DA showing a statistically reliable facilitation during washout. Pharmacological analysis of dopaminergic neurones in these islands show that although desensitisation was induced at higher concentrations, most notably at 1000 μ M, it was not convincingly blocked by either DA antagonist used. These experiments did however show some suggestion that the D1-like antagonist, SCH-23390, did elicit an effect on the rate of desensitisation, however this effect was not statistically significant. Paired-pulse stimulation at logarithmic IPIs also showed that the fEPSP generated by glutamatergic activity is affected by DA both at the presynaptic and the postsynaptic terminal, with short IPIs indicating the presynaptic mediation may be through presynaptic release probability mechanisms. These results may therefore provide a foundation for both future experiments, such as the identification of underlying mechanisms, to be conducted within this region, potentially providing results that allow clinical and therapeutic alternatives to treating depression and schizophrenia to be explored. Finally, in accordance with previous studies, the results in these experiments indicate that DA indirectly mediates fEPSP responses through glutamatergic modulation, but this was not assessed directly.

5.6 Future Work

Although the conclusions drawn from this report may provide the foundation for future work to derive from, there are still a plethora of avenues which could be explored to further understand the physiological functions of the LEC. Given more time and a larger financial budget, all of these experiments could be expanded upon in various ways.

5.6.1 Refining and Expanding Current Datasets

Despite TH immunohistochemistry confirming the presence of dopaminergic fibres, thus indicating that experiments within the LEC assessing DA function are physiologically relevant, no further analysis was performed on these experiments. Immunohistochemical staining is seldom used for quantitative assessment, instead being used to qualitatively indicate the presence of a neurone, however semi-quantitative analysis may give a more accurate and conclusive interpretation of results. This can be done through optical density analysis, analysing percentages of stained profiles and the number of stained cells in the stained region (Mausset-Bonnefont *et al.*, 2003). As well as providing semi-quantitative results on the TH staining, these methods would also better indicate the presence of DA islands within the LEC, with cell count and optical density being higher in the islands. As well as these analyses, the physiological concentration of DA may also be determined *in vitro*, either by assessment through high-performance liquid chromatography (Holm *et al.*, 2016), flow cytometry (McKinnon, 2018) or by a standard western blot (Schoonover *et al.*, 2016).

The first aspects of refining current electrophysiological datasets would be to increase the number of control experiments in both ACSF changeover and vehicle application datasets. Currently, both control experiments showed an insignificantly small depression during both experiments, which has been concluded to stem from solution preparation inconsistencies. Increasing the number of experiments performed in both these controls would likely remove this depression, as currently both datasets only have five experiments in each. As well as increasing the number of control experiments in each dataset, increasing the number of nanomolar DA application experiments, most importantly 100 and 300 nM DA application would indicate whether the observed facilitation is a reliably repeatable response or if the facilitation was as a result of any inconsistencies as mentioned previously.

As well as increasing the number of experiments in each dataset, further experiments testing DA at more nanomolar concentrations may also give a better insight into the results observed. Testing the single tonic application of both 3 and 30 nM DA would complete a logarithmic scale for nanomolar concentrations of DA, which may in turn indicate a suggestion as to why 1 and 10 nM DA showed depression during its application but 100 and 300 nM DA showed facilitation. Besides from single tonic application experiments, applying 100 nM DA 30 minutes after the first application (during its washout peak) may also provide a better understanding than its application 1 hour after its first application provided. Better understanding the conditions in which facilitation is observed will allow further experiments to be conducted which may identify an underlying mechanism. These experiments would likely target biomolecules involved in LTP generation, with both presynaptic and postsynaptic

targets present which would indicate both the mechanism and the synapse at which facilitation is induced.

Another crucial conclusion of the experiments here that would need further expanding would be that D1-like receptors are implicated in desensitisation within the LEC. As most previous reports suggest that D2-like receptors are implicated in desensitisation (Nimitvilai *et al.*, 2014 and Nimitvilai and Brodie, 2010), further experimentation assessing the role of D1-like receptors may provide further evidence that DA desensitisation in the LEC differs from other regions of the cortex. Other key components of receptor desensitisation, besides from receptor function, includes: a required phosphatidylinositol turnover; PLC activation; conventional PKC presence and concentrations of residual DA within the synaptic cleft could also be assessed.

Penultimately, PPS experiments suggested that DA mediates glutamate presynaptic release probabilities, however definitively concluding this would require further experimentation. One way to assess this alteration in presynaptic release would be through bound vesicle labelling, which not only allows a comparison between presynaptic and postsynaptic activity to be drawn, but also indicates synapses which have undergone changes in presynaptic release probabilities (Xu *et al.*, 2013). Another way which changes in presynaptic release could be measured is through glutamate concentration analysis within the synaptic cleft, with greater concentrations of the neurotransmitter indicating greater presynaptic release (Scimemi and Beato, 2009). This could also be assessed through NMDAR inhibition, through AP5 application, as discussed in the following chapter.

Lastly, assessing different biological aspects of the fEPSP may show varying results to those obtained than peak amplitude. Peak amplitude was assessed due to its consistency over long durations, however analysing how the fiber volley changes during the experiment will give insight into how presynaptic activity changes throughout. Furthermore, another method for measuring induction of plasticity is through measuring the initial slope during the peak produced by postsynaptic activity. Measuring how the peak amplitude varied across the experiment yielded very few conclusions regarding plasticity, however variations in the initial slope can give a significantly better indication (Liu *et al.*, 2008).

5.6.2 Supplementary Pharmacological Experiments

The role that NMDAR, therefore glutamatergic neurones, could also be expanded upon through further experimentation using AP5. Although AP5 application showed a greater depressive effect during its coapplication with 100 μ M DA, coapplying AP5 with 100 nM DA may indicate whether AP5 would amplify the observed response or whether its application would nullify it. Understanding this would give a greater understanding into the origin of the observed facilitation, more specifically if that facilitation is DA or glutamate mediated. Secondly, AP5 could also be used during PPS experiments will allow a conclusive conclusion to be drawn to whether the observed PPF effect is through glutamatergic modulation by DA, also potentially conclude if the observed effect is through presynaptic or postsynaptic mechanisms. Inducing PPS during the coapplication of AP5 and DA may also indicate the role

which DA plays on fEPSPs, as these parameters were used previously to assess the role that GABA plays on transmission (Davies and Collingridge, 1996).

As well as AP5 application during PPS, application of the D1-like antagonist (SCH-23390) and the D2-like antagonist (sulpiride) will not only give a better understanding into the roles that each receptor plays in synaptic plasticity, as was outlined in Figure 10, but may also further show their role in how DA receptors affect glutamatergic neurones. In addition to this, as SCH-23390 application (D1-like inhibition) showed no desensitisation, so testing this across a longer time frame may give an indication into how effective this desensitisation inhibition is and whether this affect is only seen for a limited amount of time. As well as for longer durations, repeated coapplication of 100 μ M DA and 10 μ M SCH-23390 may indicate if the observed desensitisation is a temporary effect, or if there are any downstream changes. A concentration-response curve could also be tested for both SCH-23390 and sulpiride as well, as neither of these drugs are yet to have a conclusive concentration-response curve generated for either. This way, full saturation could be identified and experiments at this saturation could be performed, with saturation discrepancies potentially providing an explanation into why desensitisation was blocked during D1-like antagonist application but not D2-like antagonist application. This concentration-curve would not only allow for more accurate experimentation in these datasets, but it would also develop knowledge and understanding for both SCH-23390 and sulpiride.

As well as the drugs used, other classifications of drugs can be used to further examine the roles that both D1-like and D2-like receptors play. Firstly, this can be done by testing other, similar DA antagonists to those used, such as SCH-39166 as a D1-like receptor antagonist or chlorpromazine as a D2-like receptor antagonist. Application of a stronger, more potent antagonist may show differing or complimentary results to those obtained, providing a more accurate conclusion to the results already obtained. This can also be done by testing drugs that target downstream signalling molecules (such as targeting PLC which has numerous targets (Huang *et al.*, 2013) or by targeting Akt using AZD5363 (Ribas *et al.*, 2015)) or by using receptor agonists rather than antagonists. These agonists, such as the D1-like agonist SKF-38392 or the D2-like agonist quinpirole, would show opposing results to those shown during antagonist application, thus would primarily be complementary to antagonist experiments already completed.

Furthermore, although Barbadin was shown to be statistically insignificant throughout its coapplication with 1000 μ M DA, analysis of Barbadin at a lower concentration of DA (such as at 100 μ M) may provide a better understanding into how the drug affects D₂ receptor transmission.

5.6.3 Implementing Clinical Relevance

Finally, experiments using genetic models of rats, for example the aforementioned FSL rats, will allow comparisons to be drawn between physiological and pathophysiological models, presenting a clinical relevance to the experiments. Completing identical experiments in the genetic model to that completed in the Sprague-Dawley rats will indicate a physiological

difference between the two, potentially bettering the understanding of the pathophysiological condition and allowing potential new clinical treatments to be derived.

6 Acknowledgments

I would firstly like to express my gratitude towards my initial lead supervisor Dr Douglas Caruana. He not only helped in designing the experiments which were conducted but also assembled the experimental apparatus which I was able to carry out experiments on. I would also like to thank him for providing information throughout the project, developing both my theoretical and practical understanding of the field. I would then like to thank my current lead supervisor, Prof. David Furness, for agreeing to become my lead supervisor in Doug's absence, and Dr Mike Evans for assisting me through the final stages of the submission. My final academic thanks must go to all the examiners for the electronic viva voce, Dr Mike Evans, Dr Arturas Volianskis and Dr Chris Adams, for agreeing to conduct the viva voce electronically during the COVID-19 pandemic. As well as academic supervisors, I must also like to deeply express my gratitude towards my co-supervisor Dr John Butcher and my MPhil colleagues Laura Harvey and Tyler Wells. I thank all three mentioned as they all helped enhance my understanding of the field, assisted the preparation of slices throughout the project as well as helping to collect data in my absence. Laura also kindly provided me with the 100 μM and 1000 μM single application DA experiment datasets to be used during the analysis, which allowed statistical comparisons to be drawn. As well as postgraduate colleagues, I would also like to thank all the undergraduate students (Eduard, Marium, Martha and Daphna) for all assisting in both electrophysiological and immunohistochemical experiments. Penultimately, I thank Keele University for allowing me to complete this Master of Philosophy, as it has given me an insight into what a career in scientific research may entail, further motivating me to pursue one. Finally, a tremendous thanks to both my wonderful family for their ongoing support, and also my girlfriend, now fiancée and soon to be wife Jiahui Kuan for all her love and support throughout.

7 References

- Abbott, L. and Nelson, S. (2000). Synaptic plasticity: Taming the beast. *Nature Neuroscience*, 3(S11), 1178-1183.
- Abelaira, H., Réus, G., Neotti, M. and Quevedo, J. (2014). The role of mTOR in depression and antidepressant responses. *Life Sciences*, 101(1-2), 10-14.
- Aberoumandi, S., Vousooghi, N., Tabrizi, B. and Karimi, P. (2019). Heroin-based crack induces hyperalgesia through β -arrestin 2 redistribution and phosphorylation of Erk1/2 and JNK in the periaqueductal gray area. *Neuroscience Letters*, 698(1), 133-139.
- Abraham, W. and Bear, M. (1996). Metaplasticity: The plasticity of synaptic plasticity. *Trends in Neurosciences*, 19(4), 126-130.
- Aggleton, J., O'Mara, S., Vann, S., Wright, N., Tsanov, M. and Erichsen, J. (2010). Hippocampal-anterior thalamic pathways for memory: Uncovering a network of direct and indirect actions. *European Journal of Neuroscience*, 31(12), 2292-2307.
- Aghajanian, G. and Rasmussen, K. (1989). Intracellular studies in the facial nucleus illustrating a simple new method for obtaining viable motoneurons in adult rat brain slices. *Synapse*, 3(4), 331-338.
- Agster, K. and Burwell, R. (2013). Hippocampal and subicular efferents and afferents of the perirhinal, postrhinal, and entorhinal cortices of the rat. *Behavioural Brain Research*, 254(1), 50-64.
- Alderton, W., Cooper, C. and Knowles, R. (2001). Nitric oxide synthases: Structure, function and inhibition. *Biochemical Journal*, 357(3), 593-615.
- Amaral, D., Insausti, R. and Cowan, W. (1987). The entorhinal cortex of the monkey: I. Cytoarchitectonic organization. *The Journal of Comparative Neurology*, 264(3), 326-355.
- Amaral, D., Scharfman, H. and Lavenex, P. (2008). The dentate gyrus: Fundamental neuroanatomical organization (dentate gyrus for dummies). *Progress in Brain Research*, 163(1), 3-22.
- Anacker, C. and Hen, R. (2017). Adult hippocampal neurogenesis and cognitive flexibility - Linking memory and mood. *Nature Reviews Neuroscience*, 18(6), 335-346.
- Anand, K. and Dhikav, V. (2012). Hippocampus in health and disease: An overview. *Annals of Indian Academy of Neurology*, 15(4), 239-262.
- Andersen, P., Gingrich, J., Bates, M., Dearry, A., Falardeau, P., Senogles, S. and Caron, M. (1990). Dopamine receptor subtypes: Beyond the D1/D2 classification. *Trends in Pharmacological Sciences*, 11(6), 231-236.
- Angst, J. and Cassano, G. (2005). The mood spectrum: Improving the diagnosis of bipolar disorder. *Bipolar Disorders*, 7(s4), 4-12.
- Ankri, L., Yarom, Y. and Uusisaari, M. (2014). Slice it hot: Acute adult brain slicing in physiological temperature. *Journal of Visualized Experiments*, 92(52068), 1-8.

- Anon, A. (2021). *Depression*. [online] WHO.int. Available at: <https://www.who.int/news-room/fact-sheets/detail/depression> [Accessed 12 Jan. 2021].
- Baldassano, C., Beck, D. and Fei-Fei, L. (2013). Differential connectivity within the parahippocampal place area. *NeuroImage*, 15(75), 228-237.
- Ballanyi, K. and Ruangkittisakul A. (2008) Brain slices. In: Binder M.D., Hirokawa N. and Windhorst U. (eds) *Encyclopaedia of neuroscience*. Springer, Berlin, Heidelberg.
- Baltaci, S., Mogulkoc, R. and Baltaci, A. (2018). Molecular mechanisms of early and late LTP. *Neurochemical Research*, 44(2), 281-296.
- Ban, T. (2007). Fifty years chlorpromazine: A historical perspective. *Neuropsychiatric Disease and Treatment*, 3(4), 495-500.
- Banerjee, A., Meredith, R., Rodríguez-Moreno, A., Mierau, S., Auberson, Y. and Paulsen, O. (2009). Double dissociation of spike timing-dependent potentiation and depression by subunit-preferring NMDA receptor antagonists in mouse barrel cortex. *Cerebral Cortex*, 19(12), 2959-2969.
- Barnes, J., Barnes, N., Costall, B., Naylor, R. and Tyers, M. (1989). 5-HT₃ receptors mediate inhibition of acetylcholine release in cortical tissue. *Nature*, 338(6218), 762-763.
- Barria, A., Muller, D., Derkach, V., Griffith, L. and Soderling, T. (1997). Regulatory phosphorylation of AMPA-type glutamate receptors by CaM-KII during long-term potentiation. *Science*, 276(5321), 2042-2045.
- Bean, B. (2007). The action potential in mammalian central neurons. *Nature Reviews Neuroscience*, 8(6), 451-465.
- Bear, M., Huber, K. and Warren, S. (2004). The mGluR theory of fragile X mental retardation. *Trends in Neurosciences*, 27(7), 370-377.
- Bear, M. and Malenka, R. (1994). Synaptic plasticity: LTP and LTD. *Current Opinion in Neurobiology*, 4(3), 389-399.
- Beaulieu, J. and Gainetdinov, R. (2011). The physiology, signalling, and pharmacology of dopamine receptors. *Pharmacological Reviews*, 63(1), 182-217.
- Beaulieu, J., Sotnikova, T., Marion, S., Lefkowitz, R., Gainetdinov, R. and Caron, M. (2005). An Akt/ β -arrestin 2/PP2A signalling complex mediates dopaminergic neurotransmission and behaviour. *Cell*, 122(2), 261-273.
- Beautrait, A., Paradis, J., Zimmerman, B., Giubilaro, J., Nikolajev, L., Armando, S., Kobayashi, H., Yamani, L., Namkung, Y., Heydenreich, F., Khoury, E., Audet, M., Roux, P., Veprintsev, D., Laporte, S. and Bouvier, M. (2017). A new inhibitor of the β -arrestin/AP2 endocytic complex reveals interplay between GPCR internalization and signalling. *Nature Communications*, 8(1), 1-16.
- Benazzi, F. (2006). Various forms of depression. *Dialogues in Clinical Neuroscience*, 8(2), 151-161.
- Bender, V., Bender, K., Brasier, D. and Feldman, D. (2006). Two coincidence detectors for spike timing-dependent plasticity in somatosensory cortex. *Journal of Neuroscience*, 26(16), 4166-4177.

- Berglöv, E. and Strömberg, I. (2009). Locus coeruleus promotes survival of dopamine neurons in ventral mesencephalon. An in oculo grafting study. In: S. Gilman, ed., *Experimental Neurology*, volume 216.1. Elsevier: Amsterdam, 158-165.
- Berlin, I., Givry-Steiner, L., Lecrubier, Y. and Puech, A. (1998). Measures of anhedonia and hedonic responses to sucrose in depressive and schizophrenic patients in comparison with healthy subjects. *European Psychiatry*, 13(6), 303-309.
- Berlucchi, G. (2002). The origin of the term plasticity in the neurosciences: Ernesto Lugaro and chemical synaptic transmission. *Journal of the History of the Neurosciences*, 11(3), 305-309.
- Berretta, N. and Jones, R. (1996). Tonic facilitation of glutamate release by presynaptic N-methyl-d-aspartate autoreceptors in the entorhinal cortex. *Neuroscience*, 75(2), 339-344.
- Beurel, E., Grieco, S. and Jope, R. (2015). Glycogen synthase kinase-3 (GSK3): Regulation, actions, and diseases. *Pharmacology & Therapeutics*, 148(1), 114-131.
- Beurel, E. and Jope, R. (2008). Differential regulation of STAT family members by glycogen synthase kinase-3. *Journal of Biological Chemistry*, 283(32), 21934-21944.
- Bi, G. and Poo, M. (1998). Synaptic modifications in cultured hippocampal neurons: Dependence on spike timing, synaptic strength, and postsynaptic cell type. *The Journal of Neuroscience*, 18(24), 10464-10472.
- Blackshaw, L., Page, A. and Young, R. (2011). Metabotropic glutamate receptors as novel therapeutic targets on visceral sensory pathways. *Frontiers in Neuroscience*, 5(40), 1-7.
- Blackstad, T. (1956). Commissural connections of the hippocampal region in the rat, with special reference to their mode of termination. *The Journal of Comparative Neurology*, 105(3), 417-537.
- Blakesley, R., Mazumdar, S., Dew, M., Houck, P., Tang, G., Reynolds, C. and Butters, M. (2009). Comparisons of methods for multiple hypothesis testing in neuropsychological research. *Neuropsychology*, 23(2), 255-264.
- Bliss, T. and Lømo, T. (1973). Long-lasting potentiation of synaptic transmission in the dentate area of the anaesthetized rabbit following stimulation of the perforant path. *The Journal of Physiology*, 232(2), 331-356.
- Blitzer, R., Connor, J., Brown, G., Wong, T., Shenolikar, S., Lyengar, R. and Landau, E. (1998). Gating of CaMKII by cAMP-regulated protein phosphatase activity during LTP. *Science*, 280(5371), 1940-1943.
- Blundon, J. and Zakharenko, S. (2008). Dissecting the components of long-term potentiation. *The Neuroscientist*, 14(6), 598-608.
- Bortolotto, Z., Fitzjohn, S. and Collingridge, G. (1999). Roles of metabotropic glutamate receptors in LTP and LTD. *Current Opinion in Neurobiology*, 9(3), 299-304.
- Bouras, R. and Chapman, C. (2003). Long-term synaptic depression in the adult entorhinal cortex in vivo. *Hippocampus*, 13(7), 780-790.

- Bourdy, R. and Barrot, M. (2012). A new control centre for dopaminergic systems: Pulling the VTA by the tail. *Trends in Neurosciences*, 35(11), 681-690.
- Bourne, J. (2001). SCH 23390: The first selective dopamine D1-Like receptor antagonist. *CNS Drug Reviews*, 7(4), 399-414.
- Bouron, A. and Reuter, H. (1999). The D1 dopamine receptor agonist SKF-38393 stimulates the release of glutamate in the hippocampus. *Neuroscience*, 94(4), 1063-1070.
- Bozzi, Y. and Borrelli, E. (2013). The role of dopamine signalling in epileptogenesis. *Frontiers in Cellular Neuroscience*, 17(7), 157.
- Braak, H. and Braak, E. (1992). The human entorhinal cortex: Normal morphology and lamina-specific pathology in various diseases. *Neuroscience Research*, 15(1-2), 6-31.
- Breese, G. and Mueller, R. (1985). SCH-23390 antagonism of a D-2 dopamine agonist depends upon catecholaminergic neurons. *European Journal of Pharmacology*, 113(1), 109-114.
- Briese, E. (1998). Normal body temperature of rats: The setpoint controversy. *Neuroscience & Biobehavioral Reviews*, 22(3), 427-436.
- Burwell, R. and Agster, K. (2008). Anatomy of the hippocampus and the declarative memory system. In: J. Byrne, ed., *Learning and Memory: A Comprehensive Reference*, 1st ed. Amsterdam: Elsevier, 47-66.
- Burwell, R. and Amaral, D. (1998). Cortical afferents of the perirhinal, postrhinal, and entorhinal cortices of the rat. *The Journal of Comparative Neurology*, 398(2), 179-205.
- Caballero-Bleda, M. and Witter, M. (1993). Regional and laminar organization of projections from the presubiculum and parasubiculum to the entorhinal cortex: An anterograde tracing study in the rat. *The Journal of Comparative Neurology*, 328(1), 115-129.
- Cachope, R., Mackie, K., Triller, A., O'Brien, J. and Pereda, A. (2007). Potentiation of electrical and chemical synaptic transmission mediated by endocannabinoids. *Neuron*, 56(6), 1034-1047.
- Cahalan, M. and Neher, E. (1992). Patch clamp techniques: an overview. *Methods in Enzymology*, 207, 3-14.
- Cajal, S. (1909). *Histologie du système nerveux de l'homme et des vertébrés tome II*. 1st ed. Paris: Maloine, 753. [In French].
- Campbell, S. and MacQueen, G. (2004). The role of the hippocampus in the pathophysiology of major depression. *Journal of Psychiatry & Neuroscience*, 29(6), 417-426.
- Campbell, S. and MacQueen, G. (2006). An update on regional brain volume differences associated with mood disorders. *Current Opinion in Psychiatry*, 19(1), 25-33.
- Canto, C., Wouterlood, F. and Witter, M. (2008). What does the anatomical organization of the entorhinal cortex tell us. *Neural Plasticity*, 2008(381243), 1-18.
- Carlson, G., Wang, Y. and Alger, B. (2002). Endocannabinoids facilitate the induction of LTP in the hippocampus. *Nature Neuroscience*, 5(8), 723-724.
- Carlsson, A. (1993). Thirty years of dopamine research. *Advances in Neurology*, 60(1), 1-10.

- Caruana, D. and Chapman, C. (2008). Dopaminergic suppression of synaptic transmission in the lateral entorhinal cortex. *Neural Plasticity*, 2008(203514), 1-14.
- Caruana, D., Sorge, R., Stewart, J. and Chapman, C. (2006). Dopamine has bidirectional effects on synaptic responses to cortical inputs in layer II of the lateral entorhinal cortex. *Journal of Neurophysiology*, 96(6), 3006-3015.
- Carulli, D., Foscarin, S. and Rossi, F. (2011). Activity-dependent plasticity and gene expression modifications in the adult CNS. *Frontiers in Molecular Neuroscience*, 4(50), 1-12.
- Castellucci, V., Pinsker, H., Kupfermann, I. & Kandel, E. R. (1970). Neuronal mechanisms of habituation and dishabituation of the gill-withdrawal reflex in *Aplysia*. *Science*, 167(1), 1745-1748.
- Castillo, P. (2012). Presynaptic LTP and LTD of excitatory and inhibitory synapses. *Cold Spring Harbor Perspectives in Biology*, 4(2), 1-23.
- Chamberlain, S., Yang, J. and Jones, R. (2008). The role of NMDA receptor subtypes in short-term plasticity in the rat entorhinal cortex. *Neural Plasticity*, 2008(872456), 1-13.
- Chater, T. and Goda, Y. (2014). The role of AMPA receptors in postsynaptic mechanisms of synaptic plasticity. *Frontiers in Cellular Neuroscience*, 8(401), 1-14.
- Chen, P., Geballe, M., Stansfeld, P., Johnston, A., Yuan, H., Jacob, A., Snyder, J., Traynelis, S. and Wyllie, D. (2015). Structural features of the glutamate binding site in recombinant NR1/NR2A N-methyl-D-aspartate receptors determined by site-directed mutagenesis and molecular modelling. *Molecular Pharmacology*, 67(5), 1470-1484.
- Chen, X., Kombian, S., Zidichouski, J. and Pittman, Q. (1999). Dopamine depresses glutamatergic synaptic transmission in the rat parabrachial nucleus in vitro. In: J. Lerma, ed., *Neuroscience*, volume 90.2. Elsevier: Amsterdam, 457-468.
- Cheng, Q., Song, S. and Augustine, G. (2018). Molecular mechanisms of short-term plasticity: Role of synapsin phosphorylation in augmentation and potentiation of spontaneous glutamate release. *Frontiers in Synaptic Neuroscience*, 10(33), 1-12.
- Chetkovich, D., Gray, R., Johnston, D. and Sweatt, J. (1991). N-methyl-D-aspartate receptor activation increases cAMP levels and voltage-gated Ca²⁺ channel activity in area CA1 of hippocampus. *Proceedings of the National Academy of Sciences*, 88(15), 6467-6471.
- Chevaleyre, V. and Siegelbaum, S. (2010). Strong CA2 pyramidal neuron synapses define a powerful disinaptic cortico-hippocampal loop. *Neuron*, 66(4), 560-572.
- Chevaleyre, V., Takahashi, K. and Castillo, P. (2006). Endocannabinoid-mediated synaptic plasticity in the CNS. *Annual Review of Neuroscience*, 29(1), 37-76.
- Christoph, G., Leonzio, R. and Wilcox, K. (1986). Stimulation of the lateral habenula inhibits dopamine-containing neurons in the substantia nigra and ventral tegmental area of the rat. *The Journal of Neuroscience*, 6(3), 613-619.

- Citri, A. and Malenka, R. (2008). Synaptic plasticity: Multiple forms, functions, and mechanisms. *Neuropsychopharmacology*, 33(1), 18-41.
- Clark, A., McCorvy, J., Watts, V. and Nichols, D. (2011). Assessment of dopamine D1 receptor affinity and efficacy of three tetracyclic conformationally-restricted analogues of SKF38393. *Bioorganic & Medicinal Chemistry*, 19(18), 5420-5431.
- Coizet, V., Dommett, E., Klop, E., Redgrave, P. and Overton, P. (2010). The parabrachial nucleus is a critical link in the transmission of short latency nociceptive information to midbrain dopaminergic neurons. *Neuroscience*, 168(1), 263-272.
- Collingridge, G. (1985). Long term potentiation in the hippocampus: mechanisms of initiation and modulation by neurotransmitters. *Trends in Pharmacological Sciences*, 6, 407-411.
- Collingridge, G., Isaac, J. and Wang, Y. (2004). Receptor trafficking and synaptic plasticity. *Nature Reviews Neuroscience*, 5(12), 952-962.
- Collingridge, G., Kehl, S. and McLennan, H. (1983). Excitatory amino acids in synaptic transmission in the schaffer collateral-commissural pathway of the rat hippocampus. *The Journal of Physiology*, 334(1), 33-46.
- Cornish-Bowden, A. (1974). A simple graphical method for determining the inhibition constants of mixed, uncompetitive and non-competitive inhibitors (Short Communication). *Biochemical Journal*, 137(1), 143-144.
- Cuellar, A., Johnson, S. and Winters, R. (2005). Distinctions between bipolar and unipolar depression. *Clinical Psychology Review*, 25(3), 307-339.
- Cui, Y., Prokin, I., Xu, H., Delord, B., Genet, S., Venance, L. and Berry, H. (2016). Endocannabinoid dynamics gate spike-timing dependent depression and potentiation. *eLife*, 5(e13185), 1-32.
- Czajkowski, R., Sugar, J., Zhang, S., Couey, J., Ye, J. and Witter, M. (2013). Superficially projecting principal neurons in layer V of medial entorhinal cortex in the rat receive excitatory retrosplenial input. *Journal of Neuroscience*, 33(40), 15779-15792.
- Dal Toso, R., Sommer, B., Ewert, M., Herb, A., Pritchett, D., Bach, A., Shivers, B. and Seeburg, P. (1989). The dopamine D2 receptor: Two molecular forms generated by alternative splicing. *The EMBO Journal*, 8(13), 4025-4034.
- Daniels, G. and Amara, S. (1999). Regulated trafficking of the human dopamine transporter. *Journal of Biological Chemistry*, 274(50), 35794-35801.
- Daoudal, G., Hanada, Y. and Debanne, D. (2002). Bidirectional plasticity of excitatory postsynaptic potential (EPSP)-spike coupling in CA1 hippocampal pyramidal neurons. *Proceedings of the National Academy of Sciences*, 99(22), 14512-14517.
- Davies, C. and Collingridge, G. (1996). Regulation of EPSPs by the synaptic activation of GABAB autoreceptors in rat hippocampus. *The Journal of Physiology*, 496(2), 451-470.

- Davis, K., Buchsbaum, M., Shihabuddin, L., Spiegel-Cohen, J., Metzger, M., Frecska, E., Keefe, R. and Powchik, P. (1998). Ventricular enlargement in poor-outcome schizophrenia. *Biological Psychiatry*, 43(11), 783-793.
- Deng, P. and Lei, S. (2008). Serotonin increases GABA release in rat entorhinal cortex by inhibiting interneuron TASK-3 K⁺ channels. *Molecular and Cellular Neuroscience*, 39(2), 273-284.
- Der-Avakian, A. and Markou, A. (2012). The neurobiology of anhedonia and other reward-related deficits. *Trends in Neurosciences*, 35(1), 68-77.
- Derkach, V., Oh, M., Guire, E. and Soderling, T. (2007). Regulatory mechanisms of AMPA receptors in synaptic plasticity. *Nature Reviews Neuroscience*, 8(2), 101-113.
- Deutch, A., Goldstein, M. and Roth, R. (1986). Activation of the locus coeruleus induced by selective stimulation of the ventral tegmental area. *Brain Research*, 363(2), 307-314.
- Devane, W., Hanus, L., Breuer, A., Pertwee, R., Stevenson, L., Griffin, G., Gibson, D., Mandelbaum, A., Etinger, A. and Mechoulam, R. (1992). Isolation and structure of a brain constituent that binds to the cannabinoid receptor. *Science*, 258(5090), 1946-1949.
- Diering, G., Heo, S., Hussain, N., Liu, B. and Haganir, R. (2016). Extensive phosphorylation of AMPA receptors in neurones. *Proceedings of the National Academy of Sciences*, 113(33), 4920-4927.
- Dietrich, D., Kirschstein, T., Kukley, M., Pereverzev, A., von der Brellie, C., Schneider, T. and Beck, H. (2003). Functional specialization of presynaptic Cav2.3 Ca²⁺ channels. *Neuron*, 39(3), 483-496.
- Ding, Q., He, X., Hsu, J., Xia, W., Chen, C., Li, L., Lee, D., Liu, J., Zhong, Q., Wang, X. and Hung, M. (2007). Degradation of Mcl-1 by β -TrCP mediates glycogen synthase kinase 3-induced tumor suppression and chemosensitization. *Molecular and Cellular Biology*, 27(11), 4006-4017.
- Dodge, F. and Rahamimoff, R. (1967). Co-operative action of calcium ions in transmitter release at the neuromuscular junction. *The Journal of Physiology*, 193(2), 419-432.
- Dowlati, Y., Herrmann, N., Swardfager, W., Liu, H., Sham, L., Reim, E. and Lanctôt, K. (2010). A meta-analysis of cytokines in major depression. *Biological Psychiatry*, 67(5), 446-457.
- Drewe, E., 1974. The effect of type and area of brain lesion on Wisconsin card sorting test performance. *Cortex*, 10(2), 159-170.
- Duclot, F. and Kabbaj, M. (2017). The role of early growth response 1 (EGR1) in brain plasticity and neuropsychiatric disorders. *Frontiers in Behavioural Neuroscience*, 11(35), 1-20.
- Dudek, S. and Bear, M. (1992). Homosynaptic long-term depression in area CA1 of hippocampus and effects of N-methyl-D-aspartate receptor blockade. *Proceedings of the National Academy of Sciences*, 89(10), 4363-4367.

- Duguid, I., Smart, T. (2009). 'Presynaptic NMDA receptors', in Van Dongen, A. (ed.) *Biology of the NMDA Receptor*. Boca Ranton: Florida, 313-328.
- Engelien, A., Tüscher, O., Hermans, W., Isenberg, N., Eidelberg, D., Frith, C., Stern, E. and Silbersweig, D. (2005). Functional neuroanatomy of non-verbal semantic sound processing in humans. *Journal of Neural Transmission*, 113(5), 599-608.
- Erulkar, S. and Rahamimoff, R. (1978). The role of calcium ions in tetanic and post-tetanic increase of miniature end-plate potential frequency. *The Journal of Physiology*, 278(1), 501-511.
- Faay, M., Czobor, P. and Sommer, I., (2018). Efficacy of typical and atypical antipsychotic medication on hostility in patients with psychosis-spectrum disorders: a review and meta-analysis. *Neuropsychopharmacology*, 43(12), 2340-2349.
- Faquih, A., Memon, R., Hafeez, H., Zeshan, M. and Naveed, S. (2019). A review of novel antidepressants: A guide for clinicians. *Cureus*, 11(3), 1-20.
- Fedotova, J. (2012). Effects of stimulation and blockade of receptor on depression-like behaviour in ovariectomized female rats. *ISRN Pharmacology*, 2012(5692), 1-8.
- Fioravante, D. and Regehr, W. (2011). Short-term forms of presynaptic plasticity. *Current Opinion in Neurobiology*, 21(2), 269-274.
- Free, R., Hazelwood, L., Cabrera, D., Spalding, H., Namkung, Y., Rankin, M. and Sibley, D. (2007). D1 and D2 dopamine receptor expression is regulated by direct interaction with the chaperone protein calnexin. *Journal of Biological Chemistry*, 282(29), 21285-21300.
- Gabrieli, J., Poldrack, R. and Desmond, J., 1998. The role of left prefrontal cortex in language and memory. *Proceedings of the National Academy of Sciences*, 95(3), 906-913.
- Gage, A., Reyes, M. and Stanton, P. (1997). Nitric-oxide-guanylyl-cyclase-dependent and -independent components of multiple forms of long-term synaptic depression. *Hippocampus*, 7(3), 286-295.
- Gallagher, S., Daly, C., Bear, M. and Huber, K. (2004). Extracellular signal-regulated protein kinase activation is required for metabotropic glutamate receptor-dependent long-term depression in hippocampal area CA1. *Journal of Neuroscience*, 24(20), 4859-4864.
- Garcia-Cabezas, M., Martinez-Sanchez, P., Sanchez-Gonzalez, M., Garzon, M. and Cavada, C. (2008). Dopamine innervation in the thalamus: Monkey versus rat. *Cerebral Cortex*, 19(2), 424-434.
- Gerdeman, G., Ronesi, J. and Lovinger, D. (2002). Postsynaptic endocannabinoid release is critical to long-term depression in the striatum. *Nature Neuroscience*, 5(5), 446-451.
- Gerfen, C. and Wilson, C. (1996). The basal ganglia. In: L. Swanson, A. Björklund and T. Hökfelt, ed., *Handbook of Chemical Neuroanatomy*, 12th ed. Amsterdam: Elsevier, 371-468.

- German, C., Baladi, M., McFadden, L., Hanson, G. and Fleckenstein, A. (2015). Regulation of the dopamine and vesicular monoamine transporters: Pharmacological targets and implications for disease. *Pharmacological Reviews*, 67(4), 1005-1024.
- Ghasemi, M., Phillips, C., Trillo, L., De Miguel, Z., Das, D. and Salehi, A. (2014). The role of NMDA receptors in the pathophysiology and treatment of mood disorders. *Neuroscience & Biobehavioral Reviews*, 47(1), 336-358.
- Gioia, D., Alexander, N. and McCool, B. (2016). Differential expression of Munc13-2 produces unique synaptic phenotypes in the basolateral amygdala of C57BL/6J and DBA/2J mice. *Journal of Neuroscience*, 36(43), 10964-10977.
- Giros, B., El Mestikawy, S., Godinot, N., Yang-Feng, T. and Caron, M. (1992). Molecular cloning, pharmacological characterization and genetic studies of the human dopamine transporter. *European Neuropharmacology*, 42(3), 383-390.
- Gladding, C., Fitzjohn, S. and Molnár, E. (2009). Metabotropic glutamate receptor-mediated long-term depression: Molecular mechanisms. *Pharmacological Reviews*, 61(4), 395-412.
- Glovaci, I. and Chapman, C. (2015). Activation of phosphatidylinositol-linked dopamine receptors induces a facilitation of glutamate-mediated synaptic transmission in the lateral entorhinal cortex. *PLOS ONE*, 10(7), e0131948.
- Gorwood, P. (2008). Neurobiological mechanisms of anhedonia. *Dialogues in Clinical Neuroscience*, 10(3), 291-299.
- Goto, Y., Yang, C. and Otani, S. (2010). Functional and dysfunctional synaptic plasticity in prefrontal cortex: Roles in psychiatric disorders. *Biological Psychiatry*, 67(3), 199-207.
- Graves, A., Moore, S., Bloss, E., Menseh, B., Kath, W. and Spruston, N. (2013). Hippocampal pyramidal neurons comprise two distinct cell types that are countermodulated by metabotropic receptors. *Neuron*, 77(2), 376.
- Habets, A., Lopes da Silva, F. and de Quartel, F. (1980). Autoradiography of the olfactory-hippocampal pathway in the cat with special reference to the perforant path. *Experimental Brain Research*, 38(3), 257-265.
- Hamam, B., Sinai, M., Poirier, G. and Chapman, C. (2007). Cholinergic suppression of excitatory synaptic responses in layer II of the medial entorhinal cortex. *Hippocampus*, 17(2), 103-113.
- Hansen, N. and Manahan-Vaughan, D. (2012). Dopamine D1/D5 receptors mediate informational saliency that promotes persistent hippocampal long-term plasticity. *Cerebral Cortex*, 24(4), 845-858.
- Harvey, L., Butcher, J., Ljubotina, D., Pettitt, G., Wells, T., Caruana, D. (2021). Persistent desensitisation of dopamine receptor function in the lateral entorhinal cortex induced by repeated exposure to dopamine. Unpublished manuscript, College of Health and Life Sciences, Aston University, Birmingham, United Kingdom.
- Hasler, G. (2010). Pathophysiology of depression: Do we have any solid evidence of interest to clinicians? *World Psychiatry*, 9(3) 155-161.

- Hawkins, K., Gavin, C., Sweatt, D. (2017). 'Long-term potentiation: A candidate cellular mechanism for information storage in the CNS', in Bryne, J. (ed.) *Learning and Memory: A Comprehensive Reference (Second Edition)*. Academic Press: Massachusetts, 33-64.
- Hebb, D. (1949). *The organization of behaviour*. 1st Edition. Wiley, New York
- Heifets, B. and Castillo, P. (2009). Endocannabinoid signaling and long-term synaptic plasticity. *Annual Review of Physiology*, 71(1), 283-306.
- Heifets, B., Chevaleyre, V. and Castillo, P. (2008). Interneuron activity controls endocannabinoid-mediated presynaptic plasticity through calcineurin. *Proceedings of the National Academy of Sciences*, 105(29), 10250-10255.
- Henze, D., Urban, N. and Barrionuevo, G. (2000). The multifarious hippocampal mossy fibre pathway: A review. *Neuroscience*, 98(3), 407-427.
- Hodgkin, A., Huxley, A. and Katz, B. (1952). Measurement of current-voltage relations in the membrane of the giant axon of *Loligo*. *The Journal of Physiology*, 116(4), 424-448.
- Holland, L. and Wagner, J. (1998). Primed facilitation of homosynaptic long-term depression and depotentiation in rat hippocampus. *The Journal of Neuroscience*, 18(3), 887-894.
- Holm, T., Isaksen, T. and Lykke-Hartmann, K. (2016). HPLC neurotransmitter analysis. *Methods in Molecular Biology*, 1377(1), 333-340.
- Horne, E. and Dell'Acqua, M. (2007). Phospholipase C is required for changes in postsynaptic structure and function associated with NMDA receptor-dependent long-term depression. *Journal of Neuroscience*, 27(13), 3523-3534.
- Hornykiewicz, O. (2002). Dopamine miracle: From brain homogenate to dopamine replacement. *Movement Disorders*, 17(3), 501-508.
- Hou, L., Antion, M., Hu, D., Spencer, C., Paylor, R. and Klann, E. (2006). Dynamic translational and proteasomal regulation of fragile X mental retardation protein controls mGluR-dependent long-term depression. *Neuron*, 51(4), 441-454.
- Huang, W., Barrett, M., Hajicek, N., Hicks, S., Harden, T., Sondek, J. and Zhang, Q. (2013). Small molecule inhibitors of phospholipase C from a novel high-throughput screen. *Journal of Biological Chemistry*, 288(8), 5840-5848.
- Hubel, D. and Wiesel, T., (1962). Receptive fields, binocular interaction and functional architecture in the cat's visual cortex. *The Journal of Physiology*, 160(1), 106-154.
- Hulme, S., Jones, O. and Abraham, W. (2013). Emerging roles of metaplasticity in behaviour and disease. *Trends in Neurosciences*, 36(6), 353-362.
- Humeau, Y., Shaban, H., Bissière, S. and Lüthi, A. (2003). Presynaptic induction of heterosynaptic associative plasticity in the mammalian brain. *Nature*, 426(6968), 841-845.
- Hunsaker, M., Chen, V., Tran, G. and Kesner, R. (2013). The medial and lateral entorhinal cortex both contribute to contextual and item recognition memory: A test of the binding of items and context model. *Hippocampus*, 23(5), 380-391.
- Insausti, R. (1993). Comparative anatomy of the entorhinal cortex and hippocampus in mammals. *Hippocampus*, 1993(3), 19-26.

- Insausti, R., Amaral, D. and Cowan, W. (1987). The entorhinal cortex of the monkey: II. cortical afferents. *The Journal of Comparative Neurology*, 264(3), 356-395.
- Isella, V., Iurlaro, S., Piolti, R., Ferrarese, C., Frattola, L., Appollonio, I., Melzi, P. and Grimaldo, M. (2003). Physical anhedonia in Parkinson's disease. *Journal of Neurology, Neurosurgery & Psychiatry*, 74(9), 1308-1311.
- Ishikawa, M., Otaka, M., Huang, Y., Neumann, P., Winters, B., Grace, A., Schluter, O. and Dong, Y. (2013). Dopamine triggers heterosynaptic plasticity. *Journal of Neuroscience*, 33(16), 6759-6765.
- Ito, H. and Schuman, E. (2011). Functional division of hippocampal area CA1 via modulatory gating of entorhinal cortical inputs. *Hippocampus*, 22(2), 372-387.
- Izumi, Y., Clifford, D. and Zorumski, C. (1992). Low concentrations of N-methyl-D-aspartate inhibit the induction of long-term potentiation in rat hippocampal slices. *Neuroscience Letters*, 137(2), 245-248.
- James, S., Abate, D., Abate, K., Abay, S., Abbafati, C., Abbasi, N., ... Murray, C. (2018). Global, regional, and national incidence, prevalence, and years lived with disability for 354 diseases and injuries for 195 countries and territories, 1990–2017: A systematic analysis for the Global Burden of Disease Study 2017. *The Lancet*, 392(10159), 1789-1858.
- Jiang, L., Sun, S., Nedergaard, M. and Kang, J. (2000). Paired-pulse modulation at individual GABAergic synapses in rat hippocampus. *The Journal of Physiology*, 523(2), 425-439.
- Jideama, N., Crawford, B., Hussain, A. and Raynor, R. (2006). Dephosphorylation specificities of protein phosphatase for cardiac troponin I, troponin T, and sites within troponin T. *International Journal of Biological Sciences*, 2(1), 1-9.
- Jo, J., Son, G., Winters, B., Kim, M., Whitcomb, D., Dickinson, B., Lee, Y., Futai, K., Amici, M., Sheng, M., Collingridge, G. and Cho, K. (2010). Muscarinic receptors induce LTD of NMDAR EPSCs via a mechanism involving Hippocalcin, AP2 and PSD-95. *Nature Neuroscience*, 13(10), 1216-1224.
- Jonas, P. (2000). The time course of signaling at central glutamatergic synapses. *Physiology*, 15(2), 83-89.
- Joseph, B., Narayanaswamy, J. and Venkatasubramanian, G. (2015). Insight in schizophrenia: Relationship to positive, negative and neurocognitive dimensions. *Indian Journal of Psychological Medicine*, 37(1), 5-11.
- Kalia, L., Gingrich, J. and Salter, M. (2004). Src in synaptic transmission and plasticity. *Oncogene*, 23(48), 8007-8016.
- Kameyama, K., Lee, H., Bear, M. and Haganir, R. (1998). Involvement of a postsynaptic protein kinase A substrate in the expression of homosynaptic long-term depression. *Neuron*, 21(5), 1163-1175.
- Kampa, B., Clements, J., Jonas, P. and Stuart, G. (2004). Kinetics of Mg²⁺ unblock of NMDA receptors: Implications for spike-timing dependent synaptic plasticity. *The Journal of Physiology*, 556(2), 337-345.

- Kang, D., Kim, K., Lee, S., Lee, Y. and Son, H. (2000). c-Fos expression by dopaminergic receptor activation in rat hippocampal neurons. *Molecules and Cells*, 10(5), 546-551.
- Kang, H., Park, P., Bortolotto, Z., Brandt, S., Colestock, T., Wallach, J., Collingridge, G. and Lodge, D. (2017). Ephedrine: A new psychoactive agent with ketamine-like NMDA receptor antagonist properties. *Neuropharmacology*, 112(A), 144-149.
- Kang-Park, M., Wilson, W., Kuhn, C., Moore, S. and Swartzwelder, H. (2007). Differential sensitivity of GABAA receptor-mediated IPSCs to cannabinoids in hippocampal slices from adolescent and adult rats. *Journal of Neurophysiology*, 98(3), 1223-1230.
- Karmarkar, U. and Buonomano, D. (2002). A model of spike-timing dependent plasticity: One or two coincidence detectors?. *Journal of Neurophysiology*, 88(1), 507-513.
- Karpa, K., Lidow, M., Pickering, M., Levenson, R. and Bergson, C. (1999). N-linked glycosylation is required for plasma membrane localization of D5, but not D1, dopamine receptors in transfected mammalian cells. *Molecular Pharmacology*, 56(5), 1071-1078.
- Keefe, K. and Gerfen, C. (1995). D1-D2 dopamine receptor synergy in striatum: Effects of intrastriatal infusions of dopamine agonists and antagonists on immediate early gene expression. *Neuroscience*, 66(4), 903-913.
- Keller, D., Erö, C. and Markram, H. (2018). Cell densities in the mouse brain: A systematic review. *Frontiers in Neuroanatomy*, 12(83), 1-21.
- Khalid, E. and Chang, J. (2020). β -arrestin-dependent signaling in GnRH control of hormone secretion from goldfish gonadotrophs and somatotrophs. *General and Comparative Endocrinology*, 287 (1133400), 1-9.
- Kilbourn, M., Sherman, P. and Pisani, T. (1992). Repeated reserpine administration reduces in vivo [18F]GBR 13119 binding to the dopamine uptake site. *European Journal of Pharmacology*, 216(1), 109-112.
- Kim, O., Gardner, B., Williams, D., Marinec, P., Cabrera, D., Peters, J., Mak, C., Kim, K. and Sibley, D. (2003). The role of phosphorylation in D1 dopamine receptor desensitization. *Journal of Biological Chemistry*, 279(9), 7999-8010.
- Klein, D. (1984). Depression and anhedonia. In: C. Clark and J. Fawcett, ed., *Anhedonia and Affect Deficit States*. New York, NY: PMA Publishing.
- Knierim, J., Neunuebel, J. and Deshmukh, S. (2013). Functional correlates of the lateral and medial entorhinal cortex: Objects, path integration and local-global reference frames. *Philosophical Transactions of the Royal Society B: Biological Sciences*, 369(1635) 20130369-20130392.
- Koga, Y., Tsurumaki, H., Aoki-Saito, H., Sato, M., Yatomi, M., Takehara, K. and Hisada, T. (2019). Roles of cyclic AMP response element binding activation in the ERK1/2 and p38 MAPK signalling pathway in central nervous system, cardiovascular system, osteoclast differentiation and mucin and cytokine production. *International Journal of Molecular Sciences*, 20(6), 1346-1394.

- Kondo, M., Tajinda, K., Colantuoni, C., Hiyama, H., Seshadri, S., Huang, B., Pou, S., Furukori, K., Hookway, C., Jaaro-Peled, H., Kano, S., Matsuoka, N., Harada, K., Ni, K., Pevsner, J. and Sawa, A. (2013). Unique pharmacological actions of atypical neuroleptic quetiapine: possible role in cell cycle/fate control. *Translational Psychiatry*, 3(4), 1-8.
- Korb, E. and Finkbeiner, S. (2011). Arc in synaptic plasticity: From gene to behaviour. *Trends in Neurosciences*, 34(11), 591-598.
- Korogod, N., Lou, X. and Schneggenburger, R. (2005). Presynaptic Ca²⁺ requirements and developmental regulation of posttetanic potentiation at the calyx of held. *Journal of Neuroscience*, 25(21), 5127-5137.
- Lai, E., Chang, C., Kao Yang, Y., Lin, S. and Lin, C. (2012). Effectiveness of sulpiride in adult patients with schizophrenia. *Schizophrenia Bulletin*, 39(3), 673-683.
- Lally, N., Nugent, A., Luckenbaugh, D., Niciu, M., Roiser, J. and Zarate, C. (2015). Neural correlates of change in major depressive disorder anhedonia following open-label ketamine. *Journal of Psychopharmacology*, 29(5), 596-607.
- Lang, U. and Borgwardt, S. (2013). Molecular mechanisms of depression: Perspectives on new treatment strategies. *Cellular Physiology and Biochemistry*, 31(6), 761-777.
- Larson, J., Wong, D. and Lynch, G. (1986). Patterned stimulation at the theta frequency is optimal for the induction of hippocampal long-term potentiation. *Brain Research*, 368(2), 347-350.
- Leal, G., Bramham, C. and Duarte, C. (2017). BDNF and hippocampal synaptic plasticity. *Vitamins and Hormones*, 104(1), 153-195.
- Lee, F., Xue, S., Pei, L., Vukusic, B., Chéry, N., Wang, Y., Wang, Y., Niznik, H., Yu, X. and Liu, F. (2002). Dual regulation of NMDA receptor functions by direct protein-protein interactions with the dopamine D1 receptor. *Cell*, 111(2), 219-230.
- Lei, S. (2012). Serotonergic modulation of neural activities in the entorhinal cortex. *International Journal of Physiology, Pathophysiology and Pharmacology*, 4(4), 201-210.
- Lerner, T. and Kreitzer, A. (2012). RGS4 is required for dopaminergic control of striatal LTD and susceptibility to parkinsonian motor deficits. *Neuron*, 73(2), 347-359.
- Levitt, M., Spector, S., Sjoerdsma, A. and Udenfriend, S. (1965). Elucidation of the rate limiting step in norepinephrine biosynthesis in the perfused guinea-pig heart. *The Journal of Pharmacology and Experimental Therapeutics*, 148(1), 1-8.
- Li, D., Chen, S., Finnegan, T. and Pan, H. (2003). Signalling pathway of nitric oxide in synaptic GABA release in the rat paraventricular nucleus. *The Journal of Physiology*, 554(1), 100-110.
- Li, X., Yu, K., Zhang, Z., Sun, W., Yang, Z., Feng, J., Chen, X., Liu, C., Wang, H., Guo, Y. and He, J. (2013). Cholecystinin from the entorhinal cortex enables neural plasticity in the auditory cortex. *Cell Research*, 24(3), 307-330.
- Lindgren, N., Usiello, A., Goiny, M., Haycock, J., Erbs, E., Greengard, P., Hokfelt, T., Borrelli, E. and Fisone, G. (2003). Distinct roles of dopamine D2L and D2S receptor isoforms in

- the regulation of protein phosphorylation at presynaptic and postsynaptic sites. *Proceedings of the National Academy of Sciences*, 100(7), 4305-4309.
- Lingenhöhl, K. and Finch, D. (1991). Morphological characterization of rat entorhinal neurons in vivo: Soma-dendritic structure and axonal domains. *Experimental Brain Research*, 84(1), 57-74.
- Lipton, P. and Eichenbaum, H. (2008). Complementary roles of hippocampus and medial entorhinal cortex in episodic memory. *Neural Plasticity*, 2008(258467), 1-8.
- Lisman, J. (1989). A mechanism for the Hebb and the anti-Hebb processes underlying learning and memory. *Proceedings of the National Academy of Sciences*, 86(23), 9574-9578.
- Liu, S. (2020). Dopamine suppresses synaptic responses of fan cells in the lateral entorhinal cortex to olfactory bulb input in mice. *Frontiers in Cellular Neuroscience*, 14(181), 1-10.
- Liu, Q., Pu, L. and Poo, M. (2005). Repeated cocaine exposure in vivo facilitates LTP induction in midbrain dopamine neurons. *Nature*, 437(7061), 1027-1031.
- Liu, X., Chu, X., Mao, L., Wang, M., Lan, H., Li, M., Zhang, G., Parelkar, N., Fibuch, E., Haines, M., Neve, K., Liu, F., Xiong, Z. and Wang, J. (2006). Modulation of D2R-NR2B interactions in response to cocaine. *Neuron*, 52(5), 897-909.
- Liu, X., Huang, F., Huang, C., Yang, Z. and Feng, X. (2008). Analysis of high-frequency stimulation-evoked synaptic plasticity in mouse hippocampal CA1 region. *Acta Physiologica Sinica*, 60(2), 284-291.
- Liu, Y., Ho, R. and Mak, A. (2012). Interleukin (IL)-6, tumour necrosis factor alpha (TNF- α) and soluble interleukin-2 receptors (sIL-2R) are elevated in patients with major depressive disorder: A meta-analysis and meta-regression. *Journal of Affective Disorders*, 139(3), 230-239.
- Llano, I., Leresche, N. and Marty, A. (1991). Calcium entry increases the sensitivity of cerebellar Purkinje cells to applied GABA and decreases inhibitory synaptic currents. *Neuron*, 6(4), 565-574.
- Llorens-Martán, M., Blazquez-Llorca, L., Benavides-Piccione, R., Rabano, A., Hernandez, F., Avila, J. and DeFelipe, J. (2014). Selective alterations of neurons and circuits related to early memory loss in Alzheimer's disease. *Frontiers in Neuroanatomy*, 27(8), 38-62.
- Loewi, O. (1921). Über humorale übertragbarkeit der herznervenwirkung. *Pflügers Archiv: European Journal of Physiology*, 189(1), 239-242. [in German].
- Lorente de Nò, R. (1934) Studies on the structure of the cerebral cortex II. Continuation of the study of the ammonic system. *Journal of Psychology and Neurology* (46), 113-177.
- Lot, T. (1993). Mechanisms of action of dopamine in the peripheral nervous system of chicks and rats. *Journal of Pharmacy and Pharmacology*, 45(10), 896-899.

- Lüscher, C. and Malenka, R. (2012). NMDA receptor-dependent long-term potentiation and long-term depression (LTP/LTD). *Cold Spring Harbor Perspectives in Biology*, 4(6), 1-15.
- Lynch, G., Dunwiddie, T. and Gribkoff, V. (1977). Heterosynaptic depression: A postsynaptic correlate of long-term potentiation. *Nature*, 266(5604), 737-739.
- Malenka, R. and Bear, M. (2004). LTP and LTD. *Neuron*, 44(1), 5-21.
- Malenka, R. and Nicoll, R., (1993). NMDA-receptor-dependent synaptic plasticity: Multiple forms and mechanisms. *Trends in Neurosciences*, 16(12), 521-527.
- Mammen, A., Kameyama, K., Roche, K. and Huganir, R. (1997). Phosphorylation of the α -amino-3-hydroxy-5-methylisoxazole4-propionic acid receptor GluR1 subunit by calcium/ calmodulin-dependent kinase II. *Journal of Biological Chemistry*, 272(51), 32528-32533.
- Mandyam, C. (2013). The interplay between the hippocampus and amygdala in regulating aberrant hippocampal neurogenesis during protracted abstinence from alcohol dependence. *Frontiers in Psychiatry*, 4(61), 1-9.
- Markram, H., Gerstner, W. and Sjöström, P. (2011). A history of spike-timing-dependent plasticity. *Frontiers in Synaptic Neuroscience*, 3(4), 1-24.
- Markram, H., Lübke, J., Frotscher, M. and Sakmann, B. (1997). Regulation of synaptic efficacy by coincidence of postsynaptic APs and EPSPs. *Science*, 275(5297), 213-215.
- Massey, P., Johnson, B., Moul, P., Auberson, Y., Brown, M., Molnar, E., Collingridge, G. and Bashir, Z. (2004). Differential roles of NR2A and NR2B-containing NMDA receptors in cortical long-term potentiation and long-term depression. *Journal of Neuroscience*, 24(36), 7821-7828.
- Masurkar, A., Srinivas, K., Brann, D., Warren, R., Lowes, D. and Siegelbaum, S. (2017). Medial and lateral entorhinal cortex differentially excite deep versus superficial CA1 pyramidal neurons. *Cell Reports*, 18(1), 148-160.
- Mausset-Bonnefont, A., de Sèze, R. and Privat, A. (2003). Immunohistochemistry as a tool for topographical semi-quantification of neurotransmitters in the brain. *Brain Research Protocols*, 10(3), 148-155.
- Mayford, M., Baranes, D., Podsypanina, K. and Kandel, E. (1996). The 3'-untranslated region of CaMKII is a cis-acting signal for the localization and translation of mRNA in dendrites. *Proceedings of the National Academy of Sciences*, 93(23), 13250-13255.
- McGuinness, L., Taylor, C., Taylor, R., Yau, C., Langenhan, T., Hart, M., Christian, H., Tynan, P., Donnelly, P. and Emptage, N. (2010). Presynaptic NMDARs in the hippocampus facilitate transmitter release at theta frequency. *Neuron*, 68(6), 1109-1127.
- McKinnon, K. (2018). Flow cytometry: An overview. *Current Protocols in Immunology*, 120(1), 1-16.
- Meffert, M., Calakos, N., Scheller, R. and Schulman, H. (1996). Nitric oxide modulates synaptic vesicle docking/fusion reactions. *Neuron*, 16(6), 1229-1236.

- Meunier, C., Chameau, P. and Fossier, P. (2017). Modulation of synaptic plasticity in the cortex needs to understand all the players. *Frontiers in Synaptic Neuroscience*, 9(2), 1-15.
- Miettinen, M., Pitkänen, A. and Miettinen, R. (1997). Distribution of calretinin-immunoreactivity in the rat entorhinal cortex: Coexistence with GABA. *The Journal of Comparative Neurology*, 378(3), 363-378.
- Miheau, J. and Barbara, V. (1999). Stimulation of 5-HT_{1A} receptors by systemic or medial septum injection induces anxiogenic-like effects and facilitates acquisition of a spatial discrimination task in mice. *Progress in Neuro-Psychopharmacology and Biological Psychiatry*, 23(6), 1113-1133.
- Millward, T., Zolnierowicz, S. and Hemmings, B. (1999). Regulation of protein kinase cascades by protein phosphatase 2A. *Trends in Biochemical Sciences*, 24(5), 186-191.
- Min, C., Zheng, M., Zhang, X., Guo, S., Kwon, K., Shin, C., Kim, H., Cheon, S. and Kim, K. (2015). N-linked glycosylation on the N-terminus of the dopamine D₂ and D₃ receptors determines receptor association with specific microdomains in the plasma membrane. *Biochimica et Biophysica Acta (BBA) - Molecular Cell Research*, 1853(1), 41-51.
- Money, K. and Stanwood, G. (2013). Developmental origins of brain disorders: roles for dopamine. *Frontiers in Cellular Neuroscience*, 7(260), 1-14.
- Morgado-Bernal, I. (2011). Learning and memory consolidation: Linking molecular and behavioural data. *Neuroscience*, 176, 12-19.
- Morishita, W., Marie, H. and Malenka, R. (2005). Distinct triggering and expression mechanisms underlie LTD of AMPA and NMDA synaptic responses. *Nature Neuroscience*, 8(8), 1043-1050.
- Morris, G., Jiruska, P., Jefferys, J. and Powell, A. (2016). A new approach of modified submerged patch clamp recording reveals interneuronal dynamics during epileptiform oscillations. *Frontiers in Neuroscience*, 10(1), 519-542.
- Motulsky, H. and Brown, R., (2006). Detecting outliers when fitting data with nonlinear regression - A new method based on robust nonlinear regression and the false discovery rate. *BMC Bioinformatics*, (9)7, 123-157.
- Moyer, C., Shelton, M. and Sweet, R. (2015). Dendritic spine alterations in schizophrenia. *Neuroscience Letters*, 601(1), 46-53.
- Mulkey, R. and Malenka, R., (1992). Mechanisms underlying induction of homosynaptic long-term depression in area CA1 of the hippocampus. *Neuron*, 9(5), 967-975.
- Nakano, T., Doi, T., Yoshimoto, J. and Doya, K. (2010). A kinetic model of dopamine- and calcium-dependent striatal synaptic plasticity. *PLoS Computational Biology*, 6(2), 1-16.
- Neher, E. and Sakmann, B. (1992). The patch clamp technique. *Scientific American*, 266(3), 44-51.
- Neveu, D. and Zucker, R. (1996). Postsynaptic levels of [Ca²⁺]_i needed to trigger LTD and LTP. *Neuron*, 16(3), 619-629.

- Nicoll, R. and Schmitz, D. (2005). Synaptic plasticity at hippocampal mossy fibre synapses. *Nature Reviews Neuroscience*, 6(11), 863-876.
- Nimitvilai, S. and Brodie, M. (2010). Reversal of prolonged dopamine inhibition of dopaminergic neurons of the ventral tegmental area. *Journal of Pharmacology and Experimental Therapeutics*, 333(2), 555-563.
- Nimitvilai, S., Herman, M., You, C., Arora, D., McElvain, M., Roberto, M. and Brodie, M. (2014). Dopamine D2 receptor desensitization by dopamine or corticotropin releasing factor in ventral tegmental area neurons is associated with increased glutamate release. *Neuropharmacology*, 82, 28-40.
- Nishi, A., Kuroiwa, M. and Shuto, T. (2011). Mechanisms for the modulation of dopamine D1 receptor signalling in striatal neurons. *Frontiers in Neuroanatomy*, 5(1), 43-75.
- Nishi, A., Matamales, M., Musante, V., Valjent, E., Kuroiwa, M., Kitahara, Y., Rebholz, H., Greengard, P., Girault, J. and Nairn, A. (2016). Glutamate counteracts dopamine/PKA signaling via dephosphorylation of DARPP-32 Ser-97 and alteration of its cytonuclear distribution. *Journal of Biological Chemistry*, 292(4), 1462-1476.
- Niswender, C. and Conn, P. (2010). Metabotropic glutamate receptors: Physiology, pharmacology, and disease. *Annual Review of Pharmacology and Toxicology*, 50(1), 295-322.
- Noel, J., Ralph, G., Pickard, L., Williams, J., Molnar, E., Uney, J., Collingridge, G. and Henley, J., (1999). Surface expression of AMPA receptors in hippocampal neurons is regulated by an NSF-dependent mechanism. *Neuron*, 23(2), 365-376.
- Nowak, L., Bregestovski, P., Ascher, P., Herbet, A. and Prochiantz, A. (1984). Magnesium gates glutamate-activated channels in mouse central neurones. *Nature*, 307(5950), 462-465.
- Nugent, F., Penick, E. and Kauer, J. (2007). Opioids block long-term potentiation of inhibitory synapses. *Nature*, 446(7139), 1086-1090.
- Oades, R. and Halliday, G. (1987). Ventral tegmental (A10) system: Neurobiology. 1. Anatomy and connectivity. *Brain Research Reviews*, 12(2), 117-165.
- Ohara, S., Inoue, K., Yamada, M., Yamawaki, T., Koganezawa, N., Tsutsui, K., Witter, M. and Lijima, T. (2009). Dual transneuronal tracing in the rat entorhinal-hippocampal circuit by intracerebral injection of recombinant rabies virus vectors. *Frontiers in Neuroanatomy*, 3(1), 1-11.
- Ohara, S., Onodera, M., Simonsen, Ø., Yoshino, R., Hioki, H., Iijima, T., Tsutsui, K. and Witter, M. (2018). Intrinsic projections of layer Vb neurons to layers Va, III, and II in the lateral and medial entorhinal cortex of the rat. *Cell Reports*, 24(1), 107-116.
- Ohno-Shosaku, T., Shosaku, J., Tsubokawa, H. and Kano, M. (2002). Cooperative endocannabinoid production by neuronal depolarization and group I metabotropic glutamate receptor activation. *European Journal of Neuroscience*, 15(6), 953-961.
- O'Keefe, J. and Nadel, L. (1978). *The hippocampus as a cognitive map*. 1st ed. Oxford: Clarendon Press, 1-570.

- Oleskevich, S., Descarries, L. and Lacaille, J. (1989). Quantified distribution of the noradrenaline innervation in the hippocampus of adult rat. *The Journal of Neuroscience*, 9(11), 3803-3815.
- O'Mara, S. (2005). The subiculum: What it does, what it might do, and what neuroanatomy has yet to tell us. *Journal of Anatomy*, 207(3), 271-282.
- Otani, S., Auclair, N., Desce, J., Roisin, M. and Crépel, F. (1999). Dopamine receptors and groups I and II mGluRs cooperate for long-term depression induction in rat prefrontal cortex through converging postsynaptic activation of MAP kinases. *The Journal of Neuroscience*, 19(22), 9788-9802.
- Otmakhova, N. and Lisman, J. (2006). Dopamine, serotonin, and noradrenaline strongly inhibit the direct perforant path-CA1 synaptic input but have little effect on the schaffer collateral input. *Annals of the New York Academy of Sciences*, 911(1), 462-464.
- Overstreet, D. (1993). The flinders sensitive line rats: A genetic animal model of depression. *Neuroscience & Biobehavioural Reviews*, 17(1) 51-68.
- Park, H., Popescu, A. and Poo, M. (2014). Essential role of presynaptic NMDA receptors in activity-dependent BDNF secretion and corticostriatal LTP. *Neuron*, 84(5), 1009-1022.
- Park, M., Penick, E., Edwards, J., Kauer, J. and Ehlers, M. (2004). Recycling endosomes supply AMPA receptors for LTP. *Science*, 305(5692), 1972-1975.
- Park, P., Kang, H., Sanderson, T., Bortolotto, Z., Georgiou, J., Zhuo, M., Kaang, B. and Collingridge, G. (2018). The role of calcium-permeable AMPARs in long-term potentiation at principal neurons in the rodent hippocampus. *Frontiers in Synaptic Neuroscience*, 10(42), 1-11.
- Patel, K., Cherian, J., Gohil, K. and Atkinson, D. (2014). Schizophrenia: Overview and treatment options. *Pharmacy and Therapeutics*, 39(9), 1-8.
- Pedrosa, R. and Soares-da-Silva, P., (2002). Oxidative and non-oxidative mechanisms of neuronal cell death and apoptosis by L-3,4-dihydroxyphenylalanine (L-DOPA) and dopamine. *British Journal of Pharmacology*, 137(8), 1305-1313.
- Pelkey, K., Lavezzari, G., Racca, C., Roche, K. and McBain, C. (2005). mGluR7 Is a metaplastic switch controlling bidirectional plasticity of feedforward inhibition. *Neuron*, 46(1), 89-102.
- Petersen, R., Moradpour, F., Eadie, B., Shin, J., Kannangara, T., Delaney, K. and Christie, B. (2013). Electrophysiological identification of medial and lateral perforant path inputs to the dentate gyrus. *Neuroscience*, 252(1), 154-168.
- Phillips, K. and Deshpande, L. (2016). Repeated low-dose organophosphate DFP exposure leads to the development of depression and cognitive impairment in a rat model of gulf war illness. *Neurotoxicology*, 52(1) 127-133.
- Pikkarainen, M., Rönkkö, S., Savander, V., Insausti, R. and Pitkänen, A. (1999). Projections from the lateral, basal, and accessory basal nuclei of the amygdala to the

- hippocampal formation in rat. *The Journal of Comparative Neurology*, 403(2), 229-260.
- Pin, J. and Duvoisin, R. (1995). The metabotropic glutamate receptors: Structure and functions. *Neuropharmacology*, 34(1), 1-26.
- Pisani, A., Centonze, D., Bernardi, G. and Calabresi, P. (2005). Striatal synaptic plasticity: Implications for motor learning and Parkinson's disease. *Movement Disorders*, 20(4), 395-402.
- Pittenger, C. and Duman, R. (2007). Stress, depression, and neuroplasticity: A convergence of mechanisms. *Neuropsychopharmacology*, 33(1), 88-109.
- Polter, A., Yang, S., Jope, R. and Li, X. (2012). Functional significance of glycogen synthase kinase-3 regulation by serotonin. *Cellular Signalling*, 24(1), 265-271.
- Popkirov, S. and Manahan-Vaughan, D. (2010). Involvement of the metabotropic glutamate receptor mGluR5 in NMDA receptor-dependent, learning-facilitated long-term depression in CA1 synapses. *Cerebral Cortex*, 21(3), 501-509.
- Prensa, L. and Parent, A. (2001). The nigrostriatal pathway in the rat: A single-axon study of the relationship between dorsal and ventral tier nigral neurons and the striosome/matrix striatal compartments. *The Journal of Neuroscience*, 21(18), 7247-7260.
- Price, C., Kim, P. and Raymond, L. (1999). D1 dopamine receptor-induced cyclic AMP-dependent protein kinase phosphorylation and potentiation of striatal glutamate receptors. *Journal of Neurochemistry*, 73(6), 2441-2446.
- Qian, J. and Noebels, J. (2001). Presynaptic Ca²⁺ channels and neurotransmitter release at the terminal of a mouse cortical neuron. *The Journal of Neuroscience*, 21(11), 3721-3728.
- Rang, H., Ritter, J., Flower, R., Henderson, G., Loke, Y. and MacEwan, D. (2019). *Rang and Dale's Pharmacology*. 9th ed. Amsterdam: Elsevier, 502.
- Rebola, N., Srikumar, B. and Mulle, C. (2010). Activity-dependent synaptic plasticity of NMDA receptors. *The Journal of Physiology*, 588(1), 93-99.
- Recce, M. and O'Keefe, J. (1989). The tetrode an improved technique for multi-unit extracellular recording. *Society for Neuroscience Abstracts*, 15(2), 1250.
- Ribas, R., Pancholi, S., Guest, S., Marangoni, E., Gao, Q., Thuleau, A., Simigdala, N., Polanska, U., Campbell, H., Rani, A., Liccardi, G., Johnston, S., Davies, B., Dowsett, M. and Martin, L. (2015). AKT antagonist AZD5363 influences estrogen receptor function in endocrine-resistant breast cancer and synergizes with fulvestrant (ICI182780) In vivo. *Molecular Cancer Therapeutics*, 14(9), 2035-2048.
- Ribot, T. (1897). *The Psychology of the Emotions*. 1st ed. London, England: Walter Scott Pub. Co.
- Riggs, R., McKenzie, A., Byrn, S., Nichols, D., Foreman, M. and Truex, L. (1987). Effect of beta-alkyl substitution on D-1 dopamine agonist activity: Absolute configuration of beta-methyldopamine. *Journal of Medicinal Chemistry*, 30(10), 1914-1918.

- Rodrigo, B., Jorge, A., Néstor, M., Damián, C., Álvarez-Tostado, C., Fiacro, J. and Gerardo, R. (2011). Quinpirole effects on the dopaminergic system. *British Journal of Pharmacology and Toxicology*, 2(6), 310-317.
- Rodríguez-Moreno, A., González-Rueda, A., Banerjee, A., Upton, A., Craig, M. and Paulsen, O. (2013). Presynaptic self-depression at developing neocortical synapses. *Neuron*, 77(1), 35-42.
- Rodríguez-Moreno, A. and Paulsen, O. (2008). Spike timing-dependent long-term depression requires presynaptic NMDA receptors. *Nature Neuroscience*, 11(7), 744-745.
- Room, P., Groenewegen, H. and Lohman, A. (1984). Inputs from the olfactory bulb and olfactory cortex to the entorhinal cortex in the cat. *Experimental Brain Research*, 56(3), 488-496.
- Rosenkranz, J. and Johnston, D. (2006). Dopaminergic regulation of neuronal excitability through modulation of I_h in layer V entorhinal cortex. *Journal of Neuroscience*, 26(12), 3229-3244.
- Rouach, N. and Nicoll, R. (2003). Endocannabinoids contribute to short-term but not long-term mGluR-induced depression in the hippocampus. *European Journal of Neuroscience*, 18(4), 1017-1020.
- Rowland, D., Weible, A., Wickersham, I., Wu, H., Mayford, M., Witter, M. and Kentros, C. (2013). Transgenically targeted rabies virus demonstrates a major monosynaptic projection from hippocampal area CA2 to medial entorhinal layer II neurons. *Journal of Neuroscience*, 33(37), 14889-14898.
- Rush, A., Wu, J., Rowan, M. and Anwyl, R. (2002). Group I metabotropic glutamate receptor (mGluR)-dependent long-term depression mediated via p38 mitogen-activated protein kinase is inhibited by previous high-frequency stimulation and activation of mGluRs and protein kinase C in the rat dentate gyrus in vitro. *The Journal of Neuroscience*, 22(14), 6121-6128.
- Sajikumar, S. and Frey, J. (2004). Late-associativity, synaptic tagging, and the role of dopamine during LTP and LTD. *Neurobiology of Learning and Memory*, 82(1), 12-25.
- Salin, P., Malenka, R. and Nicoll, R. (1996). Cyclic AMP mediates a presynaptic form of LTP at cerebellar parallel fiber synapses. *Neuron*, 16(4), 797-803.
- Sánchez-Rivera, A., Corona-Avenidaño, S., Alarcón-Angeles, G., Rojas-Hernández, A., Ramírez-Silva, M. and Romero-Romo, M., (2003). Spectrophotometric study on the stability of dopamine and the determination of its acidity constants. *Spectrochimica Acta Part A: Molecular and Biomolecular Spectroscopy*, 59(13), 3193-3203.
- Sanderson, T., Hogg, E., Collingridge, G. and Corrêa, S. (2016). Hippocampal metabotropic glutamate receptor long-term depression in health and disease: focus on mitogen-activated protein kinase pathways. *Journal of Neurochemistry*, 139(S2), 200-214.
- Sarchiapone, M., Carli, V., Camardese, G., Cuomo, C., Di Giuda, D., Calcagni, M., Focacci, C. and De Risio, S. (2006). Dopamine transporter binding in depressed patients with anhedonia. *Psychiatry Research: Neuroimaging*, 147(2-3), 243-248.

- Schoonover, K., McCollum, L. and Roberts, R. (2016). Protein markers of neurotransmitter synthesis and release in postmortem schizophrenia substantia nigra. *Neuropsychopharmacology*, 42(2), 540-550.
- Schulz, P., Cook, E. and Johnston, D. (1994). Changes in paired-pulse facilitation suggest presynaptic involvement in long-term potentiation. *The Journal of Neuroscience*, 14(9), 5325-5337.
- Schurr, A., Reid, K., Tseng, M. and Edmonds, H. (1984). The stability of the hippocampal slice preparation: An electrophysiological and ultrastructural analysis. *Brain Research*, 297(2), 357-362.
- Scimemi, A. and Beato, M. (2009). Determining the neurotransmitter concentration profile at active synapses. *Molecular Neurobiology*, 40(3), 289-306.
- Seeburg, P., Burnashev, N., Köhr, G., Kuner, T., Sprengel, R. and Monyer, H. (1995). The NMDA receptor channel: Molecular design of a coincidence detector. *Recent Progress in Hormone Research*, 50, 19-34.
- Seeman, P. (2007). Antiparkinson therapeutic potencies correlate with their affinities at dopamine D2-high receptors. *Synapse*, 61(12), 1013-1018.
- Seeman, P. and Schaus, J. (1991). Dopamine receptors labelled by [3H] quinpirole. *European Journal of Pharmacology*, 203(1), 105-109.
- Shin, R., Tully, K., Li, Y., Cho, J., Higuchi, M., Suhara, T. and Bolshakov, V. (2010). Hierarchical order of coexisting pre- and postsynaptic forms of long-term potentiation at synapses in amygdala. *Proceedings of the National Academy of Sciences*, 107(44), 19073-19078.
- Sibille, J., Zapata, J., Teillon, J. and Rouach, N. (2015). Astroglial calcium signaling displays short-term plasticity and adjusts synaptic efficacy. *Frontiers in Cellular Neuroscience*, 9(189), 1-10.
- Sibley, D., Monsma, F. and Shen, Y. (1993). Molecular neurobiology of dopaminergic receptors. *International Review of Neurobiology*, 35(1), 391-415.
- Silva, A., Kogan, J., Frankland, P. and Kida, S. (1998). CREB and memory. *Annual Review of Neuroscience*, 21(1), 127-148.
- Sjöström, P., Turrigiano, G. and Nelson, S. (2001). Rate, timing, and cooperativity jointly determine cortical synaptic plasticity. *Neuron*, 32(6), 1149-1164.
- Sjöström, P., Turrigiano, G. and Nelson, S. (2003). Neocortical LTD via coincident activation of presynaptic NMDA and cannabinoid receptors. *Neuron*, 39(4), 641-654.
- Snyder, E., Philpot, B., Huber, K., Dong, X., Fallon, J. and Bear, M. (2001). Internalization of ionotropic glutamate receptors in response to mGluR activation. *Nature Neuroscience*, 4(11), 1079-1085.
- Stahl, S., Pradko, J., Haight, B., Modell, J., Rockett, C. and Learned-Coughlin, S. (2004). A review of the neuropharmacology of bupropion, a dual norepinephrine and dopamine reuptake inhibitor. *The Primary Care Companion to The Journal of Clinical Psychiatry*, 6(4), 159-166.

- Stanton, P., Winterer, J., Bailey, C., Kyrozis, A., Raginov, I., Laube, G., Veh, R., Nguyen, C. and Müller, W. (2003). Long-term depression of presynaptic release from the readily releasable vesicle pool induced by NMDA receptor-dependent retrograde nitric oxide. *The Journal of Neuroscience*, 23(13), 5936-5944.
- Staubli, U., Larson, J. and Lynch, G. (1990). Mossy fiber potentiation and long-term potentiation involve different expression mechanisms. *Synapse*, 5(4), 333-335.
- Stoessl, A., Lehericy, S. and Strafella, A. (2014). Imaging insights into basal ganglia function, Parkinson's Disease, and dystonia. *The Lancet*, 384(9942), 532-544.
- Stolerman, I. (2010). *Encyclopedia of Psychopharmacology*. 1st ed. Berlin: Springer, 44.
- Südhof, T. (2012). Calcium control of neurotransmitter release. *Cold Spring Harbor Perspectives in Biology*, 4(1), a011353-a011374.
- Suh, J., Rivest, A., Nakashiba, T., Tominaga, T. and Tonegawa, S. (2011). Entorhinal cortex layer III input to the hippocampus is crucial for temporal association memory. *Science*, 334(6061), 1415-1420.
- Sullivan, R., Talangbayan, H., Einat, H. and Szechtman, H. (1998). Effects of quinpirole on central dopamine systems in sensitized and non-sensitized rats. *Neuroscience*, 83(3), 781-789.
- Sun, X., Zhao, Y. and Wolf, M. (2005). Dopamine receptor stimulation modulates AMPA receptor synaptic insertion in prefrontal cortex neurons. *Journal of Neuroscience*, 25(32), 7342-7351.
- Sunahara, R., Guan, H., O'Dowd, B., Seeman, P., Laurier, L., Ng, G., George, S., Torchia, J., Van Tol, H. and Niznik, H. (1991). Cloning of the gene for a human dopamine D5 receptor with higher affinity for dopamine than D1. *Nature*, 350(6319), 614-619.
- Sung, K., Choi, S. and Lovinger, D. (2001). Activation of group I mGluRs is necessary for induction of long-term depression at striatal synapses. *Journal of Neurophysiology*, 86(5), 2405-2412.
- Suzuki, W. and Amaral, D. (1994). Topographic organization of the reciprocal connections between the monkey entorhinal cortex and the perirhinal and parahippocampal cortices. *The Journal of Neuroscience*, 14(3), 1856-1877.
- Swanson, G. and Sakai, R. (2010). Ligands for ionotropic glutamate receptors. *Progress in Molecular and Subcellular Biology*, 46, 123-157.
- Swanson, L. (1982). The projections of the ventral tegmental area and adjacent regions: A combined fluorescent retrograde tracer and immunofluorescence study in the rat. *Brain Research Bulletin*, 9(1-6), 321-353.
- Tamamaki, N. and Nojyo, Y. (1993). Projection of the entorhinal layer II neurons in the rat as revealed by intracellular pressure-injection of neurobiotin. *Hippocampus*, 3(4), 471-480.
- Tang, K., Low, M., Grandy, D. and Lovinger, D. (2001). Dopamine-dependent synaptic plasticity in striatum during in vivo development. *Proceedings of the National Academy of Sciences*, 98(3), 1255-1260.

- Tang, M., Miyamoto, Y. and Huang, E. (2009). Multiple roles of β -catenin in controlling the neurogenic niche for midbrain dopamine neurons. *Development*, 136(12), 2027-2038.
- Tassin, J., Herve, D., Vezina, P., Trovero, F., Blanc, G. and Glowinski, J. (1989). Relationships between mesocortical and mesolimbic dopamine neurons. *Behavioural Pharmacology*, 1(1), 31.
- Thomas, G. and Huganir, R. (2004). MAPK cascade signalling and synaptic plasticity. *Nature Reviews Neuroscience*, 5(3), 173-183.
- Ting, J., Daigle, T., Chen, Q. and Feng, G. (2014). Acute brain slice methods for adult and aging animals: Application of targeted patch clamp analysis and optogenetics. *Methods in Molecular Biology*, 1183(1), 221-242.
- Traynelis, S., Wollmuth, L., McBain, C., Menniti, F., Vance, K., Ogden, K., Hansen, K., Yuan, H., Myers, S. and Dingledine, R. (2010). Glutamate receptor ion channels: Structure, regulation, and function. *Pharmacological Reviews*, 62(3), 405-496.
- Tritsch, N. and Sabatini, B. (2012). Dopaminergic modulation of synaptic transmission in cortex and striatum. *Neuron*, 76(1), 33-50.
- Tsukamoto, T., Asakura, M., Tsuneizumi, T., Satoh, Y., Shinozuka, T. and Hasegawa, K. (1994). The therapeutic effects and side effects in patients with major depression treated with sulpiride once a day. *Progress in Neuro-Psychopharmacology and Biological Psychiatry*, 18(3), 315-618.
- Turrigiano, G., Leslie, K., Desai, N., Rutherford, L. and Nelson, S. (1998). Activity-dependent scaling of quantal amplitude in neocortical neurons. *Nature*, 391(6670), 892-896.
- Tzounopoulos, T., Janz, R., Südhof, T., Nicoll, R. and Malenka, R. (1998). A role for cAMP in long-term depression at hippocampal mossy fiber synapses. *Neuron*, 21(4), 837-845.
- Umbriaco, D., Garcia, S., Beaulieu, C. and Descarries, L. (1995). Relational features of acetylcholine, noradrenaline, serotonin and GABA axon terminals in the stratum radiatum of adult rat hippocampus (CA1). *Hippocampus*, 5(6), 605-620.
- Undieh, A. (2010). Pharmacology of signaling induced by dopamine D1-like receptor activation. *Pharmacology & Therapeutics*, 128(1), 37-60.
- Uva, L. and de Curtis, M. (2005). Polysynaptic olfactory pathway to the ipsi- and contralateral entorhinal cortex mediated via the hippocampus. *Neuroscience*, 130(1), 249-258.
- Van Cauter, T., Camon, J., Alvernhe, A., Elduayen, C., Sargolini, F. and Save, E. (2012). Distinct roles of medial and lateral entorhinal cortex in spatial cognition. *Cerebral Cortex*, 23(2), 451-459.
- Van Groen, T., Miettinen, P. and Kadish, I. (2003). The entorhinal cortex of the mouse: Organization of the projection to the hippocampal formation. *Hippocampus*, 13(1), 133-149.

- Van Groen, T. and Wyss, J. (1990). Extrinsic projections from area CA1 of the rat hippocampus: Olfactory, cortical, subcortical, and bilateral hippocampal formation projections. *The Journal of Comparative Neurology*, 302(3), 515-528.
- Vanderwolf, C. (1992). Hippocampal activity, olfaction, and sniffing: An olfactory input to the dentate gyrus. *Brain Research*, 593(2), 197-208.
- Vasuta, C., Artinian, J., Laplante, I., Hebert-Seropian, S., Elayoubi, K. and Lacaille, J. (2015). Metaplastic regulation of CA1 schaffer collateral pathway plasticity by Hebbian mGluR1a-mediated plasticity at excitatory synapses onto somatostatin-expressing interneurons. *eNeuro*, 2(4), 1-39.
- Vaughan, R. and Foster, J. (2013). Mechanisms of dopamine transporter regulation in normal and disease states. *Trends in Pharmacological Sciences*, 34(9), 489-496.
- Vincent, P., Armstrong, C. and Marty, A. (1992). Inhibitory synaptic currents in rat cerebellar Purkinje cells: modulation by postsynaptic depolarization. *The Journal of Physiology*, 456(1), 453-471.
- Vismer, M., Forcelli, P., Skopin, M., Gale, K. and Koubeissi, M. (2015). The piriform, perirhinal, and entorhinal cortex in seizure generation. *Frontiers in Neural Circuits*, 9(27), 1-14.
- Volkow, N., Fowler, J., Wang, G. and Goldstein, R. (2002). Role of dopamine, the frontal cortex and memory circuits in drug addiction: Insight from imaging studies. *Neurobiology of Learning and Memory*, 78(3), 610-624.
- von Bernhardi, R., Bernhardi, L. and Eugeni, J. (2017). What is neural plasticity?. *Advances in Experimental Medicine and Biology*, 1015(1), 1-15.
- Waley, S. (1982). A quick method for the determination of inhibition constants. *Biochemical Journal*, 205(3), 631-633.
- Wang, G., Jiang, L., Wang, J., Zhang, J., Kong, F., Li, Q., Yan, Y., Huang, S., Zhao, Y., Liang, L., Li, J., Sun, N., Hu, Y., Shi, W., Deng, G., Chen, P., Liu, L., Zeng, X., Tian, G., Bu, Z., Chen, H. and Li, C. (2019). The G Protein-Coupled Receptor FFAR2 Promotes Internalization during Influenza A Virus Entry. *Journal of Virology*, 94(2), 1-21.
- Wang, H., Xu, J., Lazarovici, P., Quirion, R. and Zheng, W. (2018). cAMP Response Element-Binding Protein (CREB): A Possible Signaling Molecule Link in the Pathophysiology of Schizophrenia. *Frontiers in Molecular Neuroscience*, 11(255), 1-14.
- Wang, L., Fontanini, A. and Maffei, A. (2012). Experience-Dependent Switch in Sign and Mechanisms for Plasticity in Layer 4 of Primary Visual Cortex. *Journal of Neuroscience*, 32(31), 10562-10573.
- Wang, W., Jia, Y., Pham, D., Palmer, L., Jung, K., Cox, C., Rumbaugh, G., Piomelli, D., Gall, C. and Lynch, G. (2017). Atypical Endocannabinoid Signaling Initiates a New Form of Memory-Related Plasticity at a Cortical Input to Hippocampus. *Cerebral Cortex*, 28(7), 2253-2266.
- Wang, Y. and Linden, D. (2000). Expression of Cerebellar Long-Term Depression Requires Postsynaptic Clathrin-Mediated Endocytosis. *Neuron*, 25(3), 635-647.

- Wang, Y. and Salter, M., (1994). Regulation of NMDA receptors by tyrosine kinases and phosphatases. *Nature*, 369(6477), 233-235.
- Wise, R. (2006). Role of brain dopamine in food reward and reinforcement. *Philosophical Transactions of the Royal Society B: Biological Sciences*, 361(1471), 1149-1158.
- Wishart, D., Knox, C., Guo, A., Shrivastava, S., Hassanali, M., Stothard, P., Chang, Z. and Woolsey, J. (2006). DrugBank: A comprehensive resource for in silico drug discovery and exploration. *Nucleic Acids Research*, 1(34), D668-D672.
- Witter, M. (2007). The perforant path: Projections from the entorhinal cortex to the dentate gyrus. *Progress in Brain Research*, 163(1), 43-61.
- Witter, M., Doan, T., Jacobsen, B., Nilssen, E. and Ohara, S. (2017). Architecture of the entorhinal cortex: A review of entorhinal anatomy in rodents with some comparative notes. *Frontiers in Systems Neuroscience*, 11(46) 1-12.
- Witter, M., Groenewegen, H., Lopes da Silva, F. and Lohman, A. (1989). Functional organization of the extrinsic and intrinsic circuitry of the parahippocampal region. *Progress in Neurobiology*, 33(3), 161-253.
- Witter, M., Naber, P., van Haeften, T., Machielsen, W., Rombouts, S., Barkhof, F., Scheltens, P. and Lopes da Silva, F. (2000). Cortico-hippocampal communication by way of parallel parahippocampal-subicular pathways. *Hippocampus*, 10(4), 398-410.
- Woodward, R., Panicker, M. and Miledi, R. (1992). Actions of dopamine and dopaminergic drugs on cloned serotonin receptors expressed in xenopus oocytes. *Proceedings of the National Academy of Sciences*, 89(10), 4708-4712.
- Wouterlood, F., Mugnaini, E. and Nederlof, J. (1985). Projection of olfactory bulb efferents to layer I GABAergic neurons in the entorhinal area. Combination of anterograde degeneration and immunoelectron microscopy in rat. *Brain Research*, 343(2), 283-296.
- Wouterlood, F. and Nederlof, J. (1983). Terminations of olfactory afferents on layer II and III neurons in the entorhinal area: Degeneration-golgi-electron microscopic study in the rat. *Neuroscience Letters*, 36(2), 105-110.
- Wouterlood, F., van Denderen, J., van Haeften, T. and Witter, M. (2000). Calretinin in the entorhinal cortex of the rat: Distribution, morphology, ultrastructure of neurons, and co-localization with γ -aminobutyric acid and parvalbumin. *The Journal of Comparative Neurology*, 425(2), 177-192.
- Wright, D., Seroogy, K., Lundgren, K., Davis, B. and Jennes, L. (1995). Comparative localization of serotonin 1A, 1C, and 2 receptor subtype mRNAs in rat brain. *The Journal of Comparative Neurology*, 351(3), 357-373.
- Xu, H., Perez, S., Cornil, A., Detraux, B., Prokin, I., Cui, Y., Degos, B., Berry, H., de Kerchove d'Exaerde, A. and Venance, L. (2018). Dopamine-endocannabinoid interactions mediate spike-timing-dependent potentiation in the striatum. *Nature Communications*, 9(1), 1-18.
- Xu, W., Tse, Y., Dobie, F., Baudry, M., Craig, A., Wong, T. and Wang, Y. (2013). Simultaneous monitoring of presynaptic transmitter release and postsynaptic receptor trafficking

- reveals an enhancement of presynaptic activity in metabotropic glutamate receptor-mediated long-term depression. *Journal of Neuroscience*, 33(13), 5867-5877.
- Xu, X., Sun, Y., Holmes, T. and López, A. (2016). Noncanonical connections between the subiculum and hippocampal CA1. *Journal of Comparative Neurology*, 524(17), 3666-3673.
- Yamamoto, K., Gonzalez, G., Biggs, W. and Montminy, M. (1988). Phosphorylation-induced binding and transcriptional efficacy of nuclear factor CREB. *Nature*, 334(6182), 494-498.
- Yan, Q. (2000). Activation of 5-HT_{2A/2C} receptors within the nucleus accumbens increases local dopaminergic transmission. *Brain Research Bulletin*, 51(1), 75-81.
- Yang, C. and Seamans, J., (1996). Dopamine D1 receptor actions in layers V-VI rat prefrontal cortex neurons in vitro: Modulation of dendritic-somatic signal integration. *The Journal of Neuroscience*, 16(5), 1922-1935.
- Yang, H., Hu, X., Zhang, H., Xin, W., Li, M., Zhang, T., Zhou, L. and Liu, X. (2004). Roles of CaMKII, PKA, and PKC in the induction and maintenance of LTP of C-fiber-evoked field potentials in rat spinal dorsal horn. *Journal of Neurophysiology*, 91(3), 1122-1133.
- Yang, J., Woodhall, G. and Jones, R. (2006). Tonic facilitation of glutamate release by presynaptic NR2B-containing NMDA receptors is increased in the entorhinal cortex of chronically epileptic rats. *Journal of Neuroscience*, 26(2), 406-410.
- Yang, Q., Chen, S., Li, D. and Pan, H. (2007). Kv1.1/1.2 channels are downstream effectors of nitric oxide on synaptic GABA release to preautonomic neurons in the paraventricular nucleus. *Neuroscience*, 149(2), 315-327.
- Yang, Y. and Calakos, N. (2013). Presynaptic long-term plasticity. *Frontiers in Synaptic Neuroscience*, 5(8), 1-22.
- Yiannopoulou, K. and Papageorgiou, S. (2013). Current and future treatments for Alzheimer's disease. *Therapeutic Advances in Neurological Disorders*, 6(1), 19-33.
- Yuste, R. and Bonhoeffer, T. (2001). Morphological changes in dendritic spines associated with long-term synaptic plasticity. *Annual Review of Neuroscience*, 24(1), 1071-1089.
- Zhang, M., Hu, S., Tao, J., Zhou, W., Wang, R., Tai, Y., Xiao, F., Wang, Q. and Wei, W. (2019). Ginsenoside compound-K inhibits the activity of B cells through inducing IgD-B cell receptor endocytosis in mice with collagen-induced arthritis. *Inflammopharmacology*, 27(4), 845-856.
- Zhang, Y., Venkitaramani, D., Gladding, C., Zhang, Y., Kurup, P., Molnar, E., Collingridge, G. and Lombroso, P. (2008). The tyrosine phosphatase STEP mediates AMPA receptor endocytosis after metabotropic glutamate receptor stimulation. *Journal of Neuroscience*, 28(42), 10561-10566.
- Zhou, G., Lane, G., Cooper, S., Kahnt, T. and Zelano, C. (2019). Characterizing functional pathways of the human olfactory system. *eLife*, 8(e47177), 1-27.

- Zhou, Y. and Danbolt, N. (2014). Glutamate as a neurotransmitter in the healthy brain. *Journal of Neural Transmission*, 121(8), 799-817.
- Zhu, G., Briz, V., Seinfeld, J., Liu, Y., Bi, X. and Baudry, M. (2017). Calpain-1 deletion impairs mGluR-dependent LTD and fear memory extinction. *Scientific Reports*, 7(1), 1-14.
- Zhuo, M., Hu, Y., Schultz, C., Kandel, E. and Hawkins, R. (1994). Role of guanylyl cyclase and cGMP-dependent protein kinase in long-term potentiation. *Nature*, 368(6472), 635-639.
- Zorumski, C. and Izumi, Y. (2012). NMDA receptors and metaplasticity: Mechanisms and possible roles in neuropsychiatric disorders. *Neuroscience & Biobehavioral Reviews*, 36(3), 989-1000.
- Zucker, R. and Regehr, W. (2002). Short-term synaptic plasticity. *Annual Review of Physiology*, 64(1), 355-405.